

1. Report No. FHWA/TX-92+1223-1	2. Government Accession No.	3. Recipient's Catalog No.	
4. Title and Subtitle EVALUATION AND IMPLEMENTATION OF THE ROUGHNESS MEASURING SUBSYSTEM OF THE ARAN UNIT		5. Report Date February 1991	6. Performing Organization Code
7. Author(s) Jian Lu, Carl B. Bertrand, and W. Ronald Hudson		8. Performing Organization Report No. Research Report 1223-1	
9. Performing Organization Name and Address Center for Transportation Research The University of Texas at Austin Austin, Texas 78712-1075		10. Work Unit No. (TRAIS)	11. Contract or Grant No. Research Study 3-18-89/0-1223
12. Sponsoring Agency Name and Address Texas Department of Transportation (formerly State Department of Highways and Public Transportation) P. O. Box 5051 Austin, Texas 78763-5051		13. Type of Report and Period Covered Interim	
15. Supplementary Notes Study conducted in cooperation with the U. S. Department of Transportation, Federal Highway Administration Research Study Title: "Evaluation and Implementation of ARAN Unit"		14. Sponsoring Agency Code	
16. Abstract The ARAN unit, one of which has been purchased by the Texas State Department of Highways and Public Transportation (SDHPT), is a multi-function, road-quality surveying instrument. The instrument includes a pavement surface roughness measuring subsystem, a rut depth and transverse profile measuring subsystem, a gyro subsystem, a right-of-way videologging subsystem, a pavement condition videologging subsystem, and a pavement rating subsystem. To enhance our understanding of the response of this instrument (so as to apply it more efficiently to pavement management), the Center for Transportation Research (CTR) of The University of Texas at Austin has conducted a comprehensive evaluation. This report describes the procedures, methodologies, and results from the evaluation of the pavement roughness measuring subsystem of the ARAN unit. The main activities described and discussed are the field tests and data collection, the repeatability test of the roughness subsystem, the effect of the report interval on the roughness statistics, the correlation analysis and calibration models developed, the new PSI models developed, the effect of the operational speed on the roughness statistics, and the speed-effect-cancelling models developed.			
17. Key Words ARAN unit, surveying, pavement, surface roughness, rut depth, transverse profile, gyro, right-of-way, condition, videologging, subsystem, evaluation		18. Distribution Statement No restrictions. This document is available to the public through the National Technical Information Service, Springfield, Virginia 22161.	
19. Security Classif. (of this report) Unclassified	20. Security Classif. (of this page) Unclassified	21. No. of Pages 88	22. Price

**EVALUATION AND IMPLEMENTATION OF THE
ROUGHNESS MEASURING SUBSYSTEM
OF THE ARAN UNIT**

by

Jian Lu
Carl B. Bertrand
W. Ronald Hudson

Research Report Number 1223-1

Research Project 3-18-89/0-1223

Evaluation and Implementation of ARAN Unit

conducted for

**Texas State Department of Highways
and Public Transportation**

in cooperation with the

**U. S. Department of Transportation
Federal Highway Administration**

by the

CENTER FOR TRANSPORTATION RESEARCH

Bureau of Engineering Research

THE UNIVERSITY OF TEXAS AT AUSTIN

February 1991

NOT INTENDED FOR CONSTRUCTION,
PERMIT, OR BIDDING PURPOSES

W. Ronald Hudson, P.E. (Texas No. 16821)
Research Supervisor

The contents of this report reflect the views of the authors, who are responsible for the facts and the accuracy of the data presented herein. The contents do not necessarily reflect the official views or policies of the Federal Highway Administration or the State Department of Highways and Public Transportation. This report does not constitute a standard, specification, or regulation.

PREFACE

This report presents details, procedures, methodologies, and findings from the first part of Research Study 3-18-89/0-1223, Evaluation and Implementation of the Roughness Measuring Subsystem of the Automatic Road Analyzer (ARAN), conducted by the Center for Transportation Research of The University of Texas at Austin. The main objective of the study is to evaluate and implement the roughness, rut depth, and gyro measuring subsystems—including the overall system—of the ARAN unit. As part of the research study effort, some application models for the ARAN unit have been developed.

This report describes the results obtained from the first phase of the research, evaluation, and implementation of the roughness measuring subsystem of the ARAN unit. Specifically, the research results presented in this report cover field tests, roughness statistics and their report interval, repeatability, correlation analysis, new PSI model development, speed-effect analysis, and speed-effect canceling models.

We would like to express our appreciation to the Texas State Department of Highways and Public Transportation contact representatives for their cooperation in this study. In particular, we thank Mr. David Fink for assistance in the field test and data collection.

The authors are also grateful to the staff of the Center for Transportation Research, who provided support throughout this phase of the research study and report.

Jian Lu
Carl B. Bertrand
W. Ronald Hudson

February 1991

LIST OF REPORTS

Report No. 1223-1, "Evaluation and Implementation of the Roughness Measuring Subsystem of the ARAN Unit," by Jian Lu, Carl B. Bertrand, and W. Ronald Hudson, discusses the research results obtained from the evaluation and implementation of the roughness measuring subsystem of the ARAN unit. This report covers field tests, roughness statistics and their report interval, repeatability, correlation analysis, new PSI model development, speed-effect analysis, and speed-effect canceling models.

ABSTRACT

The ARAN unit, one of which has been purchased by the Texas State Department of Highways and Public Transportation (SDHPT), is a multi-function, road-quality surveying instrument. The instrument includes a pavement surface roughness measuring subsystem, a rut depth and transverse profile measuring subsystem, a gyro subsystem, a right-of-way videologging subsystem, a pavement condition videologging subsystem, and a pavement rating subsystem.

To enhance our understanding of the response of this instrument (so as to apply it more efficiently to pavement management), the Center for Transportation Research (CTR) of The University of Texas at Austin has conducted a comprehensive evaluation.

This report describes the procedures, methodologies, and results from the evaluation of the pavement roughness measuring subsystem of the ARAN unit. The main activities described and discussed are the field tests and data collection, the repeatability test of the roughness subsystem, the effect of the report interval on the roughness statistics, the correlation analysis and calibration models developed, the new PSI models developed, the effect of the operational speed on the roughness statistics, and the speed-effect-cancelling models developed.

SUMMARY

A better understanding of the ARAN unit's outputs must be developed before the instrument can be effectively put to use as a comprehensive pavement evaluation tool. This understanding would provide not only a reference for the future calibration of the instrument, but would in addition provide information regarding the ARAN's use as a pavement management and transportation planning tool. While this research effort has been divided into three subsets, this report presents only the results of the first subset, which is the evaluation and implementation of the roughness measuring subsystem of the ARAN unit.

The repeatability of the roughness measuring subsystem was evaluated using the data obtained from field tests. The ARAN unit's roughness outputs are Root Mean Square Vertical Acceleration (RMSVA), Mean Absolute Slope (MAS), and TEXTURE. While the repeatability of the roughness subsystem is influenced by several operational factors, test results from this study showed that the repeatability of the roughness outputs is statistically better than 5 percent. Another important factor which was evaluated is the report interval, which is set by the operator before the ARAN unit is used to collect roughness data. Statistical results showed that the report interval does not have a significant impact on the roughness subsystem outputs. On the other hand, test results showed that the operational speed has a significant impact on the outputs of the roughness subsystem. Two different statistical models were developed from this research to cancel the effect of the operational speed on the roughness subsystem outputs.

The modified K. J. Law profilometer was used as the standard roughness reference instrument for the correlation analysis, with two PSI models developed to estimate the serviceability index (SI) from the ARAN's roughness subsystem statistics (RMSVA, MAS, and TEXTURE).

IMPLEMENTATION STATEMENT

The results of the evaluation and implementation of the roughness measuring subsystem of the Automatic Road Analyzer unit will provide important criteria for the operation of this instrument. The results of this work will also provide some practical and theoretical references for making the ARAN unit a more effective pavement management tool. The resulting models presented in this report, and the methodologies used in this project, are not only useful to the ARAN unit, but may also be applicable to the other response-type roughness measuring systems.

TABLE OF CONTENTS

PREFACE	<i>iii</i>
LIST OF REPORTS	<i>iii</i>
ABSTRACT	<i>iii</i>
SUMMARY	<i>iv</i>
IMPLEMENTATION STATEMENT	<i>iv</i>
CHAPTER 1. INTRODUCTION	
SCOPE	1
GENERAL BACKGROUND	1
DESCRIPTION OF THE ARAN UNIT AND ITS FUNCTIONS	2
Roughness Measurement	2
Rut Depth and Transverse Profile Measurement	4
Gyro	4
Right-of-Way Videologging	4
Pavement Condition Videologging	4
Pavement Rating	4
DESCRIPTION OF ROUGHNESS MEASURING SUBSYSTEM	4
Root Mean Square Vertical Acceleration (RMSVA)	4
Mean Absolute Slope (MAS)	4
TEXTURE	4
Serviceability Index (SI)	4
CHAPTER 2. FIELD TEST AND DATA COLLECTION	
INTRODUCTION	6
TEST SITE CHOICE	6
INSTRUMENT CHOSEN FOR CORRELATION ANALYSIS	6
DESCRIPTION OF TEST PROCEDURES	6
REPORT INTERVAL, TESTING SPEED, AND PAVEMENT SURFACE CONDITION CONSIDERATIONS	6
SUMMARY OF DATA COLLECTED FROM FIELD TEST	9
CHAPTER 3. THE EFFECT OF THE REPORT INTERVAL	
INTRODUCTION	11
POSSIBLE SOURCES OF DIFFERENCES	11
METHODOLOGY USED	11
RESULTS OF THE TESTING	12
SUMMARY	12
CHAPTER 4. TEST OF REPEATABILITY	
INTRODUCTION	14
POSSIBLE INFLUENCES AFFECTING REPEATABILITIES	14
TEST PROCEDURE USED	14
RESULTS OF THE REPEATABILITY TESTING	15
SUMMARY	15
CHAPTER 5. CORRELATION ANALYSIS AND ROUGHNESS CALIBRATION MODELS	
INTRODUCTION	18
CHOICE OF THE REFERENCE INSTRUMENT	18

ROUGHNESS STATISTICS OF THE MODIFIED K. J. LAW PROFILOMETER	19
Maysmeter Output (MO)	19
Serviceability Index (SI)	19
International Roughness Index (IRI)	19
FIELD TESTS	19
Test Consideration of the Modified K. J. Law Profilometer	20
Test Considerations of the ARAN Unit	20
RESULTS	20
CONCLUSIONS	20
CHAPTER 6. NEW PSI MODEL FOR THE ARAN UNIT	
INTRODUCTION	27
NEW PSI MODEL INCLUDING TEXTURE	27
PSI EQUATION EXCLUDING TEXTURE	28
FINDINGS	30
CHAPTER 7. IMPACT OF THE ARAN UNIT OPERATIONAL SPEED ON ITS ROUGHNESS STATISTICS	
INTRODUCTION	31
REFERENCE QUARTER-CAR SIMULATION	31
AMPLITUDE FREQUENCY CHARACTERISTICS OF RQCS	32
SPEED-EFFECT CONSIDERATION	33
SPEED-EFFECT ANALYSIS BASED ON THE DATA COLLECTED FROM TEST SECTIONS	33
CONCLUSIONS	34
CHAPTER 8. SPEED-EFFECT-CANCELING MODELS FOR THE TEXAS SDHPT ARAN UNIT	
INTRODUCTION	35
SPEED-EFFECT-CANCELING MODEL 1	35
Basic Methodology of Speed-Effect-Canceling Model 1	35
Experiments and Field Tests (After Suspension Modifications)	36
Model 1 Results	36
SPEED-EFFECT-CANCELING MODEL 2	39
Experiments and Field Tests	39
Methodology of Model 2	40
Applying Speed-Effect-Canceling Model 2 to the ARAN Unit	41
Example	48
SUMMARY	48
CHAPTER 9. SUMMARY, CONCLUSIONS, AND RECOMMENDATIONS	
SUMMARY	50
CONCLUSIONS	51
RECOMMENDATION	51
REFERENCES	52
APPENDIX A	54
APPENDIX B	57
APPENDIX C	63
APPENDIX D	68

CHAPTER 1. INTRODUCTION

SCOPE

In 1982, the Texas State Department of Highways and Public Transportation (SDHPT) initiated a network-level pavement evaluation system (PES), an important aspect of which was the pavement surface condition data collection. Currently, pavement surface conditions (except pavement surface roughness) are assessed visually by field teams measuring roadway characteristics at less than normal highway speeds. Operating at such reduced speed not only makes the data collection unsafe in high-speed, high-traffic areas, but inefficient and expensive as well.

Around the same time, the Federal Highway Administration (FHWA) requested that each state change its regulation on pavement design policy and procedure; in effect, each state was required to establish a pavement management system (PMS), two important functions of which are pavement evaluation and field data collection.

In attempting to overcome problems associated with reduced data collection speed while at the same time satisfying the requirements of the FHWA, the SDHPT purchased an Automatic Road Analyzer (ARAN) in 1987. Capable of operating at 30 to 50 mph under normal traffic conditions, the ARAN unit is equipped with several important pavement surface condition surveying subsystems, which, together, define it as a comprehensive pavement surface condition survey system. Yet as a relatively new product, the ARAN unit and its several subsystems require rigorous evaluation to determine their full potential. This evaluation is the subject of the present study.

Three ARAN unit subsystems in particular have been evaluated: the roughness measuring subsystem, the rut depth measuring subsystem, and the orientation measuring subsystem. Two specific phases of research were undertaken in this effort, involving primarily:

- (1) a general subsystem evaluation, and
- (2) subsystem model development and implementation

For the general subsystem evaluation, the main activities included an analysis of repeatability, correlation, index report interval effect, testing speed

effect, dynamic and static response, accuracy, and error.

For the subsystem modeling development, the main work was conducted using methodologies to develop (1) calibration models for the problems found during the subsystem evaluation and (2) other models considered useful in implementing the ARAN unit.

Special software has been developed for the subsystem modeling implementation. Because the ARAN unit uses an IBM PC/AT as the main system control computer, this software was designed specifically for use with IBM PCs.

The multiple functioning and high operating speed of the ARAN unit commend it as an important instrument in pavement management. In addition, a comprehensive evaluation of this unit, as provided in this study, will benefit the Texas SDHPT in the following ways:

- (1) The results of the research will provide useful information about the ARAN unit with respect to the performance of the subsystems.
- (2) The models developed and implemented for the ARAN unit will render it a more powerful instrument; moreover, the methodologies of the modeling and evaluation can be used for future application on other instruments of this type.

This report includes only the results obtained from the evaluation and implementation of the roughness measuring subsystem. Specifically, these results pertain to the effects of the sampling report interval on the outputs of the subsystem, repeatability, correlation analysis, the impacts of measuring speed on the outputs of the subsystem, speed-effect-canceling models, and the PSI regression model. The measuring principles, hardware system, and software system will be described in a later report.

GENERAL BACKGROUND

Research leading to the development of roughness measuring equipment dates back more than 60 years (Ref 1). As a result of the AASHO Road Test in particular, increasing attention has focused on this research area, leading to the development of many

types of pavement roughness surveying instruments. Gradually, the use of these instruments to evaluate the ride quality of pavement surfaces grew more and more widespread, such that now the evaluation of the relative smoothness of pavement surfaces has become an important factor affecting decisions regarding maintenance and the classification of pavement inventories.

The repeatability and reliability of the static and dynamic instrument responses are among the major concerns when maintenance and classification decisions are to be based on the outputs. Moreover, the number of pavement miles within Texas and the U.S. has demanded that high-speed dynamic instruments be used for these evaluation efforts.

Generally, existing pavement roughness instruments can be divided into three classes, with each class defined by the measurement techniques and the associated measurement errors (Refs 2 and 3).

Class I: Manually operated instruments that accurately measure short wavelength profiles of the roads. The measurement interval is less than or equal to 1 foot, and the maximum error is 1.5 percent bias, or 19 inches/mile. Examples of such instruments include the rod and level, the Face Dipstick, and the TRRL beam.

Class II: Dynamic direct profiling instruments that employ a variety of methods to produce elevation data from the road surface. The measurement interval is less than or equal to 2 feet, and the maximum error is 5 percent bias, or 44 inches/mile. Examples of these instruments include the APL trailer, the GM profilometer, the K. J. Law profilometer, and the South Dakota Profiler.

Class III: Response-type road roughness measuring (RTRRM) systems, which accumulate suspension deflections (axle to body or acceleration values) from the roadway surfaces. The maximum error associated with the operation of these instruments is 10 percent, or 32 to 63 inches/mile, and the measurement interval is the test section length. Examples of these instruments include the Mays Ride Meter, the Cox Meter, the Walker Roughness Device (SIometer), the BPR Roughmeter, and the Automatic Road Analyzer (ARAN) unit.

Classifications I and II include instruments used in the measurement of the shorter wavelengths contained in the pavement surface profiles. The instruments within these classifications possess the highest resolution and the smallest acceptable maximum error.

Classification III is a category based on the assumption that the pavement surface ride quality can

be directly related to the passenger's perception of the vehicle's vibrations at a certain frequency band, rather than to the absolute surface profile; that is, the passengers are more sensitive to the vertical acceleration of the vehicle body (due to the transfer of pavement surface roughness through the vehicle suspension system) than to the actual elevation changes of the pavement surface.

The ARAN unit is defined as a Class III instrument. The vertical accelerations of the body and the axle of the unit are sampled and processed to produce three roughness indices: Root Mean Square Vertical Acceleration (RMSVA), Mean Absolute Slope (MAS), and TEXTURE (Ref 4). Relatively speaking, the smaller the values of the reported roughness indices, the better the corresponding pavement surface ride quality. In addition to the three indices, the Texas SDHPT is interested in also obtaining the serviceability index (SI), which is another roughness index. This roughness index can be obtained through a regression model with the variables RMSVA and MAS. The concept behind SI is the same as that of present serviceability index (PSI) (Ref 5).

DESCRIPTION OF THE ARAN UNIT AND ITS FUNCTIONS

The ARAN unit is a van-mounted system that measures and records a wide variety of pavement performance parameters. The entire system is mounted inside a 1986 Ford 1-ton van with a modified motorhome chassis to facilitate its operation; enlarged windows enhance operator observation, while a raised roof provides more space for equipment.

As a multi-function system, the ARAN unit (see Figure 1.1) is equipped with the following subsystems (Ref 5):

- (1) pavement surface roughness measurement,
- (2) rut depth and transverse profile measurement,
- (3) gyro,
- (4) right-of-way videologging,
- (5) pavement condition videologging, and
- (6) pavement rating.

The block diagram in Figure 1.2 shows the subsystems and their interaction. These individual subsystems have the specialized functions described below.

Roughness Measurement

This subsystem measures the accelerations of the vehicle caused by pavement surface roughness within certain wavelengths. The roughness indices reported (and which reflect the surface ride quality) include RMSVA, MAS, and TEXTURE. SI is calculated from the RMSVA and MAS data. As stated before, this subsystem is considered to be a Class III RTRRM instrument.



Figure 1.1 Outside view of the ARAN unit

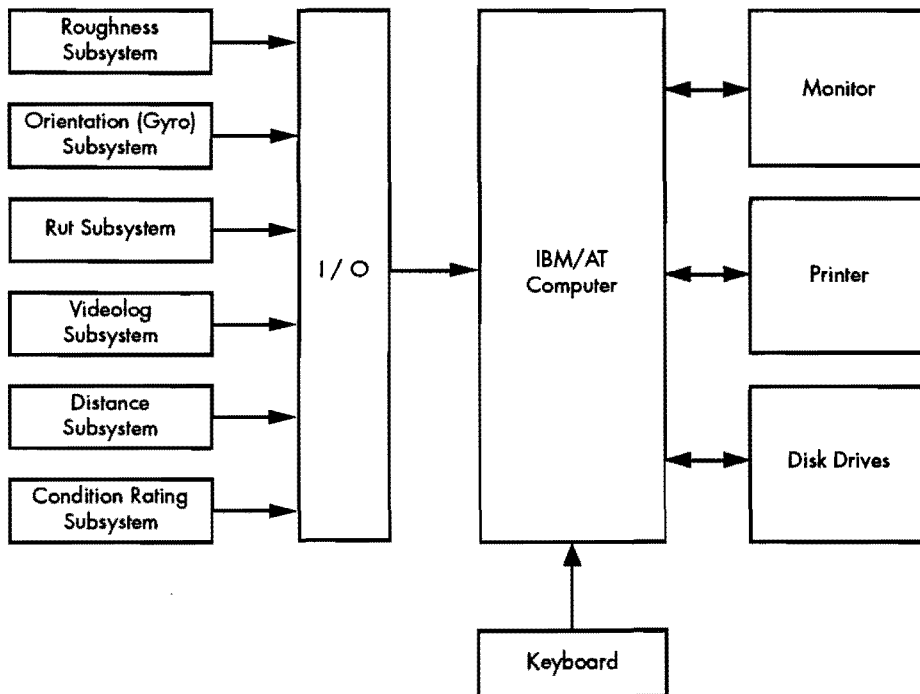


Figure 1.2 Block diagram of the ARAN unit

Rut Depth and Transverse Profile Measurement

This subsystem provides a vehicle-to-road reference measure (transverse profile) ranging from 8 feet up to 14 feet. The results obtained from this subsystem can be used to determine a measure of the rut depth in each wheelpath of the travel lane or, in conjunction with the gyro subsystem, to determine road crossfall and grade.

Gyro

This subsystem consists of two gyroscopes. The results obtained from this subsystem can be used to determine direction of travel, radius of curvature, grade, and crossfall of a roadway. Also, in conjunction with the rut depth measuring subsystem, the transverse profile can be obtained.

Right-of-Way Videologging

This subsystem consists of a color video camera and a video cassette recorder (VCR) system. It is mounted above the driver and records the view in front of the ARAN unit. These images provide reference photographs of the right-of-way.

Pavement Condition Videologging

Adapted for use in April 1990, this subsystem consists of a color video camera and a VCR system. The camera is mounted on the back of the vehicle and is pointed directly toward the pavement surface. The resulting pictures show the distress characteristics of the pavement surface.

Pavement Rating

This subsystem has two main purposes: to annotate the collected data and to inventory the roadway conditions.

DESCRIPTION OF ROUGHNESS MEASURING SUBSYSTEM

The roughness measuring subsystem block diagram is shown in Figure 1.3. This two-part subsystem is divided according to its hardware or its software. The hardware consists of axle and body accelerometers, analog signal amplifiers, analog low-pass filters, and a 12-bit analog-to-digital (A/D) converter. The software consists of digital band-pass filters passing wavelengths of 1 foot to 300 feet, digital high-pass filters passing wavelengths of 2 feet or less, and statistical models generating the reported roughness statistics (RMSVA, MAS, and TEXTURE). These roughness statistics are described below (Ref 4).

Root Mean Square Vertical Acceleration (RMSVA)

$$RMSVA = \sqrt{\frac{1}{N} \sum_{i=1}^N [a(i)]^2}$$

where $a(i)$ is the i th discrete value of filtered acceleration (which must be spatially filtered to remove any DC bias). N is the number of samples taken in the given pavement section.

Mean Absolute Slope (MAS)

MAS is the cumulative value of the absolute vertical axle or body displacement divided by the vehicle's travelled distance. Mathematically,

$$MAS = \frac{1}{2N} \left[\frac{T}{L} \right]^2 (\Delta X) \sum_{i=1}^N |Z(i)|$$

where

T = elapsed time in a test section (station), seconds;

L = station length, miles;

ΔX = sample interval of raw acceleration values;

N = $L/\Delta X$; and

$Z(i)$ = height calculated by double integrating with this equation; thus $Z(i) = Z(i-1) + a(i) + a(i-1)$.

TEXTURE

The accelerometer signal, once it passes through an A/D converter, follows one of two signal paths (see Figure 1.3). One signal path is through the high-pass filter, while the other is through the band-pass filter. The output of the high-pass filter allows more high-frequency (short wavelength) components of the input signal to pass, in the process eliminating the low-frequency signal (long wavelength) components. The high-frequency components of the acceleration signal represent the detailed characteristics of surface roughness, such as texturing and cracking. The output signals of the high-pass filter go through the same mathematical model used to calculate RMSVA. The result of the model is TEXTURE.

Serviceability Index (SI)

Software provided by HPI allowed the correlation equation for estimating the serviceability index of a test section to be changed. This equation, produced from ATS using Lotus 1-2-3, would thus change each time a correlation with the profilometer was performed. Mathematically, this equation is defined as:

$$SI = 5.6797 - 0.00134 \text{ RMSVA} - 0.7553 \text{ MAS}$$

Thus, the measured RMSVA and MAS outputs from the ARAN unit's roughness subsystem are used to estimate SI.

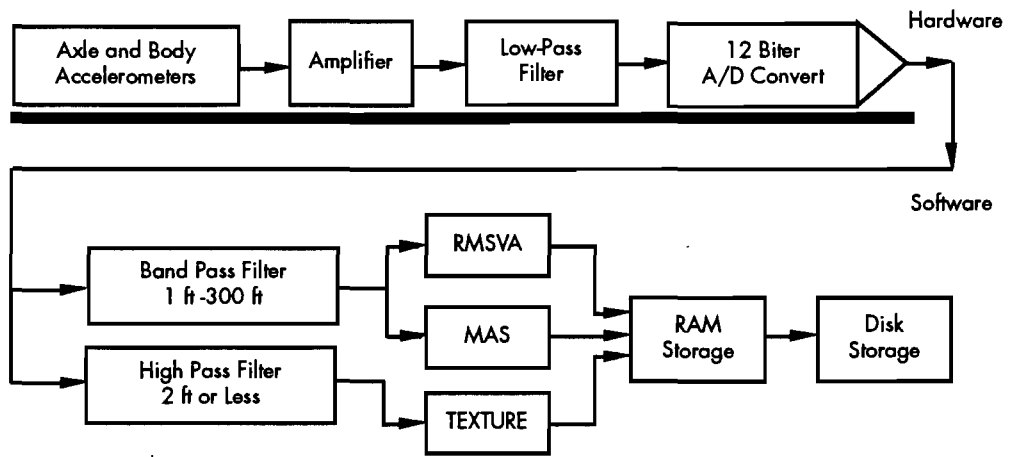


Figure 1.3 Roughness measuring subsystem

CHAPTER 2. FIELD TEST AND DATA COLLECTION

INTRODUCTION

Because most of the evaluation and modeling in this research effort were based on field testing and data collection, these activities have necessarily been assigned a higher priority. In this study the ARAN unit had to be considered a "black box"; that is, its performance had to be judged by its response (output) to a known input. The known input for the evaluation of correlativity of the roughness subsystem was the Texas SDHPT-modified K. J. Law profilometer, an instrument whose output had been verified using the FHWA HPMS Appendix J procedures (Ref 6).

TEST SITE CHOICE

In order to obtain reliable correlation for the ARAN unit, 29 test sections were chosen for the field tests. With the exception of three rigid pavement sites, all test sites were located in the Austin area. (Refer to Figures 2.1a and b for detailed map references.) Because no rigid pavements were accessible near Austin, three rigid pavement test sections near La Grange, Texas, were chosen. The data collected from the flexible and the rigid pavements were combined without consideration of the type of pavement in the study.

INSTRUMENT CHOSEN FOR CORRELATION ANALYSIS

The Texas SDHPT-modified K.J. Law profilometer, defined as a Class II pavement roughness monitoring instrument, was chosen as the standard reference instrument for correlation with the ARAN unit. From the standpoint of correlation analysis, it is better to correlate a Class III instrument with a Class I or Class II instrument. Class I and Class II instruments directly reflect the surface characteristics of a pavement, while Class III instruments reflect the response of a vehicle to, or the perception of the vehicle passengers of, the pavement surface roughness.

DESCRIPTION OF TEST PROCEDURES

The field tests were designed to consider three aspects of the ARAN roughness subsystem: (1) repeat-

ability, (2) effect of the report interval on the roughness statistics, and (3) effect of the operational speed on the roughness statistics. Several different report intervals and operational speeds were used on each test section. For each combination of speed and report interval, several repeat runs were made in order to overcome any bias caused by either environmental conditions or operator behavior, and to test the repeatability of the roughness measuring subsystem.

The ARAN unit was operated by one driver and one operator. The operator's responsibilities included signaling the computer to start acquiring data, inputting pertinent header information, setting the reference velocity and the report interval, and taking field notes, e.g., names of test sections, number of runs, and direction of travel, of each run. The driver was responsible for maintaining the correct vehicle speed and location within the travel lane. The beginning of each test section was marked so that the ARAN unit operator could start the data collection at or near the same location for each repeat run. The data were collected from October 1988 to July 1989.

REPORT INTERVAL, TESTING SPEED, AND PAVEMENT SURFACE CONDITION CONSIDERATIONS

The ARAN unit has several alternatives for the report interval. Because the most frequently used report intervals, according to SDHPT D-18 personnel, are 0.005, 0.01, 0.05, and 0.1 mile, these intervals were therefore used in evaluating the effect of the report interval on the roughness subsystem's output.

In order to evaluate the effect of the operational speed on the reported roughness statistics, different testing speeds were used. Because the response of the ARAN unit with respect to speed could be nonlinear, more than two different testing speeds had to be considered. Thus three testing speeds—30, 40, and 50 mph—were selected for use in this evaluation effort.

Three different groups of test sections were chosen to provide a range of surface roughness. These test groups included pavements with smooth surfaces (PSI = 3.5 to 5.0), pavements with medium smooth surfaces (PSI = 2.0 to 3.5), and pavements with

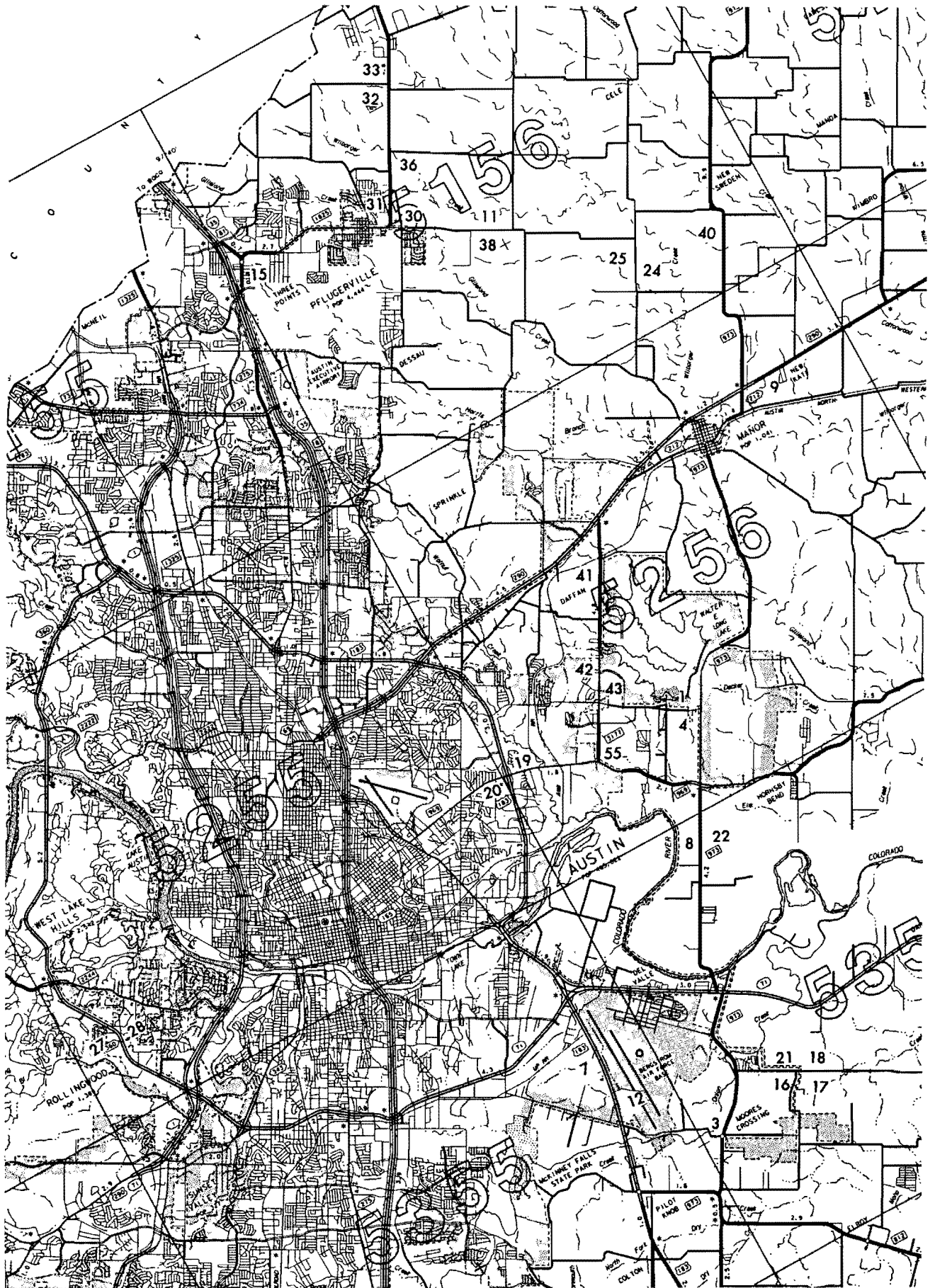


Figure 2.1(a) Map of Austin area test sites

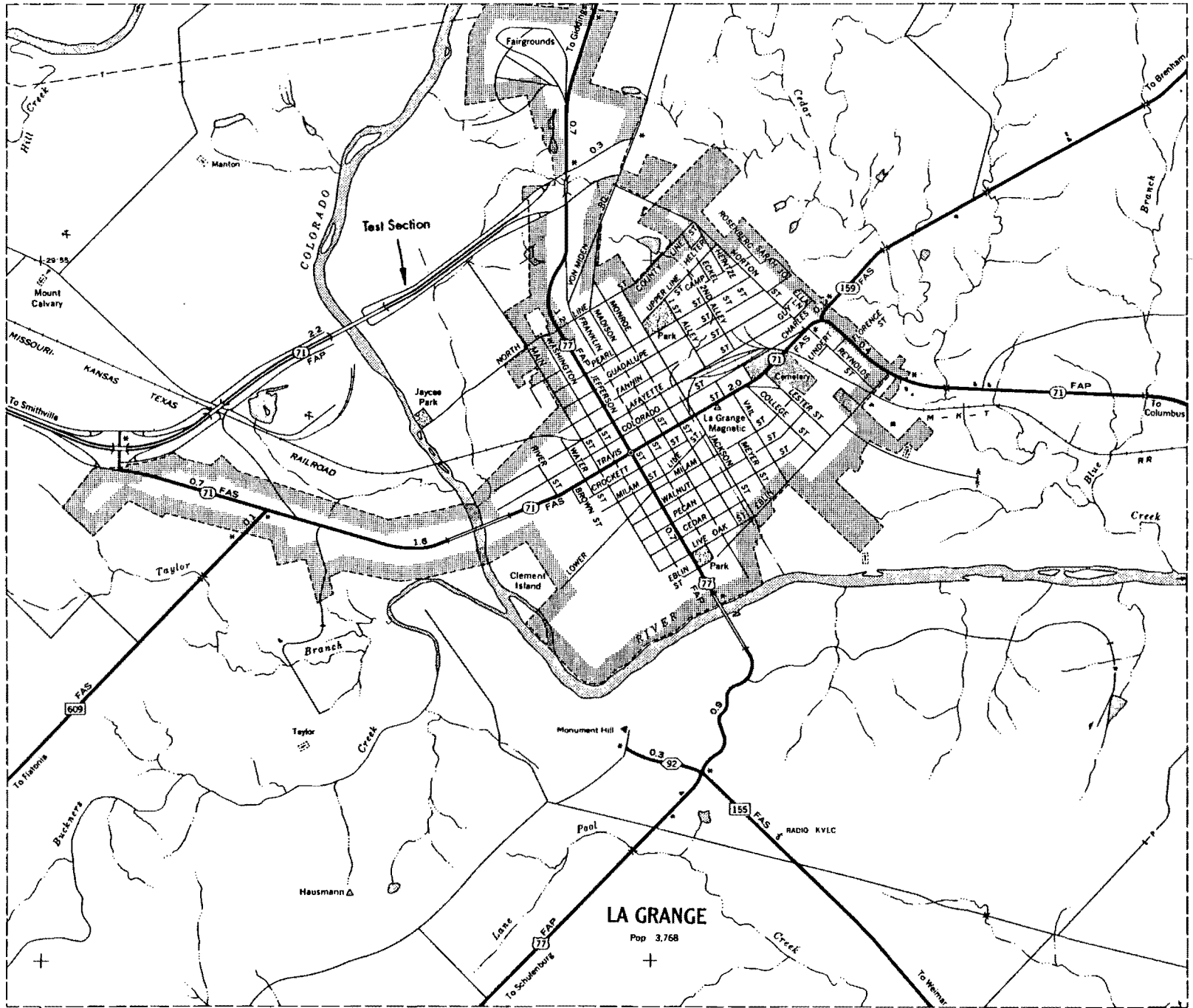


Figure 2.1(b) Map of La Grange area rigid test sites

rough surfaces (PSI = 0 to 2.0). The relative smoothnesses of these sections were ranked on the basis of the profilometer's output. The test sections chosen covered a full range of pavement conditions in terms of PSI. In addition, for each combination of the above factors, five runs were made. The factorial for the field tests is shown in Figure 2.2.

SUMMARY OF DATA COLLECTED FROM FIELD TEST

Table 2.1 shows the tabulated summary of field testing and data collection. The symbol "x" indicates that a test section was run with the instruments, the operational characteristics, and pavement conditions shown. The profilometer made five runs on each section at 20 and 50 mph. These data were then compared to the roughness statistics of the ARAN unit.

At the request of CTR personnel, the rear suspension system of the ARAN unit was modified in April 1989, following reports from SDHPT operators that driving conditions at operational speeds approaching 50 mph on rough pavements were dangerous. CTR personnel suggested the addition of extra leaf springs and heavy-duty shock absorbers. Test results showed that the response characteristics of the ARAN unit were changed by these modifications to the suspension system, and new tests had to be conducted to update the database for the analysis.

Testing Speed		30 mph	40 mph	50 mph
Report Interval (mile)				
Pavement Condition				
Smooth	.005	*		
	.01			
	.05			
	.1			
Medium	.005			
	.01			
	.05			
	.1			
Rough	.005			
	.01			
	.05			
	.1			

* Each cell represents the average of 5 runs.

Figure 2.2 Factorial for roughness field test

Table 2.1 Summary of roughness field test

Instrument				ARAN												Profilometer	
PSI				Speed (mph) and Report Interval (mile)												Speed (mph)	
Test Section	0 - 2.0 Rough	2.0 - 3.5 Middle	3.5 - 5.0 Smooth	30				40				50				20	50
				.005	.01	.05	.1	.005	.01	.05	.1	.005	.01	.05	.1		
01	x			x	x	x	x	x	x	x	x	x	x	x	x	x	x
03			x	x				x				x				x	x
04	x			x	x	x	x	x	x	x	x	x	x	x	x	x	x
07			x	x				x				x				x	x
08		x		x				x				x				x	x
09			x	x				x				x				x	x
11		x		x				x				x				x	x
12			x	x				x				x				x	x
15			x	x				x				x				x	x
16	x			x				x				x				x	x
17	x			x				x				x				x	x
18	x			x				x				x				x	x
19			x	x				x				x				x	x
20		x		x				x				x				x	x
21	x			x				x				x				x	x
22			x	x				x				x				x	x
24	x			x				x				x				x	x
25		x		x				x				x				x	x
27			x	x				x				x				x	x
28			x	x				x				x				x	x
30		x		x				x				x				x	x
31		x		x				x				x				x	x
36			x	x				x				x				x	x
38		x		x				x				x				x	x
40		x		x				x				x				x	x
41			x	x				x				x				x	x
42			x	x				x				x				x	x
43			x	x				x				x				x	x
55		x		x				x				x				x	x
LAG.3R		x		x				x				x				x	x
LAG.4L		x		x				x				x				x	x
LAG.4M		x		x				x				x				x	x

CHAPTER 3. THE EFFECT OF THE REPORT INTERVAL

INTRODUCTION

The pavement surface roughness measuring subsystem sampling interval for the raw data is 2 inches (Ref 7), i.e., the subsystem samples the acceleration data from the accelerometers every 2 inches. If a test pavement section is divided into L subsections, and in each subsection M data are sampled by the roughness measuring subsystem, then the statistical roughness outputs RMSVA, MAS, and TEXTURE are reported from these M acceleration data. In the ARAN unit, the reported statistics of each test section are the mean values of the statistical roughness outputs calculated in each subsection (L). The length of each subsection is called the result report interval, or report interval.

Several report intervals can be selected by the ARAN operator. The most frequently used report intervals are 0.005, 0.01, 0.05, and 0.1 mile, as was discussed previously. The smaller the report interval, the greater the memory space required for storing results in the ARAN unit computer, and the greater the storing frequency. Such requirements increase the risk of data loss. On the other hand, if the report interval is too large, detailed information regarding the roughness of the pavement section cannot be viewed in the output listing. Thus, the proper choice of report interval is an important factor in the pavement survey.

For this research effort it was important to determine whether the different report intervals would result in different summarized roughness output statistics for a particular pavement section. If the report interval does significantly affect the summarized roughness output, then some standard set-up will be necessary to ensure that the roughness data collected with the ARAN unit are comparable. The ARAN operator has the opportunity to select the report interval before data are collected.

POSSIBLE SOURCES OF DIFFERENCES

If different report intervals are used for a given pavement section, the corresponding outputs of the pavement surface roughness measuring subsystem

will be different. But if the impact of the report interval on these outputs is not statistically significant, the impact of the report interval can be ignored.

Why the different report intervals should result in different outputs of the roughness subsystem can be explained by either of the following:

- (1) For a given length of a pavement section and for a given testing speed, the shorter the report interval, the more times the subsystem must process data. A short report interval will result in less time for the subsystem to calculate the roughness outputs. In fact, the data processing has a higher priority in the ARAN's computer system than the data sampling. Consequently, a shorter report interval will result in a greater chance that data will be lost while the prior sampled data is being processed. Therefore, different report intervals could result in different roughness outputs.
- (2) The data sampled from a given pavement section constitute the reported data set. The data sampled from a subsection (report interval) constitute a subset of the reported data set. Because the models for calculating the roughness outputs are nonlinear (Ref 5), the reported mean values of the outputs from each subset depend on the data set and on the way in which the reported data set is divided into subsets.

METHODOLOGY USED

If the impact of the report interval on the statistical outputs of the roughness subsystem is not statistically significant, the impact can be ignored. One of the best methods of testing for statistical significance is the one-way analysis of variance, or one-way ANOVA (Ref 8). The basic concept of the one-way ANOVA can be described as follows.

In the statistical test, a statistical hypothesis (H_0) should be proposed. Then, according to a specified model, a statistical value, F value, can be calculated. The statistical test used in the one-way ANOVA is called the F-test. Two kinds of degrees of freedom (n_1 and n_2) should be given, where

$$n_1 = S - 1, n_2 = S(n - 1)$$

where S is the number of runs made at each report interval, and n is the number of alternative report intervals. A value, $F_{\alpha(n_1, n_2)}$, with a given significance level of α can be checked from an F-test table. If $F < F_{\alpha(n_1, n_2)}$, the statistical hypothesis, H_0 , should be accepted. If $F > F_{\alpha(n_1, n_2)}$, then H_0 should be rejected.

RESULTS OF THE TESTING

To test whether the report interval has a significant impact on the statistical outputs of the roughness subsystem, two rough test sections—ATS01 and ATS04—were run. These sections were chosen because they are relatively rough (PSI = 1.79 and PSI = 1.24, respectively). If the results of the one-way ANOVA test show that the report interval does not have a significant impact on the outputs of the roughness subsystem, then it might be deduced that the report interval would also have little impact on smoother pavements.

The following statistical hypothesis, H_0 , was proposed to test the significance of the report interval.

H_0 : The report interval does not have a significant impact on the outputs of the roughness subsystem.

The significance level is 5 percent, or $\alpha = 0.05$. Tables 3.1 through 3.6 show the data collected from the two test sections. The tables give the RMSVA, MAS, and TEXTURE values for the two test sites at the selected report intervals. The results from the analysis are for a given testing speed of 50 mph. Because the number of runs is four ($S = 4$) and the alternative report intervals are 0.005, 0.01, 0.05, and 0.1 mile ($n = 4$), the degrees of freedom are

$$n_1 = S - 1 = 3, n_2 = S(n - 1) = 15$$

Table identified in Ref 8, the statistical F value is calculated to be

$$F_{\alpha(n_1, n_2)} = F_{0.05(3, 15)} = 3.29$$

The results shown in Tables 3.1 through 3.6 show that all the calculated F values are smaller than the statistical F value, $F_{\alpha(n_1, n_2)}$. Therefore, it can be concluded that the hypothesis, H_0 , should be accepted. The report interval does not have a statistically significant impact on the outputs of the roughness subsystem.

SUMMARY

The results of the field test and analysis of the reported data show that all of the calculated F values are smaller than the statistical F values. It can therefore be concluded that the report interval does not have a significant impact on the ARAN unit roughness subsystem outputs.

Table 3.1 AT501-50 MPH-RMSVA

Run	Report Interval (mile)			
	.005	.01	.05	.1
1	596	610	653	638
2	599	647	637	665
3	628	631	643	668
4	653	629	630	649

Test Section: ATS01
Roughness: RMSVA
Speed: 50 mph
PSI: 1.79 (By Profilometer)
Roughness: Rough
Statistical Analysis:
Degree of Freedom: $N_1 = 3, N_2 = 15$
Significance Level: $\alpha = 0.05$
 $F_{\alpha}(N_1, N_2) = 3.29$
Hypothesis H_0 : Report interval has no significant impact on the subsystem outputs
Calculated F Value: $F = 3.08 < F_{\alpha}(N_1, N_2) = 3.29$
Conclusion: Accept H_0

Table 3.2 AT501-50 MPH-MAS

Run	Report Interval (mile)			
	.005	.01	.05	.1
1	3.29	3.24	3.71	3.36
2	3.47	3.16	3.40	3.46
3	3.48	3.13	3.30	3.70
4	3.18	3.37	3.38	3.48

Test Section: ATS01
Roughness: MAS
Speed: 50 mph
PSI: 1.79 (By Profilometer)
Roughness: Rough
Statistical Analysis:
Degree of Freedom: $N_1 = 3, N_2 = 15$
Significance Level: $\alpha = 0.05$
 $F_{\alpha}(N_1, N_2) = 3.29$
Hypothesis H_0 : Report interval has no significant impact on the subsystem outputs
Calculated F Value: $F = 2.71 < F_{\alpha}(N_1, N_2) = 3.29$
Conclusion: Accept H_0

Table 3.3 AT501-50 MPH-TEXTURE

Run	Report Interval (mile)			
	.005	.01	.05	.1
1	155	166	171	164
2	158	172	168	176
3	166	168	169	171
4	188	174	172	172

Test Section: AT501
 Roughness: TEXTURE
 Speed: 50 mph
 PSI: 1.79 (By Profilometer)
 Roughness: Rough
 Statistical Analysis:
 Degree of Freedom: $N_1 = 3, N_2 = 15$
 Significance Level: $\alpha = 0.05$
 $F_{\alpha}(N_1, N_2) = 3.29$
 Hypothesis Ho: Report interval has no significant impact on the subsystem outputs
 Calculated F Value: $F = .193 < F_{\alpha}(N_1, N_2) = 3.29$
 Conclusion: Accept Ho

Table 3.4 AT504-50 MPH-RMSVA

Run	Report Interval (mile)			
	.005	.01	.05	.1
1	755	810	792	756
2	721	774	793	750
3	722	754	782	755
4	810	714	757	786

Test Section: AT501
 Roughness: RMSVA
 Speed: 50 mph
 PSI: 1.24 (By Profilometer)
 Roughness: Rough
 Statistical Analysis:
 Degree of Freedom: $N_1 = 3, N_2 = 15$
 Significance Level: $\alpha = 0.05$
 $F_{\alpha}(N_1, N_2) = 3.29$
 Hypothesis Ho: Report interval has no significant impact on the subsystem outputs
 Calculated F Value: $F = .600 < F_{\alpha}(N_1, N_2) = 3.29$
 Conclusion: Accept Ho

Table 3.5 AT504-50 MPH-MAS

Run	Report Interval (mile)			
	.005	.01	.05	.1
1	4.48	4.53	4.49	4.35
2	4.21	4.40	4.52	4.53
3	4.22	4.36	4.52	4.56
4	4.34	4.23	4.42	4.53

Test Section: AT501
 Roughness: MAS
 Speed: 50 mph
 PSI: 1.24 (By Profilometer)
 Roughness: Rough
 Statistical Analysis:
 Degree of Freedom: $N_1 = 3, N_2 = 15$
 Significance Level: $\alpha = 0.05$
 $F_{\alpha}(N_1, N_2) = 3.29$
 Hypothesis Ho: Report interval has no significant impact on the subsystem outputs
 Calculated F Value: $F = 2.87 < F_{\alpha}(N_1, N_2) = 3.29$
 Conclusion: Accept Ho

Table 3.6 AT504-50 MPH-TEXTURE

Run	Report Interval (mile)			
	.005	.01	.05	.1
1	160	172	171	182
2	173	179	182	182
3	169	172	176	174
4	195	168	175	182

Test Section: AT501
 Roughness: TEXTURE
 Speed: 50 mph
 PSI: 1.24 (By Profilometer)
 Roughness: Rough
 Statistical Analysis:
 Degree of Freedom: $N_1 = 3, N_2 = 15$
 Significance Level: $\alpha = 0.05$
 $F_{\alpha}(N_1, N_2) = 3.29$
 Hypothesis Ho: Report interval has no significant impact on the subsystem outputs
 Calculated F Value: $F = .563 < F_{\alpha}(N_1, N_2) = 3.29$
 Conclusion: Accept Ho

CHAPTER 4. TEST OF REPEATABILITY

INTRODUCTION

The repeatability of the reported outputs of the roughness measuring subsystem is an important performance characteristic—and one worthy of investigation (Refs 9 and 10). Indeed, the quality of the roughness subsystem and its outputs is determined by its repeatability; if the roughness subsystem exhibits good repeatability, then its outputs are considered dependable.

There are two aspects of the repeatability of the roughness outputs: the systematic repeatability and the operational repeatability. The systematic repeatability reflects both the stability of the hardware systems and the accuracy of the roughness subsystem's measurement principle. The operational repeatability, on the other hand, reflects the driver's and/or the operator's behavior, as well as the environmental conditions under which the ARAN unit operates.

Under normal test conditions it is difficult to distinguish between systematic and operational repeatability by looking at the ARAN's reported outputs. The operational repeatability, normally called operator bias, is inherent to the operation of the system. If the data collected from the field tests show a good roughness output repeatability, it can be assumed that the systematic repeatability of the roughness measuring subsystem is good.

POSSIBLE INFLUENCES AFFECTING REPEATABILITIES

The systematic repeatability of the ARAN's roughness outputs may be affected by the following factors:

- (1) If the ARAN's electronic hardware is relatively sensitive to changes in temperature, then the roughness outputs collected from different runs on a given road might be different. For example, as the temperature changes, the gains of the signal amplifiers and the frequency pass bands of the filters might be changed.
- (2) The sensitivities of the axle and body accelerometers may be affected by changes in environmental temperature and humidity from run to run.

- (3) The mechanical characteristics (e.g., tire pressure, spring constants) of the suspension system of the ARAN unit are not strictly stable over time. If the differences of these characteristics are significant over time, then the roughness outputs may be significantly different.

The operational repeatability of the ARAN's roughness outputs may be affected by the following factors:

- (1) Because it is impossible for the driver to steer the ARAN unit along the exact same wheelpath and at the exact same speed on repeat runs, the operational variations could result in different roughness outputs.
- (2) Because it is unlikely that the operator of the ARAN unit will start to sample data at exactly the same pavement location during repeat runs, the consequent variation could result in differences in the roughness outputs.

TEST PROCEDURE USED

In order to test the repeatability of the roughness outputs of the ARAN unit, a number of repeat runs were made for each test section. The repeatability index used for this evaluation was

$$Re = \frac{\sqrt{\frac{1}{L} \sum_{i=1}^L (X_i - \bar{X})^2}}{\bar{X}} \quad (4)$$

where L is the number of repeat runs, X_i is the output of i th run ($i=1, 2, \dots, L$), and \bar{X} is the mean value of the X_i 's ($i=1, 2, \dots, L$). The quantity Re represents the statistical relative difference (percent) between the test runs. If Re is small, for example 5 percent, it can be said that the systematic and operational repeatability of the ARAN's roughness subsystem on a test section at a particular test speed is good.

Four test sections were selected from the Austin area: ATS01, ATS04, ATS07, and ATS12. ATS01 and ATS04 were rough sections (PSI = 1.79 and PSI = 1.24, respectively), while ATS07 and ATS12 were smooth sections (PSI = 4.53 and PSI = 4.35, respectively). It was thought that if the conclusions reached from the analysis on these four sections were the same, then the conclusions might be applicable to all pavement sections with (PSI) roughness values within this range.

The test speeds for determination of the repeatability of the roughness subsystem were 30 and 50 mph. At least six repeat runs were made at both the 30-mph and the 50-mph speeds for each test section. On some sections as many as nine repeat runs were made. The normal operational speed of the ARAN unit is between the 30-mph and 50-mph limits chosen for this evaluation. It was thought that if the conclusions from the repeatability tests at 30 and 50 mph were the same, then these conclusions could be applicable for operational speeds within this range.

RESULTS OF THE REPEATABILITY TESTING

The basic roughness outputs of the ARAN unit are RMSVA, MAS, and TEXTURE, as previously stated. The test of the operational and systematic repeatability of the ARAN roughness subsystem was based on these outputs. Table 4.1 shows the data collected in the field for each test section. The repeatability index, Re, was obtained for each test section at the 30-mph and 50-mph speeds of operation. Table 4.2 shows the resulting calculated Re values for each test section at each speed, and the mean values of Re for the RMSVA, MAS, and

TEXTURE outputs. The Re value for the output MAS on ATS07 at 30 mph is relatively high (Re = 9.257 percent). All other Re values are less than 6 percent, which indicates that the repeatability (both systematic and operational) of the roughness measuring subsystem is relatively reliable.

Figures 4.1 through 4.6 are graphic representations of the repeatabilities of RMSVA, MAS, and TEXTURE on ATS04 at 30 and 50 mph. It is believed that the differences between the repeat runs are caused mostly by driver and/or operator variations inherent in the operation of the ARAN unit.

SUMMARY

The results of the repeatability of the ARAN's roughness subsystem can be summarized as follows:

- (1) The roughness output repeatability consists of both systematic and operational repeatability. This evaluation of the repeatability of the roughness measuring subsystem is concerned only with the systematic repeatability.
- (2) The systematic repeatability is affected by the quality of the hardware system and the applicability of the roughness measurement principles. The operational repeatability is affected by the behavior of the driver and/or the operator of the ARAN unit.
- (3) The results of the field tests and the consequent analysis show that the roughness measuring subsystem has a relatively good repeatability; that is, the mean repeatability indices of RMSVA, MAS, and TEXTURE are 2.67, 4.41, and 4.09 percent, respectively.

Table 4.1 Data for repeatability test

Statistics	Run	ATS01	ATS01	ATS04	ATS04	ATS07	ATS07	ATS12	ATS12
		30 mph	50 mph						
RMSVA	1	311	584	325	728	186	322	195	303
	2	323	585	328	728	194	315	186	325
	3	318	596	327	722	190	316	188	310
	4	313	629	334	745	204	330	191	309
	5	301	610	312	749	203	309	197	305
	6	329	599	336	761	204	328	185	318
	7	321	607	358	736	-	326	-	300
	8	315	593	334	755	-	326	-	296
	9	319	624	338	721	-	-	-	-
MAS	1	3.32	3.36	3.65	4.24	1.49	1.20	1.38	1.17
	2	3.49	3.30	3.80	4.24	1.65	1.26	1.27	1.23
	3	3.39	3.29	3.76	4.22	1.25	1.20	1.25	1.25
	4	3.51	3.39	4.05	4.34	1.32	1.18	1.29	1.19
	5	3.33	3.21	3.87	4.30	1.37	1.26	1.28	1.07
	6	3.09	3.47	3.92	4.40	1.36	1.23	1.16	1.20
	7	3.58	3.13	4.02	4.31	-	1.20	-	1.17
	8	3.76	3.40	4.00	4.48	-	1.23	-	1.11
	9	3.71	3.27	3.78	4.21	-	-	-	-
TEXTURE	1	100	150	103	162	65	99	64	108
	2	100	153	107	165	60	104	65	104
	3	99	155	103	169	60	97	69	108
	4	104	162	106	172	56	91	61	103
	5	101	156	103	172	64	87	61	97
	6	107	158	103	171	60	92	67	102
	7	107	170	118	167	-	94	-	100
	8	100	168	105	160	-	92	-	99
	9	103	172	105	173	-	-	-	-

Table 4.2 Calculated Re values for each test section

Test Section and Speed	ATS01 30 mph	ATS01 50 mph	ATS04 30 mph	ATS04 50 mph	ATS07 30 mph	ATS07 50 mph	ATS12 30 mph	ATS12 50 mph
RMSVA	Re = 2.382%	Re = 2.492%	Re = 3.508%	Re = 1.881%	Re = 3.668%	Re = 2.155%	Re = 2.343%	Re = 2.891%
MAS	Re = 5.679%	Re = 2.967%	Re = 3.309%	Re = 1.984%	Re = 9.257%	Re = 2.282%	Re = 5.084%	Re = 4.742%
TEXTURE	Re = 2.840%	Re = 4.665%	Re = 4.257%	Re = 2.641%	Re = 4.878%	Re = 5.264%	Re = 4.542%	Re = 3.644%
Mean Values	Re (RMSVA) = 2.665% Re (MAS) = 4.413% Re (TEXTURE) = 4.091%							

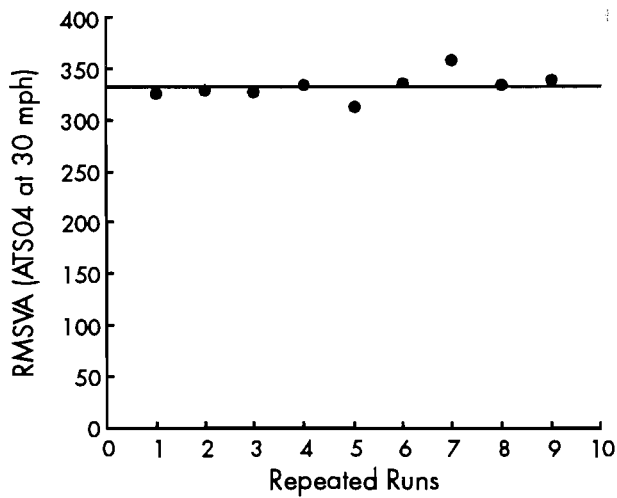


Figure 4.1 Test of repeatability for ATS04 at 30 mph – RMSVA (note: reference speed same as testing speed; the reference velocity was set in the ARAN software, with cruise control used to maintain constant velocity)

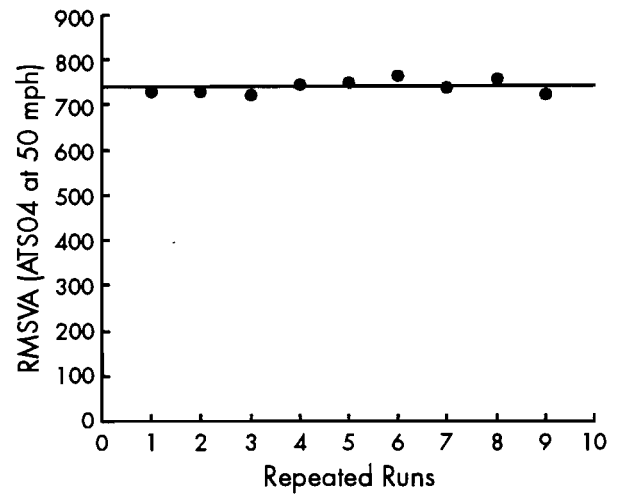


Figure 4.2 Test of repeatability for ATS04 at 50 mph – RMSVA

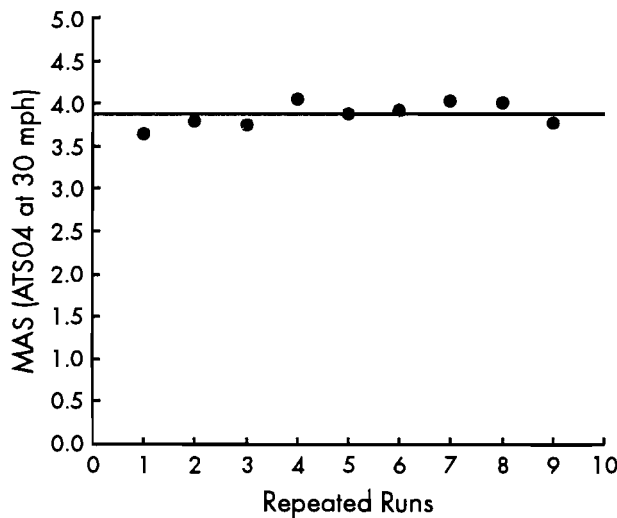


Figure 4.3 Test of repeatability for ATS04 at 30 mph – MAS

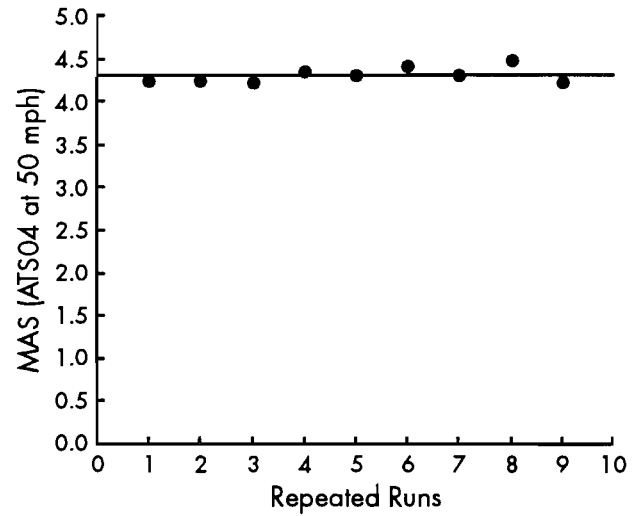


Figure 4.4 Test of repeatability for ATS04 at 50 mph – MAS

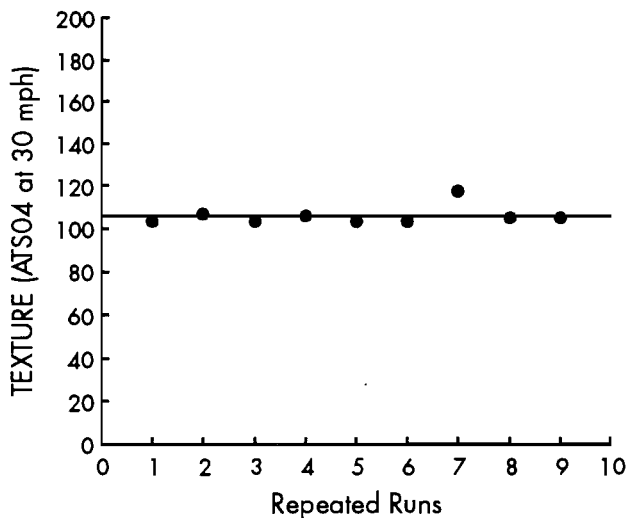


Figure 4.5 Test of repeatability for ATS04 at 30 mph – TEXTURE

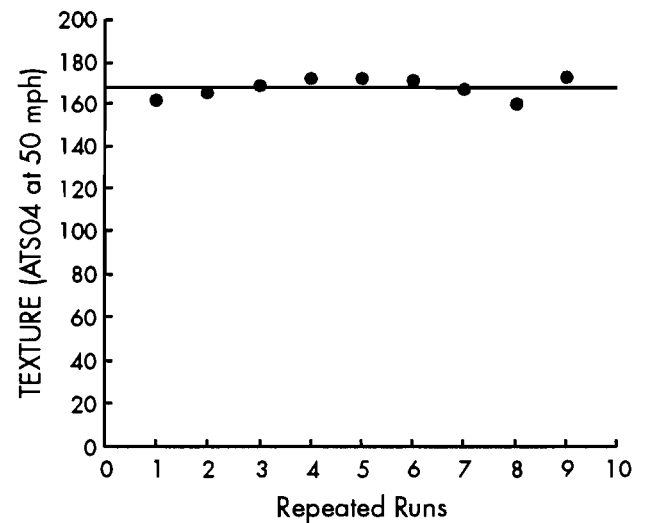


Figure 4.6 Test of repeatability for ATS04 at 50 mph – TEXTURE

CHAPTER 5. CORRELATION ANALYSIS AND ROUGHNESS CALIBRATION MODELS

INTRODUCTION

From the standpoint of instrumentation, three factors—repeatability, correlativity, and accuracy—indicate the performance of an instrument. The repeatability of an instrument can be evaluated by observing outputs on repeated runs on the same pavement surface, while the evaluation of an instrument's correlativity and accuracy must be quantified by using a standard instrument, such as that described in Ref 11. The roughness measuring subsystem of the ARAN unit, classified as a response-type road roughness measuring system, provides the statistics RMSVA, MAS, and TEXTURE, as previously described. The accuracy of these statistics could not be evaluated directly because the researchers did not have access to a reference instrument that provides the same roughness statistics as the ARAN. Accordingly, the measurement accuracy of the roughness statistics is not considered in this evaluation of the ARAN roughness subsystem. Instead, a calibration model was developed through correlation analysis with the profilometer.

This chapter evaluates the correlation between the roughness statistics from the ARAN unit and the roughness statistics generated by the Texas SDHPT modified K. J. Law profilometer. The reference statistics from the profilometer are the serviceability index (SI) (Ref 12), Maysmeter output (MO) (Refs 12 and 13), and the international roughness index (IRI) (Ref 9). The model providing RMSVA at various wavelengths from the profilometer is also available. However, since MO and SI are functions of RMSVA at the 4- and 16-foot wavelengths (Ref 13), it was considered unnecessary to use these three roughness statistics together for the correlation analysis. (It should be noted that the RMSVA of the profilometer is calculated by wavelength and the RMSVA of ARAN is based on sampling interval.)

CHOICE OF THE REFERENCE INSTRUMENT

The profilometer must meet two basic requirements before it can be used as a reference instrument for correlation. The output statistics of the reference instrument should be based on the results

of an objective measurement and should not be vehicle-dependent; if the reference instrument is vehicle-independent, the models for correlation and calibration are stable in terms of time and the vehicle's suspension system.

Two alternative approaches are available for developing the roughness statistics used in the correlation analysis and calibration of the roughness measuring subsystem of the ARAN unit. The first one is a dynamic modeling of a hypothetical device simulating the dynamic response of a vehicle with certain physical constants pre-defined. The dynamic model must have a sequence of pavement surface profiles used as the input. For example, a typical hypothetical device, called the reference quarter-car simulation (RQCS) (Ref 9), has been used as a standard reference for correlation and calibration. The corresponding statistical output of the RQCS, the quarter-car index (QI), was used for Maysmeter calibration in Brazil (Ref 9). Using RQCS makes it necessary to input the sequences of profile elevation measured by either a Class I or Class II instrument to the simulating model to develop a standard statistical output. This indirect procedure for obtaining reference standard statistical output is relatively complicated.

The second approach uses the Class II profilometric method, directly developing roughness statistics from the relatively accurate measurement of the pavement surface elevations. This method, which measures the profile elevations and directly transfers elevations into roughness statistics, is comparatively simple, with the resulting roughness statistics relatively vehicle-independent.

The modified K. J. Law profilometer—provided by the Texas SDHPT for the purpose of making comparisons in this test—has been chosen as the reference for the correlation analysis and calibration of the ARAN unit's roughness subsystem. The selection of this instrument was based on the following:

- (1) The modified K. J. Law profilometer is classified as a Class II pavement surface ride quality surveying instrument (Ref 2). This instrument automatically measures the pavement profile elevations at high operating speeds with good accuracy and repeatability.

- (2) The profilometer is equipped with the software to compute the roughness statistics RMSVA, SI, MO, and IRI. These statistics have been carefully evaluated (Ref 12) and are widely used in pavement surface ride quality surveys.
- (3) Because the profilometer belongs to the Texas SDHPT, it was therefore accessible for this evaluation effort.

It should be emphasized that, as a standard reference instrument, the profilometer should provide roughness statistics that are reliable and have good correlation with the roughness statistics of a standard Class I instrument. Fortunately, as one of the important activities of a Texas SDHPT research project conducted by CTR, several comparisons were made of roughness statistics obtained from the profilometer and the Class I Face Dipstick. The results of the comparisons showed that the roughness statistics of the profilometer had good correlations with that of the Face Dipstick (Ref 14). Consequently, the modified K. J. Law profilometer was considered an ideal standard reference instrument for this evaluation effort.

ROUGHNESS STATISTICS OF THE MODIFIED K. J. LAW PROFILOMETER

The modified K. J. Law profilometer develops the roughness statistics SI, MO, and IRI. These statistics, which summarize the pavement roughness characteristics from different approaches, are relatively vehicle-independent in principle because they are obtained through the processing of the raw profile elevations sequences. An explanation of each of these statistics follows.

Maysmeter Output (MO)

As explained in reference (Ref 12), MO is the calibrated Maysmeter output value given in Counts/0.2 miles. This Maysmeter estimate is developed using the RMSVA values calculated for the 4- and 16-foot base lengths from the profilometer, using the equation

$$MO = A1 + A2 \text{ RMSVA}_4 + A3 \text{ RMSVA}_{16} \quad (5.1)$$

where RMSVA₄ and RMSVA₁₆ are the RMSVA values of the profilometer for the 4-foot and 16-foot base lengths, respectively (Ref 12). The constants A1, A2, and A3 are different for different types of pavement (rigid or flexible).

Serviceability Index (SI)

The measure of riding quality with which engineers are most familiar is the serviceability index (SI). Representing the user's perception of pavement roughness, SI is given as a number between 0 and 5. Such a unitless index can be developed based on

MO or RMSVA. The model for calculating SI in the profilometer is (Ref 13):

$$SI = 5e^{-\left[\frac{\ln(32MO)}{8.4933}\right]^{9.3566}} \quad (5.2)$$

where MO is calculated by Equation 5.1. The index SI is a measure of roughness primarily in the 8- to 35-foot wavelength range (Ref 13).

International Roughness Index (IRI)

International roughness index (IRI) (Ref 9) is a well-known measure of roughness. IRI is reported in "inches/mile," as measured with a Class I or Class II instrument or as computed with a quarter-car simulation. IRI values from the profilometer are calculated from the profiles for both the left wheelpath and the right wheelpath. The reported IRI in this report is the mean value of the left wheelpath IRI and the right wheelpath IRI.

FIELD TESTS

It was necessary to conduct field experiments to verify whether adequate correlations with the Texas reference, the modified K. J. Law profilometer, were being achieved. It was also appropriate to determine the Texas SDHPT performance boundaries of the ARAN roughness subsystem in terms of testing speeds, pavement types, roughness levels, and report intervals.

In order to obtain the correlation and calibration models for the roughness measuring subsystem of the ARAN unit, 29 test sections were selected. These sections consisted of both rigid and flexible pavements and were evaluated with both the modified K. J. Law profilometer and the ARAN unit. The locations of the 26 flexible test sites are shown in Figure 2.1b. These sections, located in the Austin area, are designated "Austin Test Section," using ATS followed by a number. Three rigid pavement test sections located in La Grange are shown in Figure 2.1a, and are designated "LaG." These rigid pavement test sections were selected because of the scarcity of rigid pavements around the Austin area. This rigid pavement was newly constructed CRCP and had not yet been opened to the public at the time field tests were conducted. The models developed for this research are based on the combined data collected from both the flexible and the rigid pavement test sections.

The test sites were selected because they could provide the broadest range of roughness levels and could be safely run at the 50-mph test speed. The smooth sites were needed to ensure that the subsystem had the resolution necessary to measure smooth pavements correctly, while the rough sites ensured that the subsystem could handle the large

amplitudes generated when traveling down rough pavement. The medium sections allowed data points to be located between the two extremes.

The following test factors, which were discussed and approved by Texas SDHPT D-18 personnel familiar with the normal operation of the instrument, were considered during the field testing of the modified K. J. Law profilometer and the ARAN unit.

Test Consideration of the Modified K. J. Law Profilometer

- (1) *Testing Speed.* The most frequently used operational speeds of the profilometer are 20 and 50 mph. Therefore, each test section was run at the testing speeds of 20 and 50 mph.
- (2) *Number of Repeat Runs.* Three repeat runs were made for each test section and testing speed. The mean values of the reported roughness statistics were calculated and used as the summarized statistic. This was done to cancel the operational bias.
- (3) *Raw Data Reporting Interval.* The raw data reporting interval of the profilometer is set at 6 inches. The summary statistics are reported for the entire length of a test run.

Test Considerations of the ARAN Unit

- (1) *Testing Speed.* The ARAN unit is designed for operation in the normal traffic speed range. The field tests were conducted at speeds of 30, 40, and 50 mph for each test section.
- (2) *Number of Runs.* Three repeat runs were made at each test speed on each test section. The mean values of the repeat runs were calculated and taken as the summary statistic.
- (3) *Report Interval.* The factor of report interval does not have a statistically significant effect on the roughness statistics, as stated in Chapter 3. Therefore, it was not critical to choose a specific report interval for the correlation analysis and calibration. The report interval of 0.005 mile was chosen for every test because as much data as possible per test run was desired.
- (4) *Raw Data Sampling Interval.* The raw data sampling interval is not adjustable in the ARAN unit. The data summary interval of the roughness measuring subsystem is 6 inches.

RESULTS

Tables A.1 and A.2 (Appendix A) show the roughness statistics collected from the field tests using the ARAN unit and the modified K. J. Law profilometer, respectively. These test sections are divided into three roughness-level groups, as previously mentioned. This wide roughness distribution, shown in Table 2.1, makes the correlation analysis results suitable across the wide roughness levels that are normally found in the Texas highway network.

The linear model proposed for the research evaluation effort is

$$\text{Roughness (Prof)} = A + B \text{ Roughness (ARAN)} \quad (5.3)$$

where A and B are constants, and Roughness (Prof) is the estimation of the roughness statistic corresponding to one of the profilometer outputs – SI, MO, or IRI. Roughness (ARAN) is the roughness statistic (RMSVA, MAS, and TEXTURE) measured and generated by the ARAN unit. Two statistical indices showing the correlativity of the two instruments are used. One is the R² value and the other is the root mean square error (RMSE), defined by

$$\text{RMSE} = \sqrt{\frac{1}{N} \sum_{i=1}^N (x_i - y_i)^2} \quad (5.4)$$

where N is the number of test sections (N = 29), x_i is the estimation of the roughness statistic of the profilometer at ith test section, and y_i is the roughness statistic measured by the ARAN unit at ith test section. Figures 5.1 through 5.12 show the correlations between the roughness statistics of the ARAN unit at 50 mph and the modified K. J. Law profilometer at 20 mph. These figures show typical correlations between the data reported by the two instruments. The comprehensive correlation analysis results are shown in Table 5.1.

CONCLUSIONS

- (1) Different testing speeds of the ARAN unit result in different correlation models in terms of parameters A and B, as can be seen from Table 5.1. This indicates that the testing speed has a direct impact on the roughness statistics measured and reported by the ARAN unit.
- (2) The roughness indices MAS and SI from the ARAN unit correlate well with the roughness statistics obtained from the modified K. J. Law profilometer.
- (3) Table 5.2 lists the correlativity level in terms of the R² values, from the best to the worst. From this table, it can be concluded that the correlation between the ARAN unit and the profilometer, from the best to the worst, is as follows: MAS, SI, RMSVA, and TEXTURE.
- (4) TEXTURE and RMSVA have relatively poor correlation with the roughness statistics from the profilometer. This can be explained as follows:
 - (a) The statistic TEXTURE is sensitive to roughness with short wavelengths (e.g., 1 to 2 feet) because one band-pass filter is used, as described in Chapter 1. The statistics MO, IRI, and SI from the profilometer are sensitive to roughnesses with longer wavelengths.

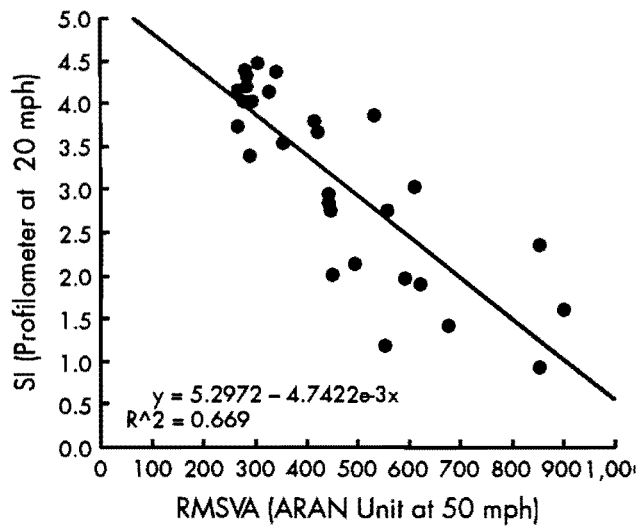


Figure 5.1 Correlation between RMSVA of the ARAN unit at 50 mph and SI of the profilometer at 20 mph

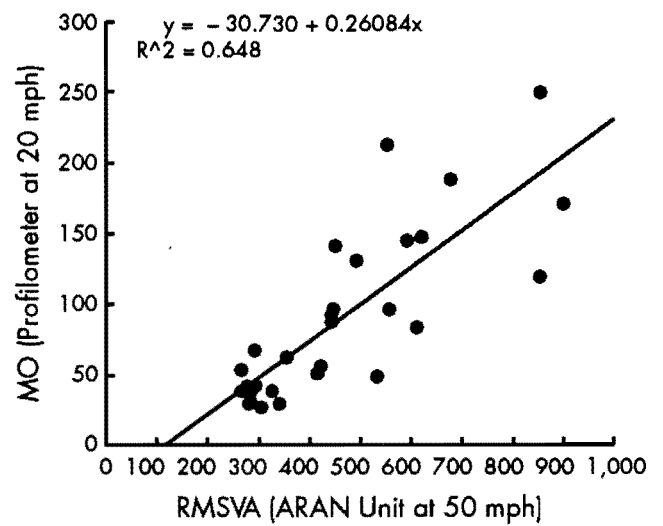


Figure 5.2 Correlation between RMSVA of the ARAN unit at 50 mph and MO of the profilometer at 20 mph

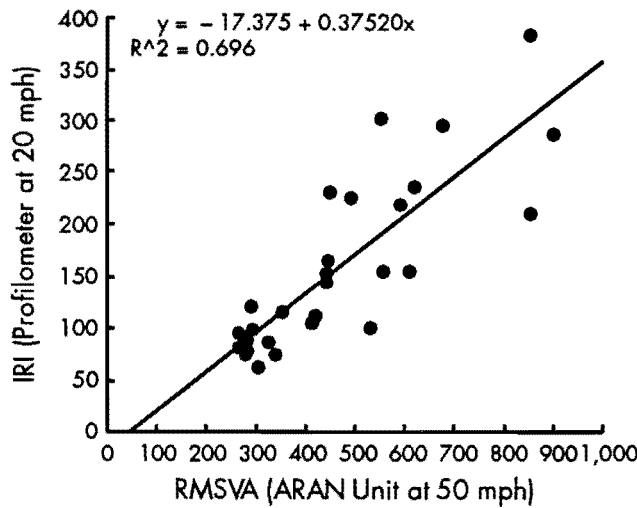


Figure 5.3 Correlation between RMSVA of the ARAN unit at 50 mph and IRI of the profilometer at 20 mph

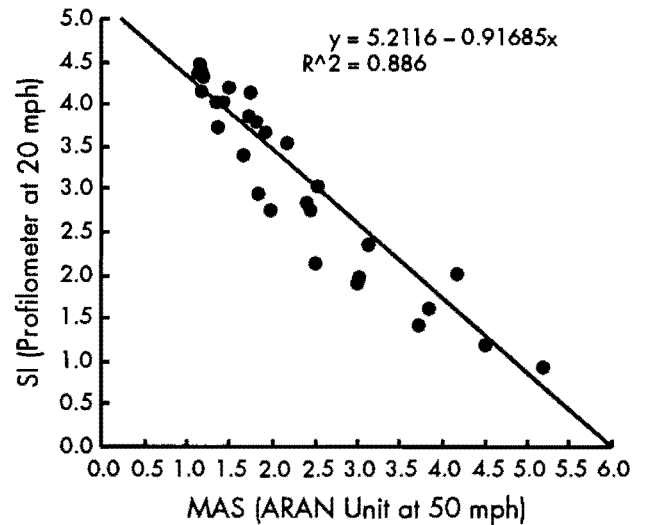


Figure 5.4 Correlation between MAS of the ARAN unit at 50 mph and SI of the profilometer at 20 mph

(b) The base length for calculating RMSVA from the ARAN unit is 2 inches (Ref 7), and the base lengths for calculating MO from the profilometer are 4 and 16 feet (see Eq 5.1). Therefore, MO is more sensitive to roughnesses with longer wavelengths than is the RMSVA from the ARAN unit. IRI from the profilometer is a statistic of accumulated slope which is sensitive to roughness with longer

wavelengths. It is reasonable then that ARAN RMSVA has relatively poor correlation with the roughness statistics from the profilometer.

(c) MAS is calculated by a model similar to that of IRI (Refs 5 and 9). MAS is generally more sensitive to longer surface wavelengths than is ARAN RMSVA. Therefore, MAS has relatively good

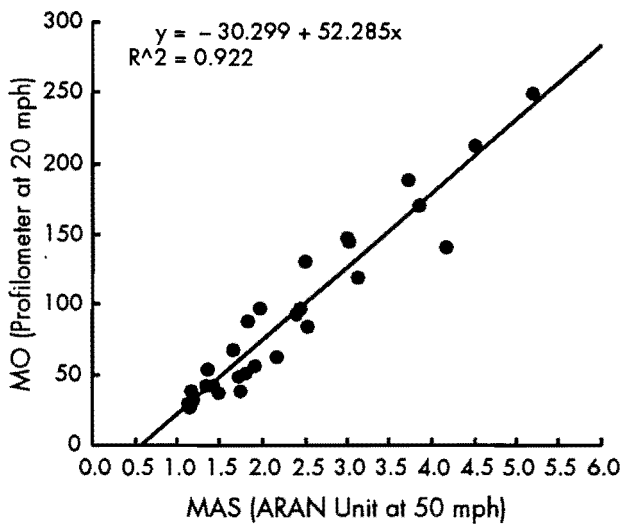


Figure 5.5 Correlation between MAS of the ARAN unit at 50 mph and MO of the profilometer at 20 mph

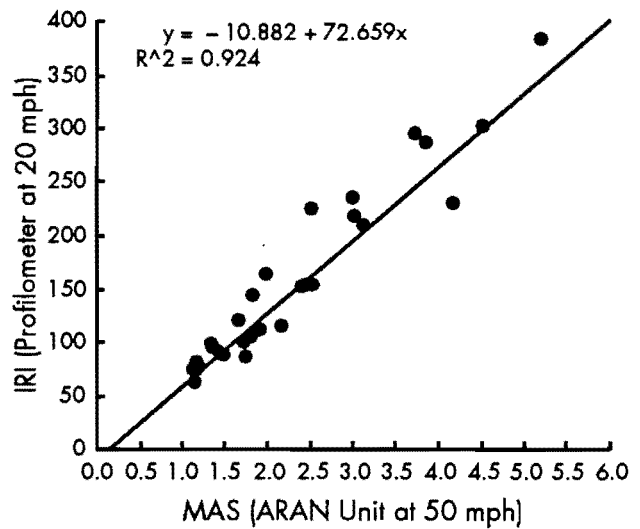


Figure 5.6 Correlation between MAS of the ARAN unit at 50 mph and IRI of the profilometer at 20 mph

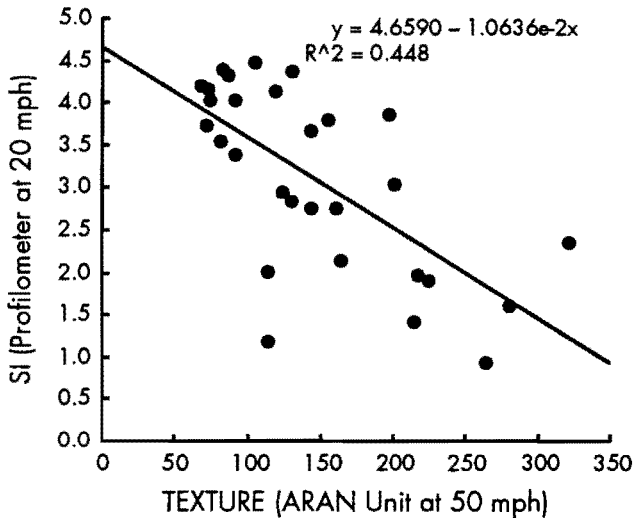


Figure 5.7 Correlation between TEXTURE of the ARAN unit at 50 mph and SI of the profilometer at 20 mph

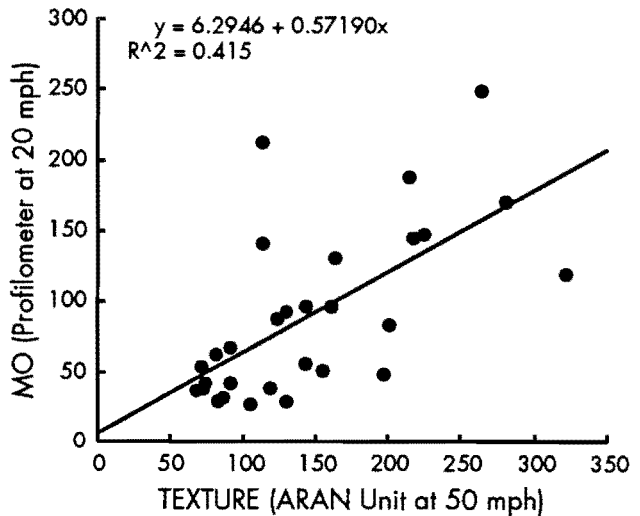


Figure 5.8 Correlation between TEXTURE of the ARAN unit at 50 mph and IRI of the profilometer at 20 mph

correlation with the roughness statistics from the profilometer.

- (5) After the ARAN unit is put into use for a period of time, the suspension system characteristics of the unit will change. In this case, updated correlation models should be determined.
- (6) The correlation models developed from these field tests are speed-dependent. If no speed-

effect-cancelling model is implemented, the correlation models should be used only for a given operation speed.

- (7) In order to estimate the roughness statistics corresponding to those of the profilometer, it is recommended that MAS or SI be used, because they both have relatively good correlation with the roughness statistics from the profilometer.

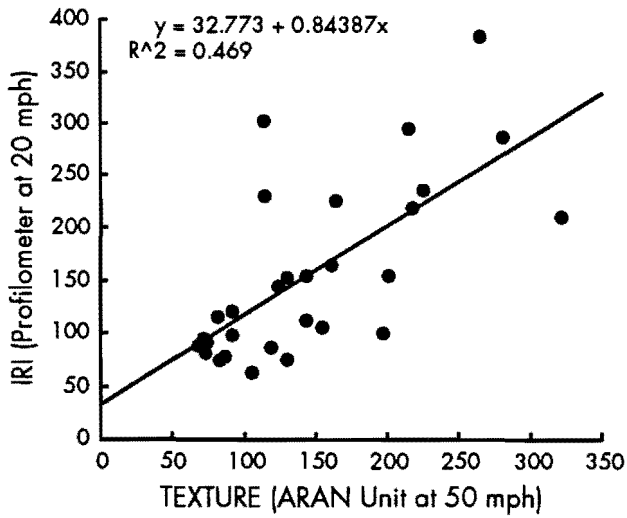


Figure 5.9 Correlation between TEXTURE of the ARAN unit at 50 mph and IRI of the profilometer at 20 mph

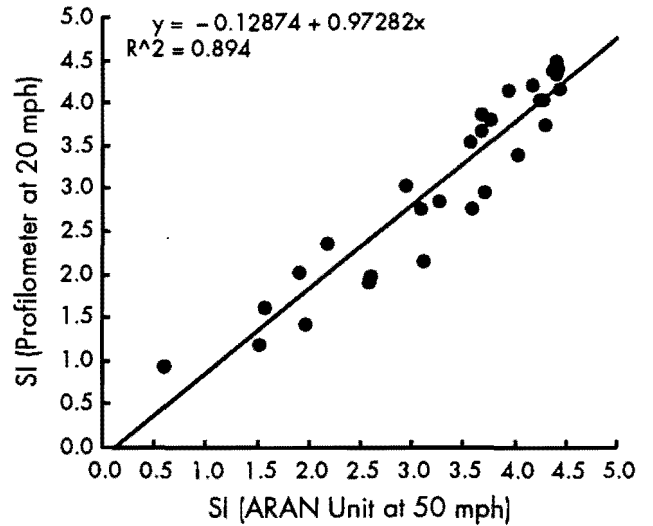


Figure 5.10 Correlation between SI of the ARAN unit at 50 mph and SI of the profilometer at 20 mph

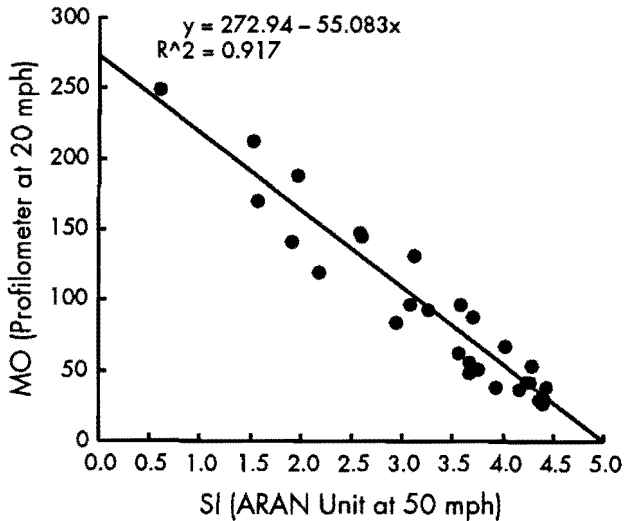


Figure 5.11 Correlation between SI of the ARAN unit at 50 mph and MO of the profilometer at 20 mph (NOTE: $SI = 5.6797 - 0.00134 MAS$, as described in Chapter 1 of this report)

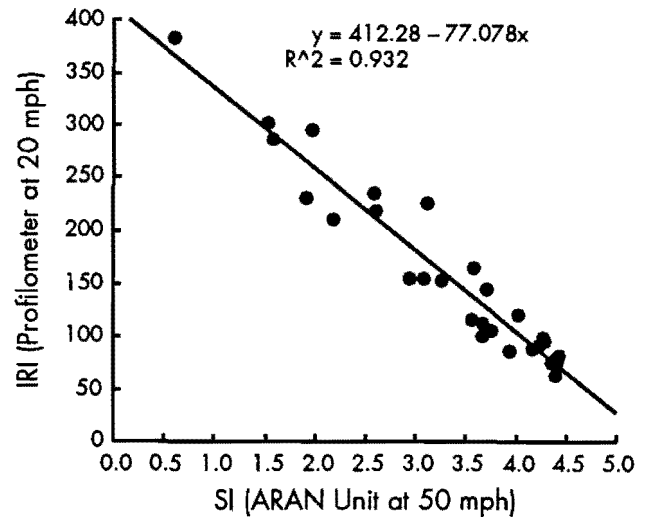


Figure 5.12 Correlation between SI of the ARAN unit at 50 mph and IRI of the profilometer at 20 mph

Table 5.1 Summary of correlation analysis of roughness statistics for ARAN versus the profilometer

		Profilometer						
		SI		MO (counts / .2 mi)		IRI (in. / mi)		
		20 mph	50 mph	20 mph	50 mph	20 mph	50 mph	
ARAN	RMSVA (mg)	30 mph	A = 4.9065 B = - 7.0212E-3 R ² = 0.521 RMSE = 0.763	A = 4.9190 B = - 7.3044E-3 R ² = 0.514 RMSE = 0.778	A = - 4.8636 B = 0.36917 R ² = 0.461 RMSE = 43.64	A = - 6.5906 B = 0.39226 R ² = 0.436 RMSE = 48.76	A = 18.688 B = 0.53548 R ² = 0.504 RMSE = 58.13	A = 19.625 B = 0.56516 R ² = 0.455 RMSE = 67.72
		40 mph	A = 5.1249 B = - 5.5126E-3 R ² = 0.577 RMSE = 0.692	A = 5.1435 B = - 5.7276E-3 R ² = 0.568 RMSE = 0.733	A = - 18.579 B = 0.29593 R ² = 0.533 RMSE = 40.64	A = - 21.563 B = 0.31553 R ² = 0.508 RMSE = 45.58	A = - 1.3517 B = 0.42964 R ² = 0.583 RMSE = 53.30	A = - 2.8514 B = 0.45707 R ² = 0.534 RMSE = 62.57
		50 mph	A = 5.2972 B = - 4.7422E-3 R ² = 0.669 RMSE = 0.612	A = 5.3222 B = - 4.9264E-3 R ² = 0.657 RMSE = 0.653	A = - 30.730 B = 0.26084 R ² = 0.648 RMSE = 35.27	A = - 35.607 B = 0.28046 R ² = 0.628 RMSE = 39.62	A = - 17.375 B = 0.37520 R ² = 0.696 RMSE = 45.50	A = - 21.563 B = 0.40275 R ² = 0.650 RMSE = 54.27
	MAS (slope * 1,000)	30 mph	A = 5.4152 B = - 0.94085 R ² = 0.900 RMSE = 0.337	A = 5.4761 B = - 0.99013 R ² = 0.907 RMSE = 0.339	A = - 42.140 B = 53.749 R ² = 0.940 RMSE = 14.52	A = - 50.653 B = 58.922 R ² = 0.947 RMSE = 14.95	A = - 27.190 B = 74.634 R ² = 0.941 RMSE = 20.23	A = - 39.584 B = 83.156 R ² = 0.946 RMSE = 21.23
		40 mph	A = 5.3098 B = - 0.93483 R ² = 0.891 RMSE = 0.351	A = 5.3698 B = - 0.98577 R ² = 0.902 RMSE = 0.349	A = - 35.778 B = 53.261 R ² = 0.926 RMSE = 16.16	A = - 44.199 B = 58.607 R ² = 0.940 RMSE = 15.94	A = - 18.783 B = 74.136 R ² = 0.931 RMSE = 21.61	A = - 30.764 B = 82.833 R ² = 0.942 RMSE = 22.10
		50 mph	A = 5.2116 B = - 0.91685 R ² = 0.886 RMSE = 0.360	A = 5.2686 B = - 0.96777 R ² = 0.899 RMSE = 0.355	A = - 30.299 B = 52.285 R ² = 0.922 RMSE = 16.58	A = - 38.338 B = 57.606 R ² = 0.938 RMSE = 16.16	A = - 10.882 B = 72.659 R ² = 0.924 RMSE = 22.69	A = - 22.322 B = 81.351 R ² = 0.939 RMSE = 22.70

Modal: Index (prof) = A+B Index (ARAN)

Table 5.1 (continued)

		Profilometer						
		SI		MO (counts / .2 mi)		IRI (in. / mi)		
		20 mph	50 mph	20 mph	50 mph	20 mph	50 mph	
ARAN	RMSVA (mg)	30 mph	A = 4.5438 B = -1.5897E-2 R ² = 0.451 RMSE = 0.788	A = 4.5362 B = -1.6478E-2 R ² = 0.442 RMSE = 0.833	A = 13.589 B = 0.84265 R ² = 0.406 RMSE = 45.83	A = 12.638 B = 0.89953 R ² = 0.388 RMSE = 50.82	A = 44.024 B = 1.2380 R ² = 0.455 RMSE = 60.93	A = 46.320 B = 1.3071 R ² = 0.411 RMSE = 70.38
		40 mph	A = 4.6382 B = -1.4275E-2 R ² = 0.478 RMSE = 0.769	A = 4.6233 B = -1.4697E-2 R ² = 0.462 RMSE = 0.818	A = 7.2714 B = 0.76888 R ² = 0.444 RMSE = 44.33	A = 6.2754 B = 0.81724 R ² = 0.421 RMSE = 49.44	A = 34.423 B = 1.1326 R ² = 0.500 RMSE = 58.34	A = 35.684 B = 1.2005 R ² = 0.455 RMSE = 67.68
		50 mph	A = 4.6590 B = -1.0636E-2 R ² = 0.448 RMSE = 0.791	A = 4.6434 B = -1.0942E-2 R ² = 0.432 RMSE = 0.841	A = 6.2946 B = 0.57190 R ² = 0.415 RMSE = 45.49	A = 5.0451 B = 0.60918 R ² = 0.394 RMSE = 50.55	A = 32.773 B = 0.84387 R ² = 0.469 RMSE = 60.16	A = 34.498 B = 0.89060 R ² = 0.432 RMSE = 69.66
	MAS (slope * 1,000)	30 mph	A = -0.71964 B = 1.0990 R ² = 0.903 RMSE = 0.332	A = -0.97400 B = 1.1548 R ² = 0.908 RMSE = 0.339	A = 306.27 B = -62.191 R ² = 0.926 RMSE = 16.21	A = 330.45 B = -67.935 R ² = 0.926 RMSE = 17.72	A = 458.10 B = -86.789 R ² = 0.936 RMSE = 20.93	A = 499.04 B = -96.100 R ² = 0.929 RMSE = 24.38
		40 mph	A = -0.42014 B = 1.0348 R ² = 0.890 RMSE = 0.352	A = -0.66333 B = 1.0886 R ² = 0.897 RMSE = 0.358	A = 288.76 B = -58.394 R ² = 0.908 RMSE = 18.05	A = 311.86 B = -63.943 R ² = 0.912 RMSE = 19.24	A = 434.79 B = -81.820 R ² = 0.925 RMSE = 22.58	A = 473.62 B = -90.713 R ² = 0.921 RMSE = 25.74
		50 mph	A = -0.12874 B = 0.97282 R ² = 0.894 RMSE = 0.347	A = -0.35743 B = 1.0235 R ² = 0.901 RMSE = 0.351	A = 272.94 B = -55.083 R ² = 0.917 RMSE = 17.09	A = 294.79 B = -60.398 R ² = 0.924 RMSE = 17.88	A = 412.28 B = -77.078 R ² = 0.932 RMSE = 21.47	A = 449.05 B = -85.571 R ² = 0.931 RMSE = 24.11

Modal: Index (prof) = A+B Index (ARAN)

Table 5.2 Correlativity level of the correlation analysis

Correlation Pair			Correlativity Level	
ARAN Output	Speed (mph)	Profilometer Output	Speed (mph)	R ²
MAS	30	MO	50	0.947
MAS	30	IRI	50	0.946
MAS	40	IRI	50	0.942
MAS	30	IRI	20	0.941
MAS	30	MO	20	0.940
MAS	40	MO	50	0.940
MAS	50	IRI	50	0.939
MAS	50	MO	50	0.938
SI	30	IRI	20	0.936
SI	50	IRI	20	0.932
MAS	40	IRI	20	0.931
SI	50	IRI	50	0.931
SI	30	IRI	50	0.929
MAS	40	MO	20	0.926
SI	30	MO	50	0.926
SI	30	MO	20	0.926
SI	40	IRI	20	0.925
MAS	50	IRI	20	0.924
SI	50	MO	50	0.924
MAS	50	MO	20	0.922
SI	40	IRI	50	0.921
SI	50	MO	20	0.917
SI	40	MO	50	0.912
SI	40	MO	20	0.908
SI	30	SI	50	0.908
MAS	30	SI	50	0.907
SI	30	SI	20	0.903
MAS	40	SI	50	0.902
SI	50	SI	50	0.901
MAS	30	SI	20	0.900
MAS	50	SI	50	0.899
SI	40	SI	50	0.897
SI	50	SI	20	0.894
MAS	40	SI	20	0.891
SI	40	SI	20	0.890
MAS	50	SI	20	0.886

Table 5.2 (continued)

Correlation Pair			Correlativity Level	
ARAN Output	Speed (mph)	Profilometer Output	Speed (mph)	R ²
RMSVA	50	IRI	20	0.696
RMSVA	50	SI	20	0.669
RMSVA	50	SI	50	0.657
RMSVA	50	MO	20	0.648
RMSVA	50	MO	50	0.628
RMSVA	50	IRI	50	0.588
RMSVA	40	IRI	20	0.583
RMSVA	40	SI	20	0.577
RMSVA	40	SI	50	0.568
RMSVA	40	IRI	50	0.534
RMSVA	40	MO	20	0.533
RMSVA	30	SI	20	0.521
RMSVA	30	SI	50	0.514
RMSVA	40	MO	50	0.508
RMSVA	30	IRI	20	0.504
TEXTURE	40	IRI	20	0.500
TEXTURE	40	SI	20	0.478
TEXTURE	50	IRI	20	0.469
TEXTURE	40	SI	50	0.462
RMSVA	30	MO	20	0.461
RMSVA	30	IRI	50	0.455
TEXTURE	40	IRI	50	0.455
TEXTURE	30	IRI	20	0.455
TEXTURE	30	SI	20	0.451
TEXTURE	50	SI	20	0.448
TEXTURE	40	MO	20	0.444
TEXTURE	30	SI	50	0.442
RMSVA	30	MO	50	0.436
TEXTURE	50	IRI	50	0.432
TEXTURE	50	SI	50	0.432
TEXTURE	40	MO	50	0.421
TEXTURE	50	MO	20	0.415
TEXTURE	30	IRI	50	0.411
TEXTURE	30	MO	20	0.406
TEXTURE	50	MO	50	0.394
TEXTURE	30	MO	50	0.388

CHAPTER 6. NEW PSI MODEL FOR THE ARAN UNIT

INTRODUCTION

HPI, the manufacturer of the ARAN unit, provided software for changing the correlation equation, which was then created by running ATS and performing a correlation with the serviceability index (SI) from the profilometer. This equation is:

$$SI = 5.6797 - 0.00134 \text{ RMSVA} - 0.7553 \text{ MAS} \quad (6.1)$$

Because the modified K. J. Law profilometer is considered by the Texas SDHPT to be the reference instrument for calibration of all its roughness monitoring equipment, it was necessary that the SI model obtained from the ARAN unit be directly calibrated to the SI from the profilometer.

In addition, it can be expected that the operational speeds of the ARAN unit will significantly affect its roughness statistics (this is addressed in Chapter 5 and discussed further in Chapter 7). The model estimating SI values should be used for a given operational speed.

Because of these disadvantages a new present serviceability index (PSI) model including TEXTURE was proposed by CTR staff. This new model is

$$PSI = A + B \text{ RMSVA} + C \text{ MAS} + D \text{ TEXTURE} \quad (6.2)$$

where A, B, C, and D are constant coefficients. These constant coefficients were obtained through a linear regression analysis of the ARAN unit's roughness output and that of the modified K. J. Law profilometer. Therefore, the PSI value resulting from this model is an estimate of the PSI values corresponding to the profilometer. According to the definitions of RMSVA, MAS, and TEXTURE, these variables are independent of each other. Conceptually, the more independent variables the model includes, the better the model will be.

Because the correlation analysis in Chapter 5 showed that TEXTURE had little correlation with the output of the profilometer, another model was generated. This model excludes the TEXTURE statistic and has the following form:

$$PSI = A + B \text{ RMSVA} + C \text{ MAS} \quad (6.3)$$

It should be noted that this new PSI model has the same form as the original SI model. The new model has the advantage of being obtained through the regression analysis of the ARAN unit and the modified K. J. Law profilometer. The data were collected in Texas.

		Profilometer	
		20 mph	50 mph
ARAN	30 mph	Model 1	Model 2
	40 mph	Model 3	Model 4
	50 mph	Model 5	Model 6

Figure 6.1 PSI modeling factorial

NEW PSI MODEL INCLUDING TEXTURE

The standard testing speeds used while conducting the field tests were presented in Chapter 5. The factorial used in the modeling of the new PSI is shown in Figure 6.1. The data collected by the ARAN unit and the profilometer during the field tests are shown in Tables A.1 and A.2, respectively. A FORTRAN program (MULT REGRESSION), developed by the CTR staff and included in Appendix D, was used to process the data in Tables A.1 and A.2. The resulting models correspond to the regression models seen in Figure 6.1.

Table 6.1 has the form of Equation 6.2 and represents the models from Figure 6.1. The R^2 values of the linear fits are also included in the table.

The sensitivities of PSI to each roughness statistic can be compared in terms of the absolute value level of each coefficient. In the resulting models, the absolute value level of coefficient C is much higher than that of either B or D. Coefficients B and D are at the same relative level. Because coefficient C was defined for MAS it can be said that PSI is more sensitive to MAS than to either RMSVA or TEXTURE. In fact, the analysis results in Chapter 5 show that the R^2 values for MAS are much higher than those

Table 6.1 Models from Eq 6.2 as defined

Model	Coefficients				R ² Value
	A	B	C	D	
1	5.4898	-0.001007	-0.873430	0.000206	0.904
2	5.5465	-0.001126	-0.930580	0.000801	9.915
3	5.4323	-0.001702	-0.855272	0.002919	0.896
4	5.4979	-0.002143	-0.917207	0.004613	0.907
5	5.3507	-0.000795	-0.795375	-0.000344	0.895
6	5.3837	-0.000722	-0.865102	-0.000118	0.904

for either RMSVA or TEXTURE. This means that the correlation of MAS with the profilometer SI is better than that of RMSVA or TEXTURE.

Greater RMSVA or MAS values for the ARAN unit represent poorer serviceability or smaller PSI values. Mathematically, this relationship requires that the signs of coefficients B and C be negative. Because TEXTURE reflects only the detail (short wavelength) characteristics of a pavement surface, it does not have an obvious direct relationship with PSI. Therefore, the sign of the coefficient of TEXTURE could be either positive or negative. From the resulting equations, shown in Table 6.1, it can be seen that the signs for coefficients B and C are negative. Coefficient D is both positive and negative.

Table 6.2 R² values of correlation between the new PSI including TEXTURE (ARAN) and SI (profilometer)

		Profilometer	
		20 mph	50 mph
ARAN	30 mph	0.904	0.915
	40 mph	0.896	0.907
	50 mph	0.895	0.904

Table 6.3 R² values of correlation between the original SI (ARAN) and SI (profilometer)

		Profilometer	
		20 mph	50 mph
ARAN	30 mph	0.903	0.908
	40 mph	0.890	0.897
	50 mph	0.894	0.901

A comparison can be made between the new PSI model including TEXTURE and the original SI equation by considering the R² values resulting from the correlation analysis. The R² values resulting from the new PSI equation are listed in Table 6.2 and correspond to the factorial shown in Figure 6.1. The R² values of the correlation between original SI for the ARAN unit and SI from the profilometer are shown in Table 6.3. All of the R² values from the new PSI equation are greater than those from the original SI

equation. It can be concluded that, because of changes in the characteristics of the ARAN van, the new PSI equation fits the profilometer output better than the original SI equation.

The correlations of the new PSI equations using TEXTURE from the ARAN unit and the SI from the profilometer at different speeds are presented in Figures 6.2 to 6.7. The equation for these correlations is

$$SI(Prof) = a + b PSI(ARAN) \quad (6.4)$$

From these figures and the resulting linear equations, it can be seen that

$$a \approx 0, \quad b = 1.$$

Therefore, the six new PSI models including TEXTURE that correspond to the different speed of operations can be used effectively to estimate the SI values from the profilometer.

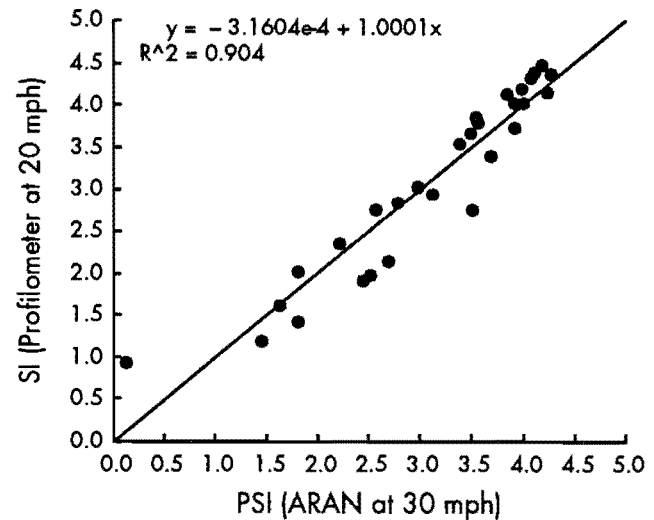


Figure 6.2 Correlation of new PSI with TEXTURE (ARAN) at 30 mph vs. SI (PROF) at 20 mph

PSI EQUATION EXCLUDING TEXTURE

The second set of PSI equations does not include TEXTURE. These equations have the same form as the PSI model shown in Eq 6.3. The factorial for equations omitting TEXTURE is the same as for equations that include TEXTURE (Figure 6.1).

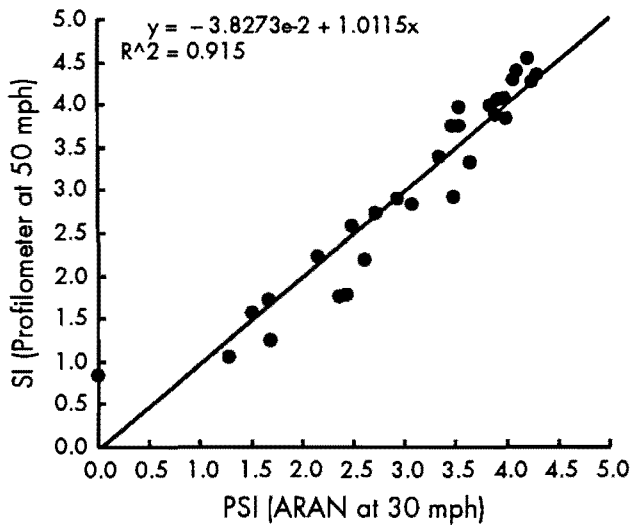


Figure 6.3 Correlation of new PSI with TEXTURE (ARAN) at 30 mph vs. SI (PROF) at 50 mph

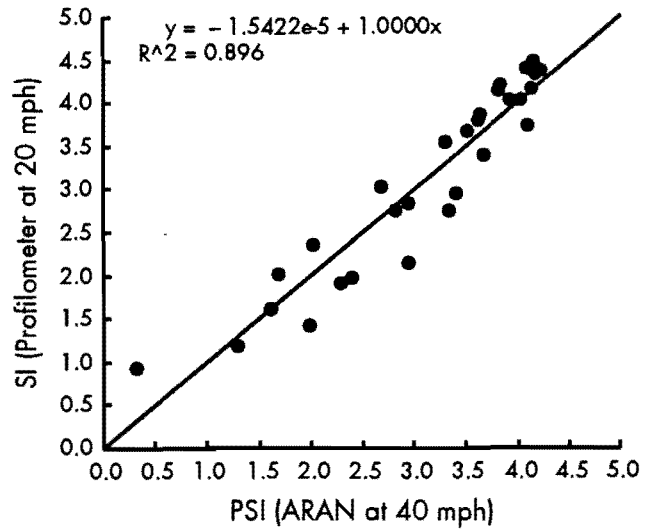


Figure 6.4 Correlation of new PSI with TEXTURE (ARAN) at 40 mph vs. SI (PROF) at 20 mph

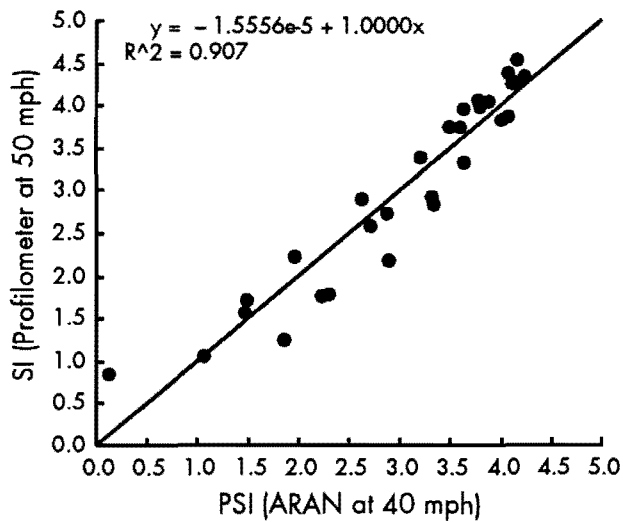


Figure 6.5 Correlation of new PSI with TEXTURE (ARAN) at 40 mph vs. SI (PROF) at 50 mph

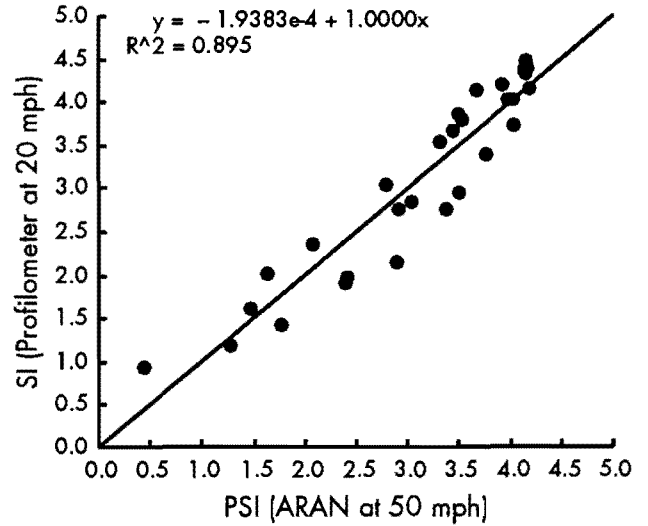


Figure 6.6 Correlation of new PSI with TEXTURE (ARAN) at 50 mph vs. SI (PROF) at 20 mph

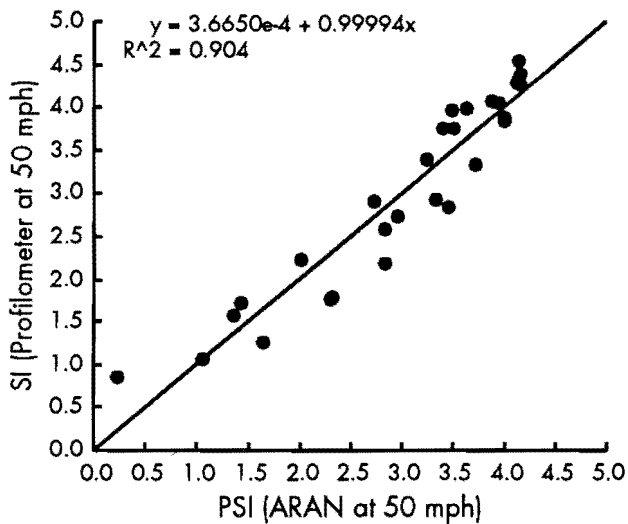


Figure 6.7 Correlation of new PSI with TEXTURE (ARAN) at 50 mph vs. SI (PROF) at 50 mph

Table 6.4 represents the coefficients from the new PSI equations excluding TEXTURE, which have the form of Equation 6.3. The program MULT REGRESSION was again used with the data from the test sections. These data can be seen in Tables A.1 and A.2.

As shown in Table 6.4 and discussed in the previous section, the second new PSI equation excluding TEXTURE has the same sign and sensitivity qualities

Table 6.4 Models from Equation 6.3 and Figure 6.1

Model	Coefficients			R ² Value
	A	B	C	
1	5.4879	-0.000924	-0.873794	0.904
2	5.5391	-0.000801	-0.931996	9.916
3	5.3875	-0.000647	-0.867200	0.894
4	5.4269	-0.000475	-0.936057	0.904
5	5.3546	-0.000951	-0.787525	0.895
6	5.3850	-0.000775	-0.862404	0.904

as does the equation including TEXTURE. It can also be seen that the new PSI equations excluding TEXTURE are not significantly different from the ones that include TEXTURE. In this case, it is reasonable to use the equations without TEXTURE because they are simpler and just as valid.

FINDINGS

- (1) The new PSI equations are derived from multiple regressions and are statistically sound.
- (2) The new PSI equations including TEXTURE and excluding TEXTURE are better than the old SI model.
- (3) Any PSI equation used with the ARAN should be used at the given operational speeds.
- (4) The study shows that while the ARAN system changes over time and speed and must be recalibrated, the equation form seems stable.

CHAPTER 7. IMPACT OF THE ARAN UNIT OPERATIONAL SPEED ON ITS ROUGHNESS STATISTICS

INTRODUCTION

As stated in Chapter 1, the roughness measuring subsystem of the ARAN unit is classified as a Class III roughness measuring instrument, or, more specifically, as a response-type road roughness measuring system (RTRRMS) (Refs 2 and 15). It can be assumed that the roughness statistics of the ARAN unit are speed-dependent; that is, the reporting statistics on the same road surface will be different if the operational speed differs. But how do the operational speeds affect the roughness statistics? Conceptually, this impact of the operational speeds on the roughness statistics depends on both the suspension system of the ARAN unit and on the pavement surface conditions. Intuitively, it appears that, if the pavement surfaces are quite rough, as speed increases, the passengers in a vehicle will feel more uncomfortable. On the other hand, if the pavement surfaces are smooth, as vehicle speed increases, the passengers' perception of the ride will not be as unfavorable. In fact, what the passengers are sensitive to are the amplitudes and frequencies of the pavement surface profiles. The change in vehicle speed is equivalent to changing the frequency of the profiles (Ref 11).

During the evaluation of the roughness measuring subsystem of the ARAN unit, a reference quarter-car simulation (RQCS) (Ref 4) model was used to simulate the suspension system of the ARAN unit. This model was used to describe qualitatively the impact of the operational speeds on the roughness statistics. A series of field tests were conducted with the ARAN unit operating at 30, 40, and 50 mph. This chapter describes the analysis of the impact of the operational speed.

REFERENCE QUARTER-CAR SIMULATION

The results obtained by an RTRRMS are based on the response of the vehicle to pavement surface profiles or slopes. As mentioned before, accurate modeling of the suspension system of the vehicle equipped with a roughness measuring system is very complicated and expensive. A simplified reference simulation of an RTRRMS, called the reference

quarter-car simulation (RQCS), can be used in the analysis of the dynamic characteristics of an RTRRMS with certain boundary conditions. Figure 7.1 shows the RQCS with these parameters:

$$K_1 = K_t/M_s = 653 \text{ sec}^{-2}$$

$$K_2 = K_s/M_s = 63.3 \text{ sec}^{-2}$$

$$U = M_u/M_s = 0.15$$

$$C = C_s/M_s = 6.00 \text{ sec}^{-1}$$

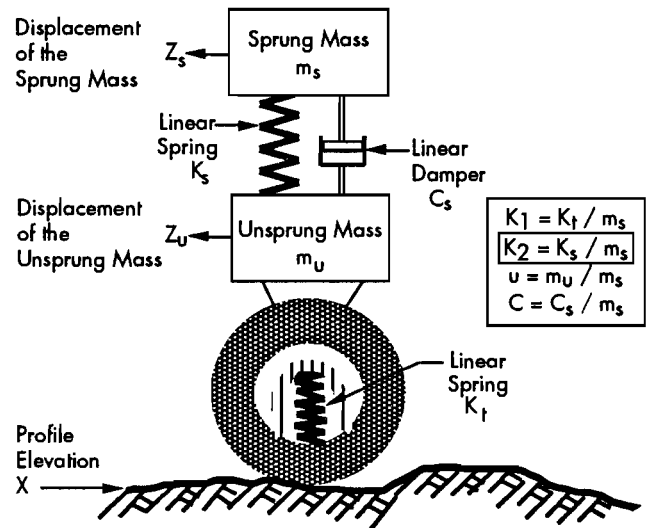


Figure 7.1 The reference quarter-car simulation

The dynamic model shown in Fig 7.1 is defined mathematically by two second-order differential equations:

$$d^2Z_s/dt^2 + C[(dZ_s/dt) - (dZ_u/dt)] + K_2(Z_s - Z_u) = 0 \quad (7.1)$$

and

$$d^2Z_s/dt^2 + U(d^2Z_u/dt^2) + K_1Z_u = K_1X \quad (7.2)$$

where X , Z_s , and Z_u are defined as shown in Fig 7.1. Since Eqs 7.1 and 7.2 are linear and constant equations, they can be used only in a relatively narrow range.

AMPLITUDE FREQUENCY CHARACTERISTICS OF RQCS

Equations 7.1 and 7.2 describe the dynamic relationship of the displacements (Z_s and Z_u) and the profile elevation (X). Some RTRRMS devices measure vehicle vertical acceleration instead of displacement (Ref 16). In order to consider the amplitude frequency characteristics with vehicle axle vertical acceleration as the output, Equations 7.1 and 7.2 need to be changed using

$$a_s = d^2Z_s/dt^2 \quad (7.3)$$

and

$$a_u = d^2Z_u/dt^2 \quad (7.4)$$

where a_s is the vehicle body vertical acceleration, and a_u is the vehicle axle vertical acceleration.

One of the best methods for frequency characteristics analysis is the Laplace Transform method (Ref 17). By taking the Laplace Transform of both sides of Eqs 7.1, 7.2, 7.3, and 7.4, the following equations in the frequency domain can be obtained:

$$S^2Z_s(S) + CS [Z_s(S) - Z_u(S)] + K_2 [Z_s(S) - Z_u(S)] = 0 \quad (7.5)$$

$$S^2Z_s(S) + US^2Z_u(S) + K_1 Z_u(S) = K_1X(S) \quad (7.6)$$

$$As(S) = S^2Z_s(S) \quad (7.7)$$

$$Au(S) = S^2Z_u(S) \quad (7.8)$$

where S is the Laplace factor, and $Z_s(S)$, $Z_u(S)$, $A_s(S)$, $A_u(S)$, and $X(S)$ are the Laplace Transforms of Z_s , Z_u , a_s , a_u , and X , respectively. From the above equations, the transfer function of axle vertical acceleration, a_u , to profile elevation, X , is expressed by

(For equations 7.9 and 7.10 please see below)

where

$H(S)$ = the transfer function,

$A_1 = K_1$, $A_2 = K_1C$, $A_3 = K_1K_2$, and

$B_1 = U$, $B_2 = UC+C$, $B_3 = UK_2+K_2+K_1$,

$B_4 = K_1C$, $B_5 = K_1K_2$.

The amplitude frequency characteristics of RQCS (a_u is the output, X is the input) are expressed by

(For equation 7.11 see below)

where

$\omega = S/j$,

$j = \sqrt{-1}$, and

$w =$ the angle frequency (1/sec).

Figure 7.2 shows the relative amplitude frequency characteristics with the maximum value of $|H(j2\pi f)|$, as the reference value, and the independent variable is frequency (Hz,1/sec) with the transformation $f = \omega/2\pi$. From Figure 7.2, it can be seen that the RQCS behaves like a band-pass filter. The RQCS has the maximum sensitivity when frequency reaches approximately 12 Hz.

A comprehensive subjective-ride research study on the relative importance of pavement profile frequency in ride comfort was conducted by the Michi-

$$H(S) = \frac{A_u(S)}{X(S)} = \frac{K_1S^4 + K_1CS^3 + K_1K_2S^2}{US^4 + (UC+C)S^3 + (UK_2+K_2+K_1)S^2 + K_1CS + K_1K_2} \quad (7.9)$$

$$H(S) = \frac{A_1S^4 + A_2S^3 + A_3S^2}{B_1S^4 + B_2S^3 + B_3S^2 + B_4S + B_5} \quad (7.10)$$

$$|H(j\omega)| = \left| \frac{A_u(j\omega)}{X(j\omega)} \right| = \sqrt{\frac{(A_1\omega^4 - A_3\omega^2)^2 + A_2^2\omega^6}{[B_1\omega^4 - B_3\omega^2 + B_5]^2 + [B_4\omega - B_2\omega^3]^2}} \quad (7.11)$$

gan Department of Transportation (Ref 18). The results indicated that the curve roughness frequencies ranging from 1.5 to 37 Hz at 50 mph correlated most strongly with the subjective ratings. Further, human sensitivity to vertical vibration is suspected to be at its maximum in the range of 5 to 6 Hz (Ref 11). This human sensitivity frequency band is, unfortunately, contained in the pass band of RQCS. In other words, if an RTRRMS fits the RQCS well, the RTRRM system responds to the roughness at the frequencies to which passengers are most sensitive.

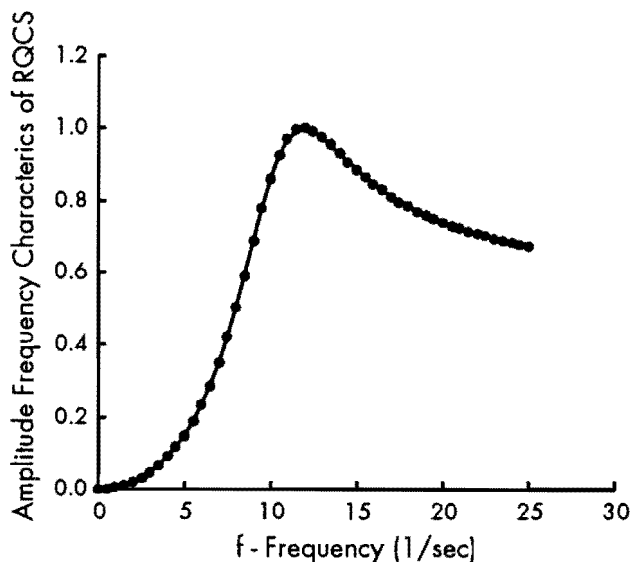


Figure 7.2 Amplitude frequency characteristics of axle acceleration due to elevation changes using the RQCS transfer function

SPEED-EFFECT CONSIDERATION

Figure 7.2 shows the amplitude frequency characteristics of axle acceleration resulting from elevation changes with input to the RQCS. As seen from this figure, the plot of amplitude frequency characteristics versus frequency is nonlinear; as frequency changes, the response of the RQCS is not constant, for example, the ride comfort perceived by the passenger is not the same. Because the pavement profile frequency is proportional to the operational speed, different operational speeds will result in different roughness statistics being reported.

RQCS is a simplified simulation of the ARAN unit, and, therefore, it cannot accurately describe the response of the ARAN unit to changes in the operational speed. As a result, the RQCS can be used only to indicate qualitatively that the roughness statistics of the ARAN unit are speed-dependent.

SPEED-EFFECT ANALYSIS BASED ON THE DATA COLLECTED FROM TEST SECTIONS

To what extent changes in the operational speeds affect the roughness statistics of the ARAN unit depends on the pavement surface conditions. The rougher the pavement surface, the more sensitive to speed the reported roughness statistics are. In order to gain a better understanding of the effect of the operational speed on the ARAN's roughness output, four sections having different roughness levels were chosen for testing. These four test sections are ATS04, ATS09, ATS19, and ATS20. The roughness statistics of the four test sections are shown in Table A.2. The roughness levels, as determined by the profilometer, ranged from smooth to rough, in the following order: ATS19, ATS09, ATS20, and ATS04.

The following discussion and the figures presented illustrate the relationship of operational speed on the ARAN's roughness outputs.

Figure 7.3 shows the curves of RMSVA from the four test sections versus the testing speed. It can be seen that, as the speed increases, the measured RMSVA for a given test section also increases. It can also be observed that the RMSVA from the roughest test section is more sensitive to speed than is the RMSVA from the smoother test sections.

Figure 7.4 shows the curves of MAS from the four test sections versus the testing speed. MAS is not as sensitive to speed as is the RMSVA statistic. For the smooth test sections, as the speed increases, MAS will actually decrease slightly. For the roughest test section, as speed increases, MAS will increase slightly.

Figure 7.5 shows the curves of TEXTURE versus the testing speed. TEXTURE is affected by speed in the same way as RMSVA, because they use the same statistical model to generate the reported numbers. The magnitude of the changes in TEXTURE caused by increased speed is significantly smaller than that seen in RMSVA.

SI, obtained by the model shown in Equation 6.1, is the function of RMSVA and MAS. As discussed earlier in this chapter and in Chapter 6, because RMSVA is speed-dependent, and because MAS decreases slightly with speed, SI should also be speed-dependent. Figure 7.6 illustrates how SI is affected by the testing speed. The speed effect is quite significant for the rough section, but for smoother sections, the speed effect is not as great. As the operating speed increases, the SI will decrease, but the amount of decrease depends on the test pavement surface conditions.

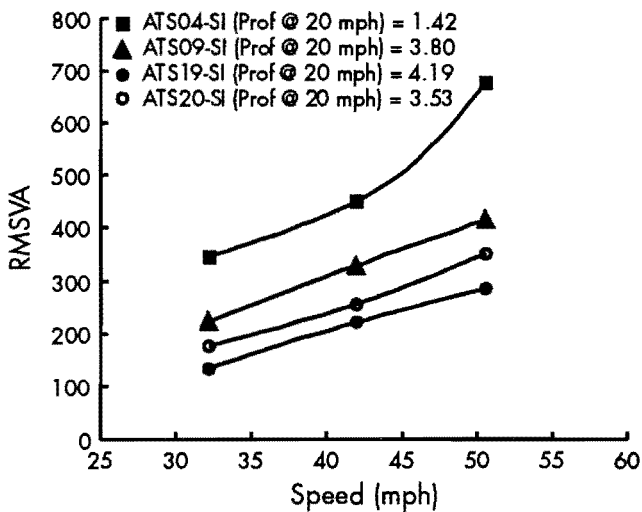


Figure 7.3 Operational speed impact on ARAN RMSVA

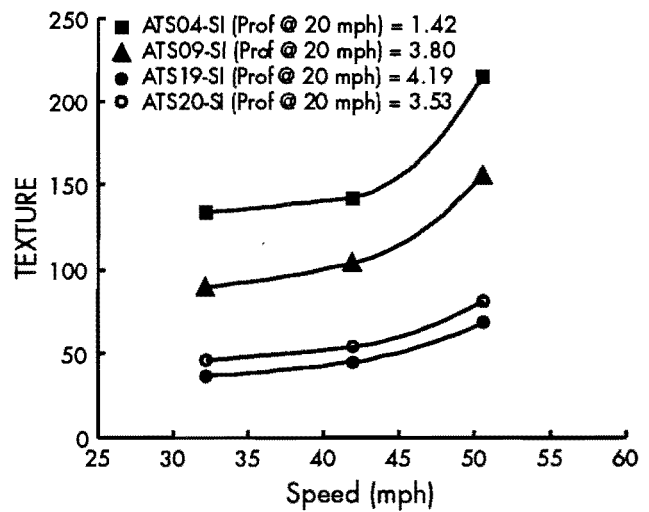


Figure 7.5 Operational speed impact on ARAN TEXTURE

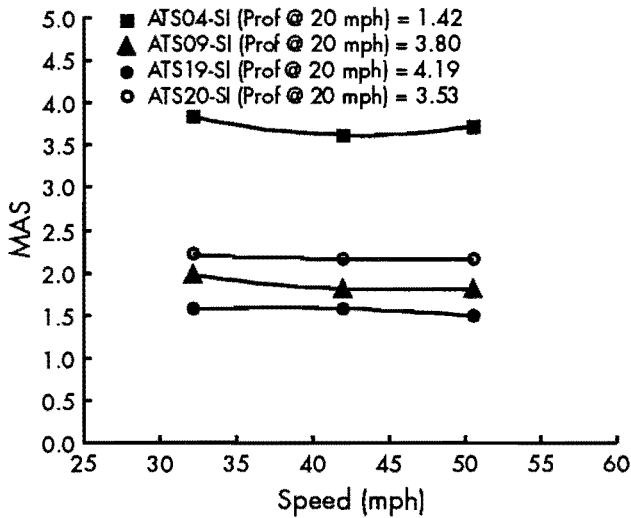


Figure 7.4 Operational speed impact on ARAN MAS

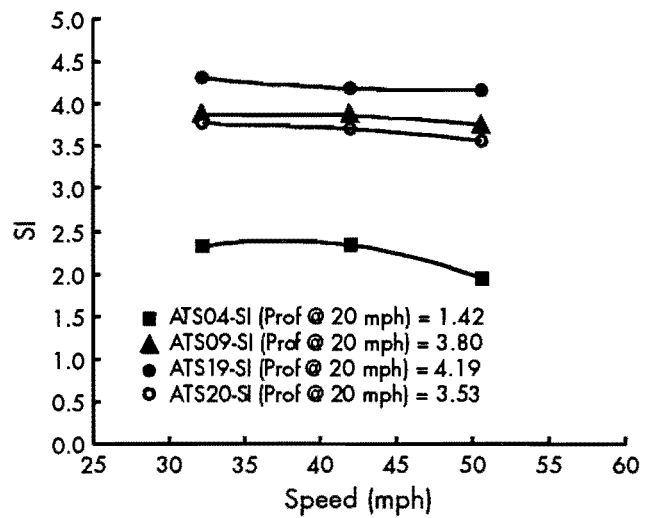


Figure 7.6 Operational speed impact on ARAN SI

CONCLUSIONS

- (1) The ARAN unit is classified as a Class III RTRRM instrument, and therefore its roughness statistics should be speed-dependent.
- (2) The spectral function of the suspension system of the ARAN unit is not constant, as shown in Figure 7.2. The speed-dependency of the ARAN unit is, therefore, nonlinear. The ARAN unit is sensitive to changes in operational speed only at certain roughness wavelengths.
- (3) The effect of the operational speed on the roughness statistics of the ARAN unit also depends on the roughness level of the test pavements.
- (4) The typical effects of the operational speed on the roughness statistics of the ARAN unit are shown in Figures 7.3 to 7.6. RMSVA and TEXTURE are more sensitive to changes in the operational speed than are MAS and SI.

CHAPTER 8. SPEED-EFFECT-CANCELING MODELS FOR THE TEXAS SDHPT ARAN UNIT

INTRODUCTION

Chapter 7 described the speed-effect analysis for the ARAN unit. While the results of theoretical and field-data experiments showed that the operational speed does affect the roughness outputs of the ARAN unit, in practical situations two basic problems regarding the operation of the ARAN unit are often encountered.

First, in order to correlate the roughness outputs of the ARAN unit with the outputs of other roughness measuring systems, a standard operational speed is required for evaluating the pavement roughness. But in some cases (e.g., in heavily trafficked areas or on very rough pavements), the ARAN unit may not be capable of running at the required operational speed. According to the results of the speed-effect analysis in Chapter 7 and Refs 4, 9, 10, and 19, the biased operational speed will result in errors in the roughness outputs.

Second, during repeat runs of the ARAN unit a constant operational speed is required. Yet sometimes, for considerations of safety or other reasons, the driver cannot maintain a constant speed. Therefore, the non-constant operational speed will result in errors in the roughness outputs. (Note that all RTRRM's share this limitation.)

Because it is believed that these two problems could be remedied by statistical models based on field-test data and experiments, this chapter presents two speed-effect-canceling models. Model 1 is based on the correlation of results from the ARAN unit and the modified K. J. Law profilometer, which were presented in Chapter 5. For different operational speeds, the ARAN unit will have different correlations with the profilometer. The relationships between the operational speed and the correlation equations could be obtained with this model. Model 2 is based on the response of the roughness outputs of the ARAN unit to different operational speeds; that is, if the statistical relationship of the response of the ARAN unit to speed is found, then, according to the relationship, the standard roughness outputs at a standard speed can be calculated.

This chapter describes the methodologies employed to derive both Model 1 and Model 2, with the

resulting models for the Texas SDHPT ARAN unit also presented. The detailed results can be found in Ref 4.

SPEED-EFFECT-CANCELING MODEL 1

Speed-effect-canceling Model 1 is based on the results of correlation analysis between the ARAN and the modified K. J. Law profilometer. Therefore, this model can be used for canceling the speed effect.

It was previously found that the correlations between the ARAN RMSVA and TEXTURE statistics with the roughness statistics output from the profilometer are poorer than for MAS. It is therefore unnecessary to apply speed-effect-canceling Model 1 to RMSVA and TEXTURE.

Basic Methodology of Speed-Effect-Canceling Model 1

If the variables Output(ARAN) and Output (Profilometer) are used to indicate the roughness statistics of the ARAN and the profilometer, respectively, then, at a given operational speed of the ARAN unit, V_A , and at a given operational speed of the profilometer, V_P , the two variables are correlated by using the following linear equation:

$$\text{Output(profilometer)} = a + b \text{ Output(ARAN)} \quad (8.1)$$

where a and b are constant parameters of correlation at given speeds V_A and V_P .

From the results of the correlation analysis in Chapter 5, it was found that at different speeds the correlation equation, Equation 5.1, should be different or the parameters a and b should be the functions of the speed, V_A , if V_P is given. Mathematically, if V_P is given, the roughness statistics of the ARAN unit operated at any reasonable speed, V_A , could be correlated with the roughness statistics of the profilometer by

$$\text{Output}\{\text{profilometer}(V_P)\} = a(V_A) + b(V_A)\text{Output}\{\text{ARAN}(V_A)\}. \quad (8.2)$$

According to Equation 8.2, $a(V_A)$ and $b(V_A)$ are functions of the speed of the ARAN, V_A , and are expressed by the second-order polynomial functions

$$a(V_A) = A_1 + A_2 V_A + A_3 V_A^2 \quad (8.3)$$

and

$$b(V_A) = B_1 + B_2 V_A + B_3 V_A^2 \quad (8.4)$$

where A_i and B_i ($i = 1, 2, \text{ and } 3$) are constants.

Consequently, the correlation or calibration of the ARAN unit with the profilometer for a given speed of the profilometer, V_p , could be expressed by

$$\begin{aligned} \text{Output[prof.}(V_p)] &= (A_1 + A_2 V_A + A_3 V_A^2) \\ &+ (B_1 + B_2 V_A + B_3 V_A^2) \times \text{Output} \\ &[\text{ARAN}(V_A)] \end{aligned} \quad (8.5)$$

Two important points should be mentioned here:

- (1) In Equation 8.5, V_A is a variable that changes within a reasonable range, say 30 to 50 mph. V_p should be given. The modified K. J. Law profilometer normally runs at 20 or 50 mph, so in the model V_p is chosen to be one of these two speeds.
- (2) Equations 8.3 and 8.4 could take other forms, but, as the results of field experiments and data analysis show, the second-order polynomial function is sufficient to fit $a(V_A)$ and $b(V_A)$.

Experiments and Field Tests (After Suspension Modifications)

During June and July 1989, a series of tests were conducted at both the Austin and the La Grange test sections. The chosen report interval was 0.005 mile for every section; testing speeds were 30, 40, and 50 mph. While the data from the flexible pavements (Austin test sections) and the rigid pavements (La Grange test sections) were combined, the test sections covered the roughness spectrum (smooth, medium smooth, and rough). The data from these field tests are presented in Table A.1. The reference velocity in the ARAN software used was selected to correspond to the testing speed; for example, if the testing speed was 30 mph, then a 30-mph reference speed was used.

Model 1 Results

It should be understood that Model 1 is based on the results of the correlation analysis that was reported in Chapter 5. The results of the analysis of the correlation between the ARAN unit and the modified K. J. Law profilometer are presented in Table 5.1.

V_A	$a(V_A)$	$b(V_A)$
x	x	x
x	x	x
x	x	x

Figure 8.1 Sample matrix for Model 1

Given the speed of the profilometer, V_p (20 or 50 mph), the parameters of the correlation in Equations 8.1 and 8.2 are functions of the speed of the ARAN, V_A . This relationship can be expressed using the matrix shown in Figure 8.1. Using both the matrix in Figure 8.1 and curve-fitting techniques, the coefficients in Equations 8.3 and 8.4, A_i and B_i ($i=1, 2, 3$), can be calculated. Thus, speed-effect-canceling Model 1, shown in Equation 8.5, can be obtained.

Because the ARAN unit cannot maintain exactly 30, 40, or 50 mph on repeat runs, V_A is taken as the mean value of the speed used during the repeat runs at each test section. From Table A.1 we have

$$V_A = 32.23 \text{ mph,}$$

$$V_A = 41.92 \text{ mph, and}$$

$$V_A = 50.53 \text{ mph.}$$

V_A	$a(V_A)$	$b(V_A)$
32.23	5.4152	-0.94085
41.92	5.3098	-0.93483
50.53	5.2116	-0.91685

Figure 8.2 Matrix of profilometer SI at 20 mph versus ARAN MAS

(1) Correlation between the ARAN MAS and SI (profilometer)

The profilometer was operated at 20 mph ($V_p = 20$). The data from Table 5.1 give the matrix shown in Figure 8.2. From the model shown in Equation 8.5, we obtain the coefficients

$$A_1 = 5.7744,$$

$$A_2 = -1.1121 \times 10^{-2},$$

$$A_3 = 0,$$

$$B_1 = -0.85256,$$

$$B_2 = -5.3229 \times 10^{-3}, \text{ and}$$

$$B_3 = 8.0165 \times 10^{-5}.$$

V_A	$a(V_A)$	$b(V_A)$
32.23	5.4761	-0.99013
41.92	5.3698	-0.98577
50.53	5.2686	-0.96777

Figure 8.3 Matrix of profilometer SI at 50 mph versus ARAN MAS

The profilometer was also operated at 50 mph ($V_p = 50$). The data from Table 5.1 give the matrix shown in Figure 8.3. From the model shown in Equation 8.5, we obtain the following coefficients

$$A_1 = 5.8424,$$

$$A_2 = -1.1331 \times 10^{-2},$$

$$A_3 = 0,$$

$$B_1 = -0.88350,$$

$$B_2 = -6.1978 \times 10^{-3}, \text{ and}$$

$$B_3 = 8.9653 \times 10^{-5}.$$

Figures B.1 and B.2 give the curves of the correlation parameters a and b , respectively, as functions of the average speed V_A with a given V_p ($V_p = 20$ and 50 mph). Figures B.7 and B.8 give the corrected correlations of MAS (ARAN) versus SI (profilometer), respectively, at $V_p = 20$ and 50 mph from the resulting speed-effect-canceling Model 1.

(2) *Correlation between the ARAN MAS and MO (profilometer)*

V_A	$a(V_A)$	$b(V_A)$
32.23	-42.140	53.749
41.92	-35.778	53.261
50.53	-30.299	52.285

Figure 8.4 Matrix of profilometer MO at 20 mph versus ARAN MAS

The profilometer was operated at 20 mph ($V_p = 20$). The data from Table 5.1 give the matrix shown in Figure 8.4. From the model shown in Equation 8.5 we have the coefficients

$$A_1 = -62.972,$$

$$A_2 = 0.64725,$$

$$A_3 = 0,$$

$$B_1 = 50.721,$$

$$B_2 = 0.20489, \text{ and}$$

$$B_3 = -3.4424 \times 10^{-3}.$$

V_A	$a(V_A)$	$b(V_A)$
32.23	-50.653	58.922
41.92	-44.199	58.607
50.53	-38.338	57.606

Figure 8.5 Matrix of profilometer MO at 50 mph versus ARAN MAS

The profilometer was also operated at 50 mph ($V_p = 50$). The resulting matrix is shown in Fig 8.5 and the coefficients are

$$A_1 = -72.359,$$

$$A_2 = 0.67281,$$

$$A_3 = 0,$$

$$B_1 = 53.786,$$

$$B_2 = 0.30685,$$

$$B_3 = -4.5764 \times 10^{-3}.$$

Figures B.3 and B.4 give the curves of a and b , respectively, versus V_A at $V_p = 20$ and 50 mph. Figures B.9 and B.10 show the corrected correlations of the ARAN MAS versus MO (profilometer) with $V_p = 20$ and 50 mph, respectively.

(3) *Correlation between the ARAN MAS and IRI (profilometer)*

The profilometer was operated at 20 mph ($V_p = 20$).

V_A	$a(V_A)$	$b(V_A)$
32.23	-27.190	74.634
41.92	-18.783	74.136
50.53	-10.882	72.659

Figure 8.6 Matrix of profilometer IRI at 20 mph versus ARAN MAS

The resulting matrix is shown in Figure 8.6 and the coefficients are

$$A_1 = -55.967,$$

$$A_2 = 0.89066,$$

$$A_3 = 0,$$

$$B_1 = 67.420,$$

$$B_2 = 0.43545, \text{ and}$$

$$B_3 = -6.5657 \times 10^{-3}.$$

V_A	$a(V_A)$	$b(V_A)$
32.23	-39.584	83.156
41.92	-30.764	82.833
50.53	-22.322	81.351

Figure 8.7 Matrix of profilometer IRI at 50 mph versus ARAN MAS

The profilometer was also operated at 50 mph ($V_P = 50$). The matrix is shown in Figure 8.7 and the coefficients are

$$A_1 = -70.064,$$

$$A_2 = 0.94259,$$

$$A_3 = 0,$$

$$B_1 = 73.985,$$

$$B_2 = 0.52904, \text{ and}$$

$$B_3 = -7.5843 \times 10^{-3}.$$

Figures B.5 and B.6 show the curves of a and b , respectively, versus V_A at $V_P = 20$ and 50 mph. Figures B.11 and B.12 show the corrected correlations of ARAN MAS against the profilometer IRI with $V_P = 20$ and 50 mph, respectively.

(4) Correlation between the ARAN SI and SI (profilometer).

The profilometer was operated at 20 mph ($V_P = 20$).

V_A	$a(V_A)$	$b(V_A)$
32.23	-0.71964	1.0990
41.92	-0.42014	1.0348
50.53	-0.12874	0.97282

Figure 8.8 Matrix of profilometer SI at 20 mph versus ARAN SI

The matrix is shown in Figure 8.8 and the coefficients are

$$A_1 = -1.4990,$$

$$A_2 = 1.9011 \times 10^{-2},$$

$$A_3 = 1.6045 \times 10^{-4},$$

$$B_1 = 1.2702,$$

$$B_2 = -4.3028 \times 10^{-3}, \text{ and}$$

$$B_3 = -3.1323 \times 10^{-5}.$$

V_A	$a(V_A)$	$b(V_A)$
32.23	-0.9740	1.1548
41.92	-0.6633	1.0886
50.53	-0.3574	1.0235

Figure 8.9 Matrix of profilometer SI at 50 mph versus ARAN SI

The profilometer was also operated at 50 mph ($V_P = 50$). The matrix is shown in Figure 8.9 and the coefficients are

$$A_1 = -1.7513,$$

$$A_2 = 1.8011 \times 10^{-2},$$

$$A_3 = 1.8948 \times 10^{-4},$$

$$B_1 = 1.3212,$$

$$B_2 = -3.8772 \times 10^{-3}, \text{ and}$$

$$B_3 = -3.9846 \times 10^{-5}.$$

Figures B.13 and B.14 show the curves of a and b , respectively, versus V_A at $V_P = 20$ and 50 mph. Figures B.19 and B.20 show the corrected correlations of ARAN SI against the profilometer SI at $V_P = 20$ and 50 mph, respectively.

(5) Correlation between the ARAN SI and MO (profilometer)

The profilometer was operated at 20 mph ($V_P = 20$).

V_A	$a(V_A)$	$b(V_A)$
32.23	306.27	-62.191
41.92	288.76	-58.394
50.53	272.94	-55.083

Figure 8.10 Matrix of profilometer MO at 20 mph versus ARAN SI

The matrix is shown in Figure 8.10 and the coefficients are

$$A_1 = 362.27,$$

$$A_2 = -1.6839,$$

$$A_3 = -1.6602 \times 10^{-3},$$

$$B_1 = -75.359,$$

$$B_2 = 0.42140, \text{ and}$$

$$B_3 = -3.9860 \times 10^{-4}.$$

V_A	$a(V_A)$	$b(V_A)$
32.23	330.45	-67.935
41.92	311.86	-63.943
50.53	294.79	-60.398

Figure 8.11 Matrix of profilometer MO at 50 mph versus ARAN MO

The profilometer was also operated at 50 mph ($V_p = 50$).

The matrix is shown in Figure 8.11 and the coefficients are

$$A_1 = 387.55,$$

$$A_2 = -1.6587,$$

$$A_3 = -3.5030 \times 10^{-3},$$

$$B_1 = -81.231,$$

$$B_2 = 0.41295, \text{ and}$$

$$B_3 = -1.3145 \times 10^{-5}.$$

Figures B.15 and B.16 give the curves of a and b , respectively, versus V_A with $V_p = 20$ and 50 mph. Figures B.21 and B.22 give the corrected correlations of the ARAN SI against the profilometer MO at $V_p = 20$ and 50 mph, respectively.

(6) *Correlation between the ARAN SI and IRI (profilometer)*

The profilometer was operated at 20 mph ($V_p = 20$).

V_A	$a(V_A)$	$b(V_A)$
32.23	458.10	-86.789
41.92	434.79	-81.820
50.53	412.28	-77.078

Figure 8.12 Matrix of profilometer IRI at 20 mph versus ARAN SI

The matrix is shown in Figure 8.12 and the coefficients are

$$A_1 = 520.21,$$

$$A_2 = -1.5594,$$

$$A_3 = -1.1411 \times 10^{-2},$$

$$B_1 = -100.51,$$

$$B_2 = 0.35899, \text{ and}$$

$$B_3 = 2.0742 \times 10^{-3}.$$

The profilometer was also operated at 50 mph ($V_p = 50$).

V_A	$a(V_A)$	$b(V_A)$
32.23	499.04	-96.100
41.92	473.62	-90.713
50.53	449.05	-85.571

Figure 8.13 Matrix of profilometer IRI at 50 mph versus ARAN SI

The matrix is shown in Figure 8.13 and the coefficients are

$$A_1 = 566.58,$$

$$A_2 = -1.6900,$$

$$A_3 = -1.2587 \times 10^{-2},$$

$$B_1 = -110.97,$$

$$B_2 = 0.38868, \text{ and}$$

$$B_3 = 2.2557 \times 10^{-3}.$$

Figures B.17 and B.18 give the curves of a and b , respectively, versus V_A with $V_p = 20$ and 50 mph. Figures B.19 and B.20 show the corrected correlations of the ARAN SI against the profilometer IRI at $V_p = 20$ and 50 mph, respectively.

Table 8.1 summarizes the results obtained from applying speed-effect-canceling Model 1 to the data collected for this research effort.

SPEED-EFFECT-CANCELING MODEL 2

Speed-effect-canceling Model 2 is based on the statistical relationship between the roughness response and the operational speed. The model is obtained from the test data of the ARAN unit itself. The roughness outputs from the ARAN, measured at any operational speed, can then be referenced back to the roughness outputs at a desired standard speed. This model can be used to remedy the two problems stated in the introduction to this chapter.

Experiments and Field Tests

In order to include more rigid data in the models, field tests were conducted on IH-10 near Flatonia in November 1989. The Austin test section data collected in June and July 1989 were also used. Since the test sites near La Grange had not been open to the public when the testing was done, the speed-effect characteristics on the ARAN roughness data are different from those from the ATS and the IH-10 sites. The interaction between vehicles and pavement roughness on newly constructed rigid pavements probably differs from that on trafficked pavements (flexible and rigid). Therefore, the test data from La Grange were not used for the modeling. In the field tests the chosen report interval was 0.005 mile for

Table 8.1 Summary of speed-effect-canceling Model 1

			ARAN			
			MAS		SI	
			A ₁	B ₁	A ₁	B ₁
Proflometer	SI	20 mph	A ₁ = 5.7744 A ₂ = -1.1121x10 ⁻² A ₃ = 0	B ₁ = -0.85256 B ₂ = -5.3229x10 ⁻³ B ₃ = 8.0165x10 ⁻³	A ₁ = -1.4990 A ₂ = -1.9011x10 ⁻² A ₃ = 1.6045x10 ⁻⁴	B ₁ = -1.2702 B ₂ = -4.3028x10 ⁻³ B ₃ = 3.1323x10 ⁻³
		50 mph	A ₁ = 5.8424 A ₂ = -1.1331x10 ⁻² A ₃ = 0	B ₁ = -0.88350 B ₂ = -6.1978x10 ⁻³ B ₃ = 8.9653x10 ⁻⁵	A ₁ = -1.7513 A ₂ = -1.8011x10 ⁻² A ₃ = 1.8948x10 ⁻⁴	B ₁ = -1.3212 B ₂ = -3.8772x10 ⁻³ B ₃ = 3.9846x10 ⁻³
	MO	20 mph	A ₁ = -62.972 A ₂ = 0.64725 A ₃ = 0	B ₁ = 50.721 B ₂ = 0.20489 B ₃ = -3.4424x10 ⁻³	A ₁ = -362.27 A ₂ = -1.6839 A ₃ = 1.6602x10 ⁻³	B ₁ = -75.359 B ₂ = 0.42140 B ₃ = 3.9860x10 ⁻⁴
		50 mph	A ₁ = -72.359 A ₂ = 0.67281 A ₃ = 0	B ₁ = 53.786 B ₂ = 0.30685 B ₃ = -4.5766x10 ⁻³	A ₁ = -387.55 A ₂ = -1.6587 A ₃ = 3.5030x10 ⁻³	B ₁ = -81.231 B ₂ = 0.41295 B ₃ = 3.3145x10 ⁻⁵
	IRI	20 mph	A ₁ = -55.967 A ₂ = 0.89066 A ₃ = 0	B ₁ = 67.420 B ₂ = 0.43545 B ₃ = -6.5657x10 ⁻³	A ₁ = -520.21 A ₂ = -1.5594 A ₃ = 1.1411x10 ⁻²	B ₁ = -100.51 B ₂ = 0.35899 B ₃ = 2.0742x10 ⁻⁵
		50 mph	A ₁ = -70.064 A ₂ = 0.94259 A ₃ = 0	B ₁ = 73.983 B ₂ = 0.52904 B ₃ = -7.5843x10 ⁻³	A ₁ = -566.58 A ₂ = -1.6900 A ₃ = 1.2587x10 ⁻²	B ₁ = -110.97 B ₂ = 0.38868 B ₃ = 2.2557x10 ⁻³

every section and the testing speeds were 30, 40, and 50 mph.

Methodology of Model 2

The roughness outputs measured at some testing speed, V_t, can be defined as RO(V_t). For a given test section, RO(V_t) is a function of V_t (Ref 4):

$$RO(V_t) = f(V_t) \tag{8.6}$$

where f(*) is a continuous function and can be obtained with curve-fitting techniques. The function of Equation 8.6 should include some parameters, A₀, A₁, ..., A_N. That is, Equation 8.6 could be described by Equation 8.7

$$RO(V_t) = f(A_0, A_1, \dots, A_N, V_t) \tag{8.7}$$

where A₀, A₁, ..., A_N are the parameters that must be estimated. To estimate these parameters a certain

number of test section runs should be made at different testing speeds. For each test section the parameters A₀, A₁, ..., A_N and the value of RO(V_s), where V_s is the standard operating speed (say V_s = 50 mph), can be obtained. Consequently, RO(V_s) becomes the standard roughness output at V_s. The following matrix can be generated from the test section data:

Matrix					
Test Section	RO(V_s)	A₀	A₁	...	A_N
1	X1s	X10	X11	...	X1N
2	X2s	X20	X21	...	X2N
3	X3s	X30	X31	...	X3N
...
M	XM _s	XM ₀	XM ₁	...	XM _N

where M is the number of the test sections run by ARAN during the field test, and RO(V_s) is the standard roughness output for a given test section if V_s is defined as the standard operational speed. However, RO(V_s) indicates the roughness level for each

test section and the parameters A_0, A_1, \dots, A_N could be related to $RO(V_s)$ by some function

$$\begin{aligned} A_0 &= GA_0[RO(V_s)] \\ A_1 &= GA_1[RO(V_s)] \\ &\dots \dots \\ A_N &= GAN[RO(V_s)] \end{aligned} \quad (8.8)$$

where $GA_0(\cdot), GA_1(\cdot), \dots, GAN(\cdot)$ are the continuous function of $RO(V_s)$. By solving Equations 8.6 and 8.8 we have

$$RO(V_s) = \mathbf{R} [V_t, RO(V_t)] \quad (8.9)$$

where $\mathbf{R} [\cdot]$ is the speed-effect-canceling model and is the two-variable function of V_t and $RO(V_t)$. Therefore, the standard roughness output, $RO(V_s)$, can be obtained through Equation 8.9 for a test section no matter what the operational speed, V_t , and the measured roughness output at V_t is $RO(V_t)$.

This process is shown in the following example. If $RO(V_t)$ is related to the operating speed V_t by

$$RO(V_t) = A_0 + A_1 V_t \quad (8.10)$$

and the parameters A_0 and A_1 are related by

$$A_0 = a_{01} + a_{02} RO(V_s) \quad (8.11)$$

$$A_1 = a_{11} + a_{12} RO(V_s) \quad (8.12)$$

then, by substituting Equations 8.11 and 8.12 into Equation 8.10, we have

$$RO(V_t) = a_{01} + a_{02} RO(V_s) + [a_{11} + a_{12} RO(V_s)] V_t \quad (8.13)$$

or

$$RMSVA(V_s) = \frac{RMSVA(V_t) - [-36.758 + 1.403(V_t - 25)]}{0.44407 + 0.022237(V_t - 25)} \quad (8.14)$$

Equation 8.14 is the speed-effect-canceling Model 2 for the example listed above. The speed-effect-canceling model described above can also be completed with the use of a family of curves. This technique is explained in the following section.

Applying Speed-Effect-Canceling Model 2 to the ARAN Unit

During June and July 1989 a series of field tests on flexible pavements were conducted; field tests on rigid pavements took place in November 1989. Because of improper operation of the ARAN unit during the test, not all the data collected from these test sections were useful.

(1) Speed-Effect-Canceling Model for RMSVA

The test data collected from the field tests are shown in Table 8.2. Figure C.1 shows the curves of raw RMSVA data versus the testing speed. Each curve represents the data collected from a particular test section. From the curves shown in Figure C.1, Equation 8.7 has the following form:

$$RMSVA(V_t) = A + B(V_t - 25) \quad (8.15)$$

where $RMSVA(V_t)$ is the roughness output RMSVA measured at V_t , the testing speed. A and B are the parameters of the linear equation. It should be noted that for each section there is a different set of parameters A and B . If $RMSVA(V_s)$ is considered as the standard roughness output, RMSVA, measured at the standard speed, $V_s = 50$ mph, then parameters A and B should be the function of $RMSVA(V_s)$. Table 8.3 lists the data for A, B , and $RMSVA(V_s)$ for each test section. If A and B are related to $RMSVA(V_s)$ by mathematical functions, and if the curve fit is relatively good, then the speed-effect-canceling model can be obtained. Figures C.2 and C.3 show the relationships of coefficients A and B with $RMSVA(V_s)$, respectively. From these figures it can be observed that a linear function gives a relatively good fit through all of the data points. Also, the relationships of A and B with $RMSVA(V_s)$ have the following forms:

$$A = -36.758 + 0.4440 RMSVA(V_s) \quad (8.16)$$

$$B = 1.4703 + 2.2237 \times 10^{-3} RMSVA(V_s) \quad (8.17)$$

when Equations 8.16 and 8.17 are substituted into Equation 8.15, the mathematical model for canceling the speed effect becomes

$$RMSVA(V_s) = \frac{RMSVA(V_t) - [-36.758 + 1.403(V_t - 25)]}{0.44407 + 0.022237(V_t - 25)} \quad (8.18)$$

The measured RMSVA at speed V_t can be referenced to the standard output, $RMSVA(V_s)$, using Equation 8.18, regardless of the actual operational speed, V_t . Figure C.4 shows a family of curves for canceling the speed effect for the Texas SDHPT ARAN unit.

To obtain these equations, first notice, from Equation 8.18, that, for a given $RMSVA(V_s)$, $RMSVA(V_t)$ is a function of V_t . Therefore, a curve of $RMSVA(V_t)$ versus V_t can be obtained. By changing $RMSVA(V_s)$, another curve of $RMSVA(V_t)$ versus V_t can be obtained, and so on.

Calculations using Figure C.4 are easily made. For instance, if the ARAN unit measures roughness data

Table 8.2 Field test data for RMSVA

Test Section	Speed (mph)	RMSVA	Test Section	Speed (mph)	RMSVA	Test Section	Speed (mph)	RMSVA
ATS01	31.10	311.8	ATS22	32.07	148.0	IH1-I	32.27	164.0
	40.48	433.0		42.43	227.7		40.43	234.0
	49.98	591.4		50.83	285.0		50.93	351.0
ATS03	32.20	240.0	ATS24	31.90	324.0	IH2-I	33.07	216.3
	42.23	343.3		41.97	515.3		40.97	287.7
	49.80	423.0		50.80	621.3		50.85	391.5
ATS07	32.00	176.0	ATS25	32.33	157.0	IH3-I	33.00	214.0
	42.27	268.0		42.60	233.0		41.10	299.0
	50.00	306.7		50.10	289.3		50.83	412.3
ATS08	32.30	157.0	ATS27	32.40	135.7	IH1-O	31.87	183.7
	41.67	233.0		41.37	186.7		41.50	264.7
	50.87	289.3		51.40	264.3		50.67	401.0
ATS09	32.47	222.3	ATS28	31.73	131.0	IH2-O	32.87	269.0
	42.10	329.7		41.70	187.3		41.97	362.3
	50.87	416.0		51.00	265.3		50.97	507.7
ATS12	32.43	178.3	ATS30	32.70	496.3	IH3-O	33.10	263.7
	42.37	263.3		41.87	691.0		41.27	370.7
	50.70	339.0		50.93	856.3		50.77	497.7
ATS15	32.90	174.0	ATS31	33.65	259.5			
	42.03	246.0		43.33	385.7			
	51.00	293.0		50.33	448.0			
ATS16	30.83	436.7	ATS36	33.20	308.0			
	41.17	653.0		42.00	396.0			
	50.90	856.3		51.00	533.0			
ATS18	31.17	233.3	ATS41	32.53	161.0			
	41.60	342.3		42.50	253.0			
	49.60	449.0		50.60	325.3			
ATS19	31.97	133.7	ATS42	32.80	160.7			
	42.13	221.0		42.57	231.7			
	50.83	285.0		49.27	277.3			
ATS20	32.60	176.0	ATS43	31.87	148.3			
	42.37	256.0		42.10	227.0			
	51.33	353.3		49.93	279.0			
ATS21	31.87	530.0	ATS55	32.87	372.3			
	40.83	722.7		41.73	542.3			
	50.10	899.7		49.27	608.7			

at any speed V_t , the measured RMSVA(V_t) must be converted to the standard roughness output, RMSVA(V_s), through V_t and RMSVA(V_t) in the figure. The corresponding RMSVA(V_s) curve can be found at the intersection of the RMSVA(V_t) and V_t .

(2) *Speed-Effect-Canceling Model for MAS*

The test data collected from field tests are shown in Table 8.4. Figure C.5 shows the curves obtained by plotting raw MAS data versus the testing speed,

Table 8.3 Data for the parameters A and B and the Standard RMSVA at $V_s=50$

Test Section	A	B	RMSVA(V_s)
ATS01	215.495	14.813	585.820
ATS03	164.904	10.393	424.729
ATS07	129.496	7.352	313.286
ATS08	108.022	7.127	286.207
ATS09	145.485	10.537	408.910
ATS12	112.270	8.788	331.970
ATS15	125.986	6.578	290.449
ATS16	314.855	20.907	837.530
ATS18	154.775	11.779	449.250
ATS19	79.452	8.038	280.405
ATS20	100.222	9.447	336.395
ATS21	394.455	20.273	901.280
ATS22	97.466	7.318	280.408
ATS24	225.160	15.806	620.310
ATS25	175.765	12.747	494.440
ATS27	82.058	6.787	251.743
ATS28	79.962	6.953	253.799
ATS30	348.735	19.751	842.510
ATS31	165.480	11.408	450.680
ATS36	196.430	12.650	512.680
ATS41	92.898	9.098	320.335
ATS42	105.864	7.093	283.194
ATS43	99.765	7.260	281.258
ATS55	270.711	14.553	634.536
IH1-I	86.370	10.074	338.220
IH2-I	134.185	9.881	381.200
IH3-I	123.045	11.139	401.520
IH1-O	94.610	11.532	382.910
IH2-O	156.390	13.182	485.940
IH3-O	155.970	13.246	487.120

Vt. Each curve represents the data collected from a particular test section. From these curves the relationship between MAS and Vt has the following form:

$$\text{MAS}(V_t) = A + B(V_t - 25) \quad (8.19)$$

where MAS(Vt) is the ARAN roughness output MAS measured at speed Vt and A and B are the parameters. If Vs = 50 mph is taken as the standard operational speed and MAS(Vs) is taken as the standard roughness output MAS, then A and B should be the function of MAS(Vs). Table 8.5 lists the data for A, B, and MAS(Vs), and Figures C.6 and C.7 show the relationships of A and B with MAS(Vs), respectively. It can be seen that the linear equations fit the data points of Figures C.6 and C.7 with adequate correlation. From curve-fitting techniques the following relationship can be obtained:

$$A = 0.42896 + 0.88363 \text{ MAS}(V_s) \quad (8.20)$$

$$B = -1.71582 \times 10^{-2} + 4.6547 \times 10^{-3} \text{ MAS}(V_s) \quad (8.21)$$

By substituting Equations 8.20 and 8.21 into Equation 8.19, we get the speed-effect-canceling model for MAS:

$$\begin{aligned} \text{MAS}(V_t) &= 0.42896 + 0.88363 \text{ MAS}(V_s) \\ &+ [-1.71582 \times 10^{-2} + 4.6547 \times 10^{-3} \text{ MAS}(V_s)](V_t - 25) \end{aligned} \quad (8.22)$$

or

$$\text{MAS}(V_s) = (\text{MAS}(V_t) - [0.42896 - 1.71582 \times 10^{-2} (V_t - 25)] / [0.88363 + 4.6567 \times 10^{-3} (V_t - 25)]) \quad (8.23)$$

Equation 8.23 is the speed-effect-canceling model for MAS. Like RMSVA, the model can also be implemented by the use of a family of curves. Figure C.8 shows the realization of the model. The development

and use of Figure C.8 are the same as that for RMSVA, which was described previously.

(3) Speed-Effect-Canceling Model for TEXTURE

As stated before, the ARAN unit gives a significantly different response to rigid and flexible pavements if the TEXTURE roughness output is considered. Therefore, the speed-effect-canceling model for TEXTURE should be divided into two submodels. One model is for the TEXTURE of flexible pavements, and the other is for the TEXTURE of rigid pavements.

(a) *Speed-Effect-Canceling Model for the TEXTURE of Flexible Pavements.* The test data are listed in Table 8.6. Figure C.9 gives the curves for fitting of raw TEXTURE (flexible pavements) versus the testing speed Vt. From the figure it is known that the relationship between TEXTURE and Vt can be approached by

$$\text{TEXTURE}(V_t) = e^{A + B(V_t - 25)} \quad (8.24)$$

Table 8.7 lists the data for A, B, and TEXTURE(Vs) when Vs = 50 mph. Figures C.10 and C.11 show the relationships of A and B with TEXTURE(Vs), respectively. The functions for curve fitting are

$$A = -1.1694 + 2.5151 \log [\text{TEXTURE}(V_s)] \quad (8.25)$$

$$B = 4.6775 \times 10^{-2} - 8.5003 \times 10^{-3} \log [\text{TEXTURE}(V_s)] \quad (8.26)$$

From Equations 8.24, 8.25, and 8.26, we have

$$\begin{aligned} \text{Ln} [\text{TEXTURE}(V_t)] &= -1.1694 + 2.5151 \\ &\log[\text{TEXTURE}(V_s)] + \{4.6775 \times 10^{-2} - 8.5003 \times \\ &10^{-3} \log[\text{TEXTURE}(V_s)]\} (V_t - 25) \end{aligned} \quad (8.27)$$

or See Equation 8.28 below

or See Equation 8.29 below

$$\text{Log}[\text{TEXTURE}(V_s)] = \frac{\text{Ln} [\text{TEXTURE}(V_t)] - [1.1694 + 4.6775 \times 10^{-2} (V_t - 25)]}{2.5151 - 8.5003 \times 10^{-3} (V_t - 25)} \quad (8.28)$$

$$\text{TEXTURE}(V_s) = 10^{\left[\frac{\text{Ln} [\text{TEXTURE}(V_t)] - [-1.1694 + 4.6775 \times 10^{-2} (V_t - 25)]}{2.5151 - 8.5003 \times 10^{-3} (V_t - 25)} \right]} \quad (8.29)$$

Table 8.4 Field test data for MAS

Test Section	Speed (mph)	MAS	Test Section	Speed (mph)	MAS	Test Section	Speed (mph)	MAS
ATS01	31.10	3.08	ATS21	31.87	3.85	IH3-O	33.10	2.21
	40.48	3.16		40.83	3.72		41.27	1.94
	49.98	3.02		50.10	3.85		50.77	2.02
ATS03	32.20	2.03	ATS22	32.07	1.46	IH2-S	33.73	2.15
	42.23	1.91		42.43	1.25		41.20	1.95
	49.80	1.91		50.83	1.19		48.87	1.92
ATS04	32.60	3.84	ATS24	31.90	3.14	IH3-S	32.13	1.97
	40.52	3.62		41.97	3.28		40.77	1.92
	50.13	3.72		50.80	3.00		48.87	1.75
ATS07	32.00	1.30	ATS27	32.40	1.66			
	42.27	1.24		41.37	1.37			
	50.00	1.15		51.40	1.37			
ATS08	32.30	1.90	ATS28	31.73	1.29			
	41.67	1.81		41.70	1.33			
	50.87	1.67		51.00	1.18			
ATS09	32.47	1.97	ATS30	32.70	3.23			
	42.10	1.81		41.87	3.41			
	50.87	1.80		50.93	3.12			
ATS12	32.43	1.20	ATS31	33.65	2.00			
	42.37	1.18		43.33	2.09			
	50.70	1.13		50.33	1.98			
ATS15	32.90	1.51	ATS36	33.20	1.89			
	42.03	1.38		42.00	1.75			
	51.00	1.33		51.00	1.72			
ATS17	31.30	4.37	ATS42	32.80	1.62			
	42.20	4.36		42.57	1.50			
	51.23	4.52		49.27	1.42			
ATS18	31.17	3.96	ATS43	31.87	1.42			
	41.60	4.01		42.10	1.33			
	49.60	4.18		49.93	1.17			
ATS19	31.97	1.57	IH3-I	33.00	1.89			
	42.13	1.58		41.10	1.64			
	50.83	1.49		50.83	1.67			
ATS20	32.60	2.21	IH2-O	32.87	2.70			
	42.37	2.16		41.97	2.45			
	51.33	2.16		50.97	2.49			

Equation 8.29 is the speed-effect-canceling model for the TEXTURE of flexible pavements. Figure C.12 shows the implementation of the model with associated family of curves.

(b) *Speed-Effect-Canceling Model for the TEXTURE of Rigid Pavements.* The test data from field tests are listed in Table 8.8. The curves of raw

TEXTURE data versus V_t are shown in Fig C.13. These curves can be mathematically described by

$$\text{TEXTURE}(V_t) = A + B (V_t - 25) + C (V_t - 25)^2 \quad (8.30)$$

Table 8.9 lists the parameters A, B, and C which can be related to the standard TEXTURE(V_s) at the

Table 8.5 Data for the parameters A and B and the standard MAS AT $V_s=50$ mph

Test Section	A	B	MAS(V_s)
ATS01	3.2164	-3.2026E-3	3.136
ATS03	2.2436	-7.0897E-3	2.066
ATS04	3.9830	-6.2395E-3	3.827
ATS07	1.5697	-8.2005E-3	1.365
ATS08	2.3084	-1.2377E-3	2.277
ATS09	2.2513	-9.3593E-3	2.017
ATS12	1.3279	-3.7734E-3	1.234
ATS15	1.8246	-9.9575E-3	1.576
ATS17	4.1157	7.2383E-3	4.297
ATS18	3.5775	1.1584E-2	3.867
ATS19	1.7173	-4.0968E-3	1.615
ATS20	2.2906	-2.7063E-3	2.223
ATS21	3.8034	8.0853E-5	3.805
ATS22	1.9107	-1.4618E-2	1.545
ATS24	3.4272	-6.9115E-3	3.254
ATS27	2.0910	-1.4964E-2	1.717
ATS28	1.4986	-5.5918E-3	1.359
ATS30	3.5036	-5.9821E-3	3.354
ATS31	2.0468	-5.5212E-4	2.033
ATS36	2.1874	-9.5270E-3	1.949
ATS42	2.0183	-1.2153E-2	1.714
ATS43	1.8680	-1.3591E-2	1.528
IH3-I	2.2259	-1.1827E-2	1.930
IH2-O	3.0345	-1.1632E-2	2.744
IH3-O	2.4837	-1.0236E-2	2.228
IH2-S	2.6315	-1.5141E-2	2.253
IH3-S	2.4101	-1.3061E-2	2.084

Table 8.6 Field test data for TEXTURE on flexible pavements

Test Section	Speed (mph)	TEXTURE	Test Section	Speed (mph)	TEXTURE
ATS01	31.10	121.8	A TS21	31.87	173.7
	40.48	139.0		40.83	204.0
	49.98	217.6		50.10	280.3
ATS03	32.20	84.3	A TS22	32.07	46.7
	42.23	103.0		42.43	62.7
	49.80	143.7		50.83	86.3
ATS04	32.60	133.8	A TS27	32.40	37.7
	40.52	142.6		41.37	50.3
	50.13	214.8		51.40	72.0
ATS07	32.00	70.0	A TS28	31.73	39.0
	42.27	82.3		41.70	52.3
	50.00	105.7		51.00	73.0
ATS08	32.30	48.7	A TS30	32.70	214.3
	41.67	63.3		41.87	233.3
	50.87	91.3		50.93	321.2
ATS09	32.47	89.0	A TS31	33.65	101.5
	42.10	103.3		43.33	120.7
	50.87	155.5		50.33	161.3
ATS12	32.43	73.3	A TS36	33.20	112.5
	42.37	84.0		42.00	129.7
	50.70	129.7		51.00	197.7
ATS15	32.90	56.3	A TS41	32.53	65.3
	42.03	65.3		42.50	82.0
	51.00	92.0		50.60	119.3
ATS17	31.30	67.3	A TS42	32.80	47.7
	42.20	85.0		42.57	56.7
	51.23	114.7		49.27	75.0
ATS18	31.17	76.3	A TS43	31.87	45.3
	41.60	87.7		42.10	60.7
	49.60	114.0		49.93	83.0
ATS19	31.97	36.3			
	42.13	44.7			
	50.83	68.0			
ATS20	32.60	46.0			
	42.37	53.7			
	51.33	81.3			

Table 8.7 Data for the parameters A and B and the standard TEXTURE on flexible pavements at Vs=50mph

Test Section	A	B	TEXTURE (Vs)
ATS01	4.5623	3.0770E-2	206.758
ATS03	4.1906	2.9759E-2	139.014
ATS04	4.6322	2.7550E-2	204.578
ATS07	4.0701	2.2515E-2	102.819
ATS08	3.6206	3.3825E-2	87.028
ATS09	4.2192	3.0016E-2	143.969
ATS12	4.0138	3.0676E-2	119.188
ATS15	3.7838	2.7100E-2	86.600
ATS17	4.0243	2.6570E-2	108.695
ATS18	4.1775	2.1369E-2	111.244
ATS19	3.3224	3.2927E-2	63.154
ATS20	3.5539	3.0187E-2	74.334
ATS21	4.9515	2.6296E-2	272.844
ATS22	3.6002	3.2569E-2	82.634
ATS27	3.3714	3.4086E-2	68.275
ATS28	3.4349	3.2495E-2	69.915
ATS30	5.1572	2.2190E-2	302.460
ATS31	4.3586	2.7162E-2	154.107
ATS36	4.4168	3.1731E-2	183.108
ATS41	3.8997	3.2952E-2	112.562
ATS42	3.6305	2.6764E-2	73.670
ATS43	3.5702	3.3283E-2	81.636

standard speed, Vs = 50 mph, by linear equations. Figures C.14, C.15, and C.16 show the relationships of A, B, and C with TEXTURE(Vs). The equations are

$$A = 6.7548 + 1.0907 \text{ TEXTURE}(Vs) \quad (8.31)$$

$$B = 0.37065 - 7.2755 \times 10^{-2} \text{ TEXTURE}(Vs) \quad (8.32)$$

$$C = 4.0183 \times 10^{-3} + 2.7651 \times 10^{-3} \text{ TEXTURE}(Vs) \quad (8.33)$$

when Equations 8.31, 8.32, and 8.33 are substituted into Equation 8.30, the speed-effect-canceling model becomes

See Equation 8.34 below

Figure C.17 shows the implementation of the model with the associated family of curves. The procedure for canceling the speed effect can be completed by either applying Equation 8.34 or Figure C.17.

$$\text{TEXTURE}(Vs) = 10 \left[\frac{\ln [\text{TEXTURE}(Vt)] - \left[6.7548 - 0.37065(Vt - 25) + 4.0183 \times 10^{-3} (Vt - 25)^2 \right]}{1.0907 - 7.2755 \times 10^{-2} (Vt - 25) + 2.7651 \times 10^{-3} (Vt - 25)^2} \right] \quad (8.34)$$

Example

As an example, the case of the speed-effect-canceling for RMSVA is considered here. If the ARAN unit is operated at 40 mph ($V_t = 40$ mph) and the RMSVA measured at 40 mph is 400 mg [$\text{RMSVA}(V_t) = 400$ mg]. Substituting $\text{RMSVA}(V_t)$ and V_t into Equation 8.18 results in the standard RMSVA at 50 mph [$\text{RMSVA}(V_s)$ and $V_s = 50$ mph]. This RMSVA would be 533.3 mg. Figure C.18 shows how to obtain

$\text{RMSVA}(V_s)$ using the family of curves that were presented in Figure C.4. The resulting $\text{RMSVA}(V_s)$ from Figure C.18 is the same as that calculated using Equation 8.18.

SUMMARY

Two different types of speed-effect-canceling models can be used with the ARAN unit. Model 1 is based on the analysis of correlation between the ARAN unit and the modified K. J. Law profilometer. The final result of Model 1 is a family of curves that indicates the different correlations at different operational speeds. Model 2 is based on the statistical relationship between the roughness response and the operational speed. The final model can relate the ARAN's roughness outputs measured at any reasonable speed to a corresponding standard roughness output at a standard speed.

From the standpoint of applicability, Model 2 is more useful than Model 1 because it considers only the ARAN unit itself. It can also be related to the other reference instruments by the corrected roughness statistics. Model 2 can be used to correct both of the problems stated in the introduction of this chapter.

The response characteristics of the suspension system of the ARAN unit may change with time. Consequently, the models for speed-effect-canceling may not be constant over time. Therefore, the models should be updated to obtain new parameters and new forms of the functions as necessary.

The methodologies of the speed-effect-canceling models presented in this chapter can be applied to other response-type road roughness measuring systems, but these systems should have relatively good repeatability and the output must include information regarding the speed of operation.

Table 8.8 Field test data for texture on rigid pavements

Test Section	Speed (mph)	TEXTURE
IH1 - I	32.27	67.0
	40.43	59.7
	50.93	104.3
IH2 - I	33.07	76.3
	40.97	70.7
	50.85	121.0
IH3 - I	33.00	76.7
	41.10	73.7
	50.83	127.7
IH1 - O	31.87	66.7
	41.50	62.0
	50.67	96.7
IH2 - O	32.87	92.7
	41.97	83.0
	50.97	128.7
IH3 - O	33.10	91.7
	41.27	84.0
	50.77	119.7
IH1 - S	32.87	69.3
	41.10	60.0
	50.07	93.3
IH2 - S	33.73	66.7
	41.20	61.0
	48.87	83.0
IH3 - S	32.13	90.0
	40.77	68.7
	48.87	100.3

Table 8.9 Data for the parameters A, B, and C and the standard TEXTURE on rigid pavement at $V_s = 50$ mph

Test Section	A	B	C	TEXTURE (V_s)
IH1 - I	104.406	-7.151	0.27557	97.875
IH2 - I	124.066	-8.550	0.32621	114.185
IH3 - I	122.435	-8.372	0.33204	120.660
IH1 - O	95.800	-5.799	0.22724	92.850
IH2 - O	146.419	-9.497	0.33943	121.125
IH3 - O	134.376	-7.426	0.26601	114.995
IH1 - S	113.861	-7.878	0.28153	92.855
IH2 - S	107.291	-6.742	0.23985	88.635
IH3 - S	150.350	-11.174	0.38032	108.700

CHAPTER 9. SUMMARY, CONCLUSIONS, AND RECOMMENDATIONS

SUMMARY

As described earlier, the ARAN unit is a multi-functional pavement evaluation surveying instrument containing several subsystems, one of which—the pavement surface roughness measuring subsystem—was evaluated in this report. The evaluation of the remaining subsystems, including an overall system evaluation of the ARAN unit, will be published in another research report for this project.

The roughness outputs of the ARAN unit consist of the statistics RMSVA, MAS, and TEXTURE. This report presents the performance of the roughness measuring subsystem of the ARAN unit in terms of RMSVA, MAS, and TEXTURE, and describes the field tests performed and the data collected. The evaluation results presented here cover the following areas: (1) the impact of the report interval on the roughness outputs, (2) the repeatability of the roughness subsystem, (3) correlation analysis and roughness calibration models developed, and (4) analysis of the impact of the operational speed on roughness statistics. As a result of this research, new PSI modeling based on RMSVA, MAS, and TEXTURE was developed and presented. Because the field tests demonstrated that the operational speed of the ARAN unit has a significant impact on the roughness outputs (as it does on all RTRRMS devices), the speed-effect-canceling models were developed and presented.

The field testing and data collection for the correlation analysis were conducted from October 1988 through July 1989. The ARAN unit and the K. J. Law profilometer were run along the same marked wheelpaths of all test sections. The factorial of the field tests includes the pavement types, report intervals, testing speeds, and roughness levels of the test sections. The roughness level of the test sections covers a wide range of surface roughness, and in order to obtain the speed-effect-canceling models, more rigid pavement test sections were chosen and evaluated. The rigid pavement additional test sites were on IH-10 near Flatonia (selected because adequate rigid pavement test sections were unavailable in the Austin area). However, the roughness range of

the new rigid pavement test sections covers only smooth and medium-smooth pavements.

Statistical tests showed that the report interval of the roughness output does not have a significant impact on the reported roughness statistics; that is, the operator of the ARAN unit can select the report interval without being concerned about its effect on the roughness outputs.

The repeatability of the roughness outputs of the ARAN unit consists of both systematic repeatability and operational repeatability. Systematic repeatability is affected by the quality of the hardware systems and the effectiveness of the measurement principles. Operational repeatability is affected by the behavior of both the driver and operator of the ARAN unit, as well as by the environmental conditions during testing. The results of the repeatability test showed that the overall repeatability of the roughness measuring subsystem is better than 5 percent, based on field tests.

The correlation analysis compared the Texas SDHPT ARAN unit with the modified K. J. Law profilometer, with the results showing good correlation between the outputs of these two instruments. However, because the correlation models developed are speed-dependent, the correlation models must be used for a given operational speed if no speed-effect-canceling model is implemented. It is recommended that MAS be used to estimate the roughness outputs corresponding to the profilometer. Unfortunately, RMSVA and TEXTURE do not correlate well with any of the profilometer's outputs.

Two PSI models, developed as a result of this research effort, are presented in this report: (1) the model including the roughness output TEXTURE, and (2) the model excluding TEXTURE. The test results demonstrated that the new PSI models developed are better than the original SI model, though they could change with time. The new PSI model excluding TEXTURE has been implemented with the PC program presented in Appendix D of this report.

The operational speed of the ARAN unit has a significant impact on its roughness outputs. The impact

of the operational speed on the roughness outputs also depends on the roughness level of the pavement surface being evaluated. With respect to the operational speed of the ARAN unit, it was found that RMSVA and TEXTURE are more sensitive than MAS.

Two speed-effect-canceling models were developed as a result of this project. The first speed-effect-canceling model, Model 1, is based on the correlation analysis of the Texas SDHPT ARAN unit and their modified K. J. Law profilometer. The final result of the first model is a family of curves, each of which indicates the different correlations at different operational speeds. The second speed-effect-canceling model, Model 2, is based on the statistical relationship between the ARAN unit's roughness outputs and its operational speed. The second model can be used to reference the roughness outputs measured at any reasonable test speed to a standard roughness output at a standard speed. The methodology used to develop the speed-effect-canceling models for the ARAN unit can be applied to other response-type road roughness measuring systems.

There are some limitations to the second speed-effect-canceling model: In order to apply the methodology to other RTRRM systems, relatively good repeatability of its output roughness statistics is required. In addition, the output of the RTRRM instrument must include the speed of operation.

CONCLUSIONS

The following conclusions were reached by the researchers after their evaluation of the ARAN unit's pavement roughness measuring subsystem.

- (1) Since the field tests covered the entire roughness range, and since the field tests have proven that the ARAN unit works well, the roughness measuring subsystem can be applied to any reasonable pavement roughness conditions.
- (2) When the operator of the ARAN unit chooses the report interval for the measurement of pavement roughness, he does not need to be concerned about the effect of the report interval on the roughness outputs. He needs to consider only the effect of the report interval on computer memory space and on the other subsystems of the ARAN unit.

- (3) The roughness measuring subsystem should be operated only at speeds between 25 mph and 60 mph, because of the inherent limitations associated with traffic safety, the filters, the computer sampling rate, the suspension response characteristics, and the driver's behavior.
- (4) The operational speed of each run should be kept as constant as possible during a survey run, because it has been shown to have a significant impact on the roughness outputs.

RECOMMENDATION

The following recommendations could enhance the performance of the ARAN unit, making it a more powerful pavement roughness monitoring instrument.

- (1) The Texas SDHPT's modified K. J. Law profilometer's response to pavement roughness and its dynamic calibration must be verified. The calibrated profilometer should be used as a reference instrument for the calibration and correlation of the ARAN unit's roughness measuring subsystem.
- (2) The coefficients of the new PSI models developed by the researchers during this evaluation will change with time due to the wear of the ARAN unit's suspension system and/or normal maintenance performed on the ARAN unit (such as rotating or changing the tires). A periodic verification of calibration procedure should be developed to make certain that roughness data collected using the ARAN unit are valid over time. The procedure should take into account the total distance traveled by the ARAN unit and/or the length of time between each verification of calibration. If the ARAN unit fails the verification, the techniques developed in this project should be used to recalculate the coefficients of the PSI models.
- (3) If only correlation analysis or the estimation of the outputs of a reference instrument is required, it is recommended that the first speed-effect-canceling model be used. Otherwise, the second speed-effect-canceling model is recommended, because it can reference the roughness outputs measured at any reasonable speed to a standard roughness output at a standard speed.
- (4) It is recommended that more research be conducted in an attempt to apply the methodology for developing the speed-effect-canceling models to other SDHPT RTRRMS instruments.

REFERENCES

1. Buchanan, J. A., and A. L. Catudal, "Standardizable Equipment for Evaluating Road Surface Roughness," Highway Research Record No.2, Highway Research Board, Washington, D. C., 1940.
2. U. S. Department of Transportation, *Highway Performance Monitoring Field Manual*, Federal Highway Administration Publication 5600.1A, Appendix J, Washington, D. C., December 1987.
3. Sayers, Michael W., Thomas D. Gillespie, and William D. O. Paterson, "Guidelines for Conducting and Calibrating Road Roughness Measurements," World Bank Technical Paper Number 46, The World Bank, Washington, D. C., U.S.A., 1986.
4. Lu, Jian, Carl Bertrand, and W. R. Hudson, "Speed Effect Analysis and Canceling Model of Response Type Road Roughness Measuring System," Transportation Research Board, Washington, D. C., January 1990.
5. Highway Products International INC., *ARAN III Manual*, Version 1.3, 1983.
6. Bertrand, Carl, Robert Harrison, and B. Frank McCullough, "Evaluation of the Performance of the Auto-Read Version of the Face Dipstick," Research Report 969-2F, Center for Transportation Research, The University of Texas at Austin, 1989.
7. Highway Products International Inc., *ARAN Data Acquisition User Guide*, 1987.
8. Ott, Lyman, *An Introduction to Statistical Methods and Data Analysis*, 3rd Edition, PWS-KENT Publishing Company, Boston, 1988.
9. Sayers, Michael W., Thomas D. Gillespie, and Cesar A. V. Queiroz, "The International Road Roughness Experiment, Establishing Correlation and a Calibration Standard for Measurement," World Bank Technical Paper Number 45, The World Bank, Washington, D. C., 1986.
10. Paterson, William D. O., Accuracy of Calibrated Roughness Surveys, *Measuring Road Roughness and its Effects on User Cost and Comfort*, ASTM STP884, T. D. Gillespie and Michael Sayers, Eds., American Society for Testing and Materials, Philadelphia, 1986, pp 66-88.
11. Gillespie, T. D., M. W. Sayers, and L. Segel, "Calibration of Response-Type Road Roughness Measuring Systems," National Cooperative Highway Research Program Report 228, Transportation Research Board, Washington, D. C., December 1982.
12. Claros, German J., W. R. Hudson, and Clyde F. Lee, "Performance of the Analog and Digital Profilometer with Wheels and with Non-Contact Transducers," Research Report 251-3F, Center for Transportation Research, The University of Texas at Austin, April 1985.
13. McKenzie, David W., W. R. Hudson, and Clyde E. Lee, "The Use of Road Profile Statistics for Maysmeter Calibration," Research Report 251-1, Center for Transportation Research, The University of Texas at Austin, August 1982.
14. Bertrand, Carl, Robert Harrison, and B. Frank McCullough, "Evaluation of the Performance of the Auto-Read Version of the Face Dipstick," Research Report 969-2F, Center For Transportation Research, The University of Texas at Austin, 1989.

15. Harrison, Robert, Carl Bertrand, and W. R. Hudson, "Measuring the Smoothness of Newly Constructed Concrete Pavement For Acceptance Specifications," Fourth International Conference on Concrete Pavement Design and Rehabilitation, Purdue University, April 1989.
16. Federal Highway Administration, "Automated Pavement Data Collection Equipment," Pavement Profile Measurement Seminar Proceedings, Vol II, FHWA-DP-88-072-004, April 1988.
17. Bogart, Jr., Theodore F., *Laplace Transforms and Control Systems Theory for Technology*, John Wiley & Sons, Inc., 1982.
18. Darlington, J. R., "A Roughness Wavelength Band Determined by Subjective Response," Unpublished Report, Michigan Department of State Highway and Transportation, February 1976.
19. Paterson, W. D. O., and T. Watanatada, Relationships Between Vehicle Speed, Ride Quality, and Road Roughness, *Measuring Road Roughness and Its Effect on User Cost and Comfort*, ASTM STP884, T. D. Gillespie and Michael Sayers, Eds., American Society for Testing and Materials, Philadelphia, 1985, pp. 89-110.

APPENDIX A. FIELD ROUGHNESS DATA FROM THE ARAN UNIT AND THE K. J. LAW PROFILOMETER

Table A.1 Field roughness test data from the ARAN unit

Test Section	Speed	RMSVA	MAS	Texture	SI	Test Section	Speed	RMSVA	MAS	Texture	SI
ATS01	31.10	311.8	3.08	121.8	2.94	ATS16	30.83	436.7	5.68	172.0	0.80
	40.48	433.0	3.16	139.0	2.71		41.17	653.0	5.41	214.7	0.72
	49.98	591.4	3.02	217.6	2.61		50.90	856.3	5.20	264.3	0.60
ATS03	32.20	240.0	2.03	84.3	3.82	ATS17	31.30	235.7	4.37	67.3	2.06
	42.23	343.3	1.91	103.0	3.78		42.20	387.3	4.36	85.0	1.87
	49.80	423.0	1.91	143.7	3.67		51.23	554.7	4.52	114.7	1.52
ATS04	32.60	346.4	3.84	133.8	2.32	ATS18	31.17	233.3	3.96	76.3	2.38
	40.52	450.4	3.62	142.6	2.34		41.60	342.3	4.01	87.7	2.19
	50.13	676.8	3.72	214.8	1.96		49.60	449.0	4.18	114.0	1.92
ATS07	32.00	176.0	1.30	70.0	4.46	ATS19	31.97	133.7	1.57	36.3	4.31
	42.27	268.0	1.24	82.3	4.38		42.13	221.0	1.58	44.7	4.19
	50.00	306.7	1.15	105.7	4.40		50.83	285.0	1.49	68.0	4.17
ATS08	32.30	157.0	1.90	48.7	4.03	ATS20	32.60	176.0	2.21	46.0	3.77
	41.67	233.0	1.81	63.3	4.00		42.37	256.0	2.16	53.7	3.71
	50.87	289.3	1.67	91.3	4.03		51.33	353.3	2.16	81.3	3.57
ATS09	32.47	222.3	1.97	89.0	3.89	ATS21	31.87	530.0	3.85	173.7	2.06
	42.10	329.7	1.81	103.3	3.87		40.83	722.7	3.72	204.0	1.90
	50.87	416.0	1.80	155.3	3.76		50.10	899.7	3.85	280.3	1.57
ATS12	32.43	178.3	1.20	73.3	4.53	ATS22	32.07	148.0	1.46	46.7	4.38
	42.37	263.3	1.18	84.0	4.44		42.43	227.7	1.25	62.7	4.43
	50.70	339.0	1.13	129.7	4.37		50.83	285.0	1.19	86.3	4.40
ATS15	32.90	174.0	1.51	56.3	4.31	ATS24	31.90	324.0	3.14	128.7	2.87
	42.03	246.0	1.38	65.3	4.31		41.97	515.3	3.28	183.7	2.51
	51.00	293.0	1.33	92.0	4.28		50.80	621.3	3.00	224.7	2.58

Table A.1 Field roughness test data from the ARAN unit (continued)

Test Section	Speed	RMSVA	MAS	Texture	SI	Test Section	Speed	RMSVA	MAS	Texture	SI
ATS25	32.33	267.0	2.91	91.7	3.12	ATS43	31.87	148.3	1.42	45.3	4.41
	42.60	405.3	2.54	127.7	3.22		42.10	227.0	1.33	60.7	4.37
	50.10	492.7	2.52	163.7	3.12		49.93	279.0	1.17	83.0	4.42
ATS27	32.40	135.7	1.66	37.7	4.24	ATS55	32.87	372.3	2.49	145.0	3.30
	41.37	186.7	1.37	50.3	4.39		41.73	542.3	2.74	174.7	2.88
	51.40	264.3	1.37	72.0	4.29		49.27	608.7	2.54	200.7	2.95
ATS28	31.73	131.0	1.29	39.0	4.53	LaG3R	31.47	298.7	2.38	92.0	3.48
	41.70	187.3	1.33	52.3	4.42		41.67	376.0	1.95	94.0	3.70
	51.00	265.3	1.18	73.0	4.43		50.67	443.0	1.84	124.7	3.70
ATS30	32.70	496.3	3.23	214.3	2.58	LaG4L	32.80	294.0	2.78	107.3	3.19
	41.87	691.0	3.41	233.3	2.18		42.07	372.3	2.52	103.7	3.28
	50.93	856.3	3.12	321.3	2.18		50.87	445.0	2.41	130.0	3.26
ATS31	33.65	259.5	2.00	101.5	3.82	LaG4M	32.70	404.3	2.90	109.7	2.95
	43.33	385.7	2.09	120.7	3.58		41.87	504.0	2.45	119.3	3.15
	50.33	448.0	1.98	161.3	3.58		50.93	556.7	2.45	114.3	3.08
ATS36	33.20	308.0	1.89	112.5	3.84						
	42.00	396.0	1.75	129.7	3.83						
	51.00	533.0	1.72	197.7	3.67						
ATS41	32.53	161.0	1.71	65.3	4.17						
	42.50	253.0	1.68	82.0	4.07						
	50.60	325.3	1.74	119.3	3.93						
ATS42	32.80	160.7	1.62	47.7	4.24						
	42.57	231.7	1.50	56.7	4.24						
	49.27	277.3	1.42	75.0	4.24						

Table A.2 Field test data from K. J. Law profilometer

Test Section	Speed	SI	M O	IRI	Test Section	Speed	SI	M O	IRI
ATS01	20	1.96	144.50	219.10	ATS28	20	4.16	37.57	80.94
	50	1.79	156.30	235.20		50	4.26	33.68	77.40
ATS03	20	3.66	56.45	111.75	ATS30	20	2.35	118.96	209.44
	50	3.76	52.59	110.78		50	2.22	126.41	211.56
ATS04	20	1.42	188.28	294.30	ATS31	20	2.75	96.62	164.74
	50	1.24	207.76	324.58		50	2.93	87.80	159.10
ATS07	20	4.46	26.28	62.98	ATS36	20	3.86	48.54	100.11
	50	4.53	23.76	61.13		50	3.96	44.79	97.72
ATS08	20	3.40	67.91	119.55	ATS41	20	4.14	38.32	85.77
	50	3.32	70.30	126.66		50	3.98	44.15	93.63
ATS09	20	3.80	51.02	105.72	ATS42	20	4.02	42.56	91.73
	50	3.75	52.76	107.71		50	4.05	41.70	90.71
ATS12	20	4.36	29.87	74.12	ATS43	20	4.39	28.94	73.82
	50	4.35	30.21	75.73		50	4.39	28.78	72.58
ATS15	20	4.02	42.47	98.12	ATS55	20	3.03	83.45	154.19
	50	3.84	49.27	106.83		50	2.90	89.51	165.99
ATS16	20	0.93	248.70	382.61	LaG3R	20	2.94	87.47	144.54
	50	0.85	264.71	410.76		50	2.84	92.41	155.15
ATS17	20	1.19	212.76	301.38	LaG4L	20	2.84	92.85	152.14
	50	1.05	231.16	334.54		50	2.73	97.61	160.39
ATS18	20	2.01	140.82	230.49	LaG4M	20	2.76	96.37	154.51
	50	1.72	161.58	270.10		50	2.58	105.55	156.92
ATS19	20	4.19	36.43	88.66					
	50	4.07	40.88	94.43					
ATS20	20	3.53	61.75	115.33					
	50	3.39	67.23	126.02					
ATS21	20	1.62	170.38	285.71					
	50	1.56	175.39	290.76					
ATS22	20	4.33	31.23	77.16					
	50	4.28	32.94	81.27					
ATS24	20	1.91	147.40	236.30					
	50	1.76	158.63	264.10					
ATS25	20	2.15	131.25	225.83					
	50	2.19	128.38	234.23					
ATS27	20	3.73	53.78	95.57					
	50	3.87	48.08	89.26					

APPENDIX B. FIGURES RELATED TO THE SPEED-EFFECT-CANCELING MODEL 1

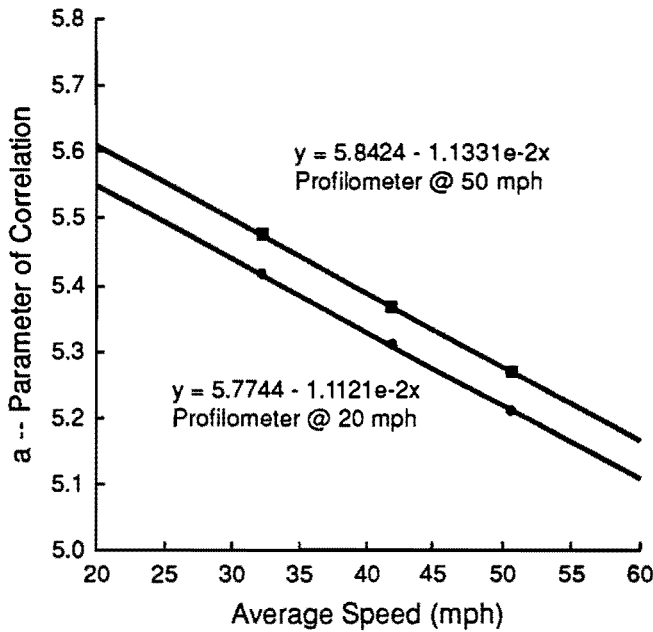


Fig B.1 Parameter of correlation (A) between MAS (ARAN) and SI (Profilometer), as a function of average speed.

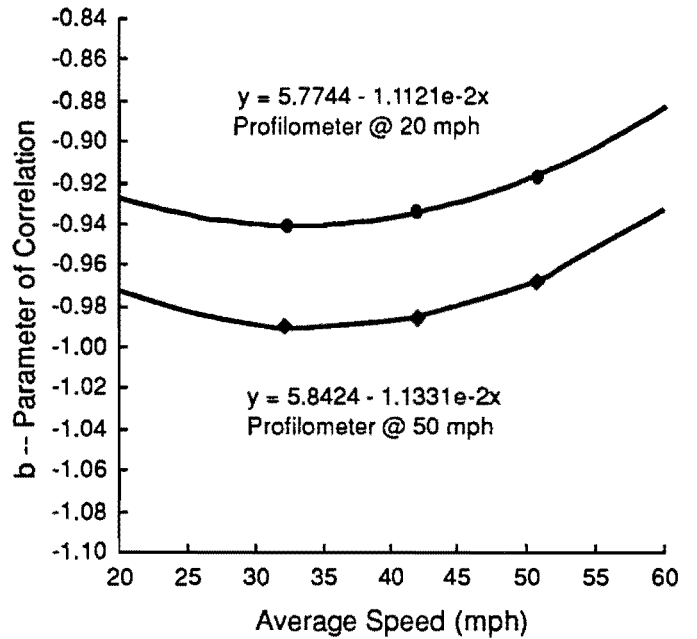


Fig B.2 Parameter of correlation (B) between MAS (ARAN) and SI (Profilometer), as a function of average speed.

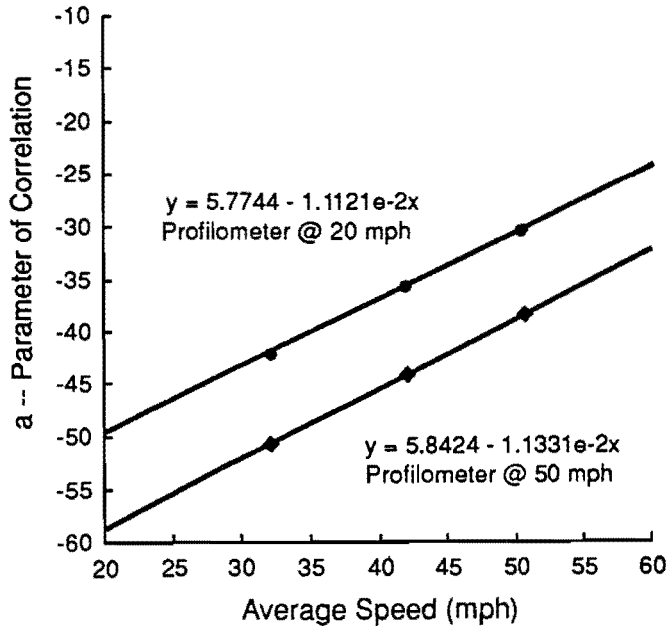


Fig B.3 Parameter of correlation (A) between MAS (ARAN) and MO (Profilometer), as a function of average speed.

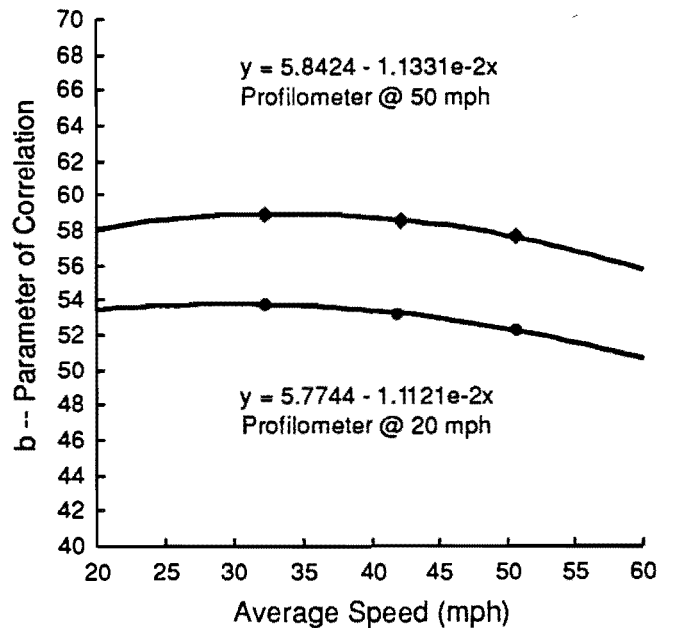


Fig B.4 Parameter of correlation (B) between MAS (ARAN) and MO (Profilometer), as a function of average speed.

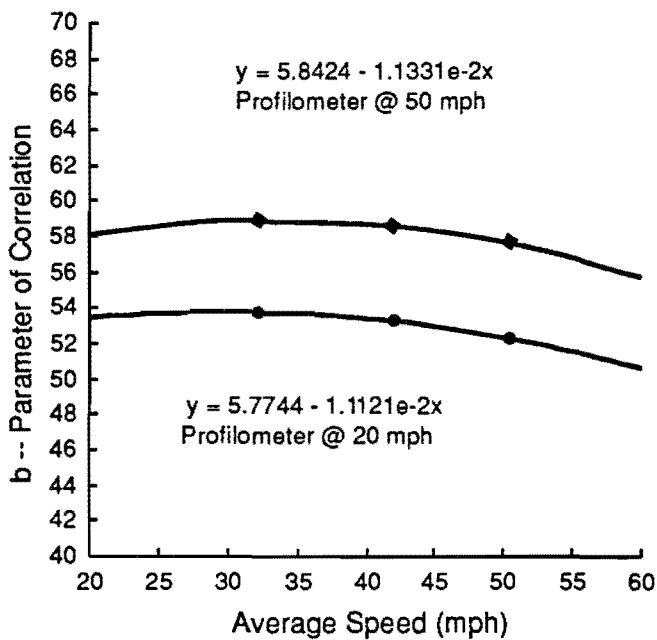


Fig B.5 Parameter of correlation (A) between MAS (ARAN) and IRI (Profilometer), as a function of average speed.

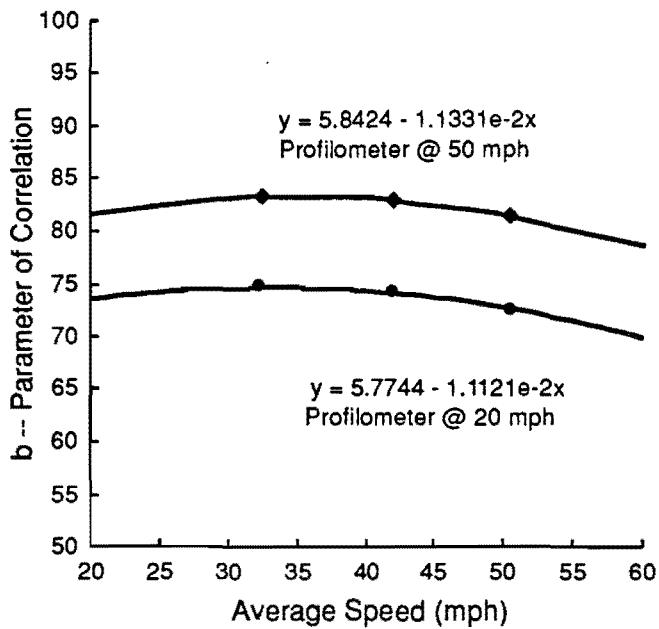


Fig B.6 Parameter of correlation (B) between MAS (ARAN) and IRI (Profilometer), as a function of average speed.

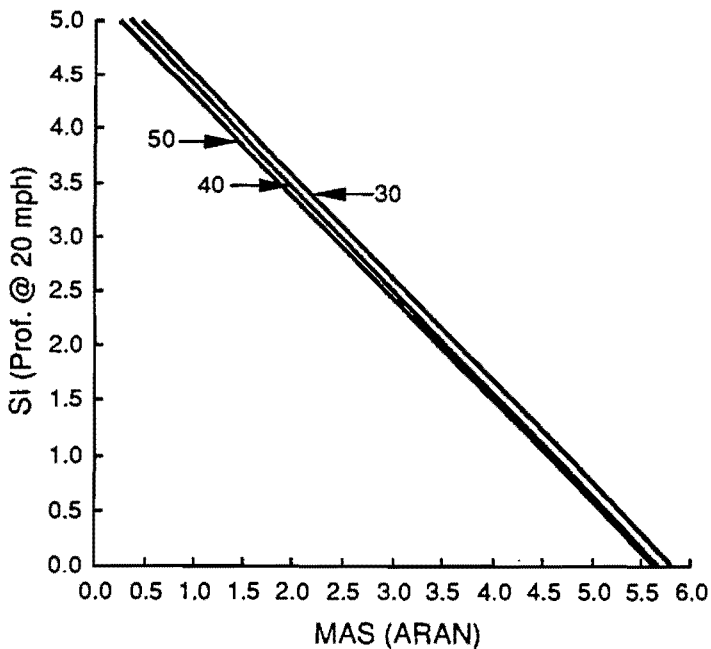


Fig B.7 Correlations between MAS (ARAN) and SI profilometer at 20 mph.

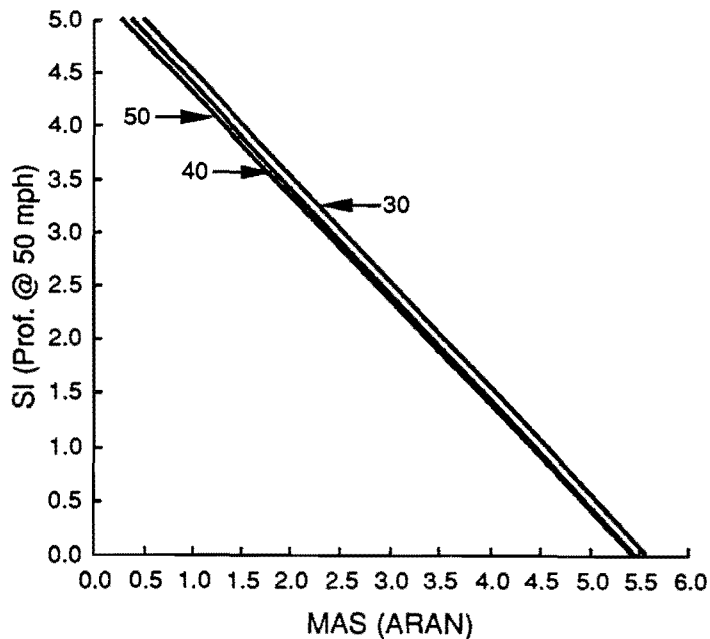


Fig B.8 Correlations between MAS (ARAN) and SI profilometer at 50 mph.

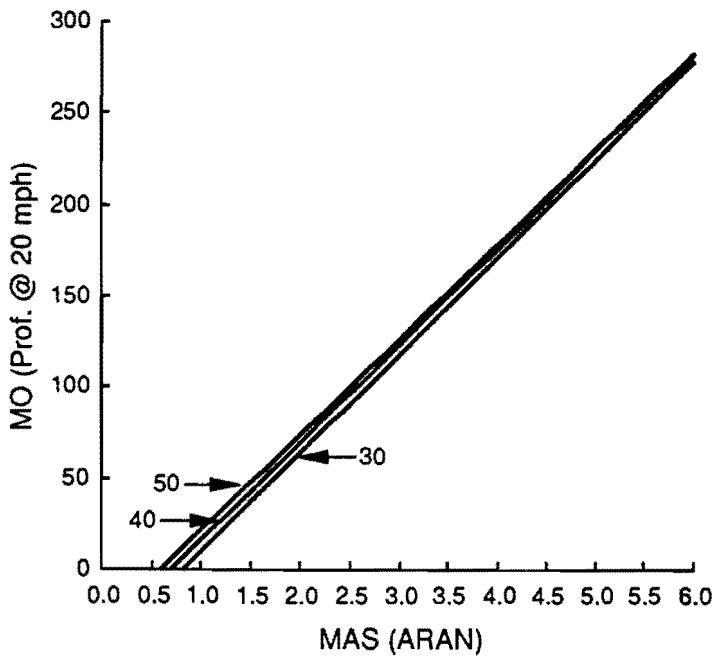


Fig B.9 Correlations between MAS (ARAN) and MO profilometer at 20 mph.

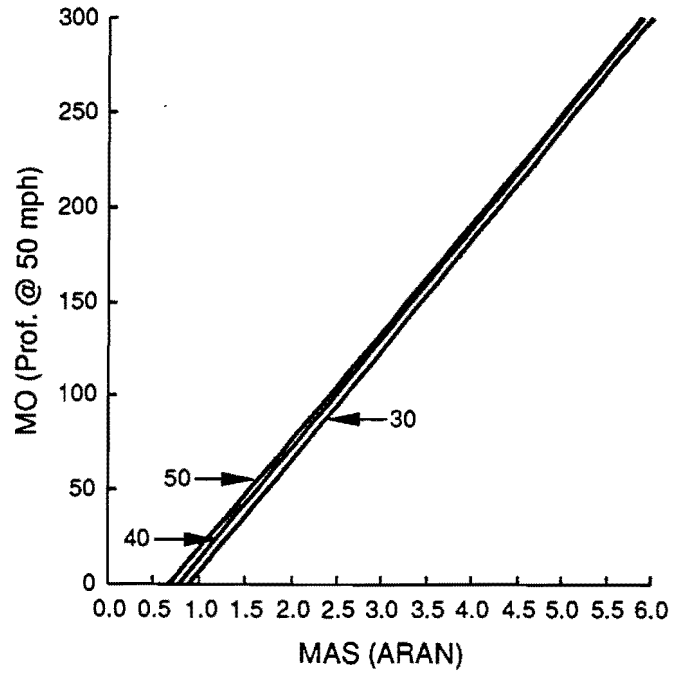


Fig B.10 Correlations between MAS (ARAN) and MO profilometer at 50 mph.

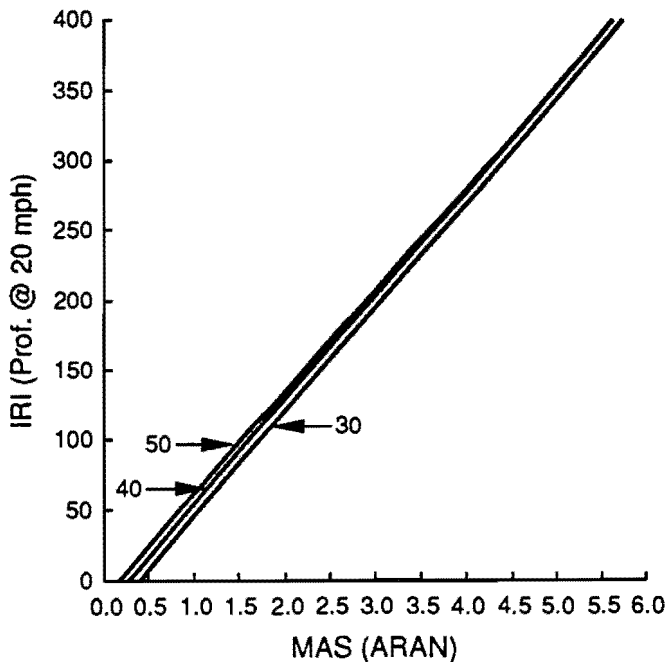


Fig B.11 Correlations between MAS (ARAN) and IRI profilometer at 20 mph.

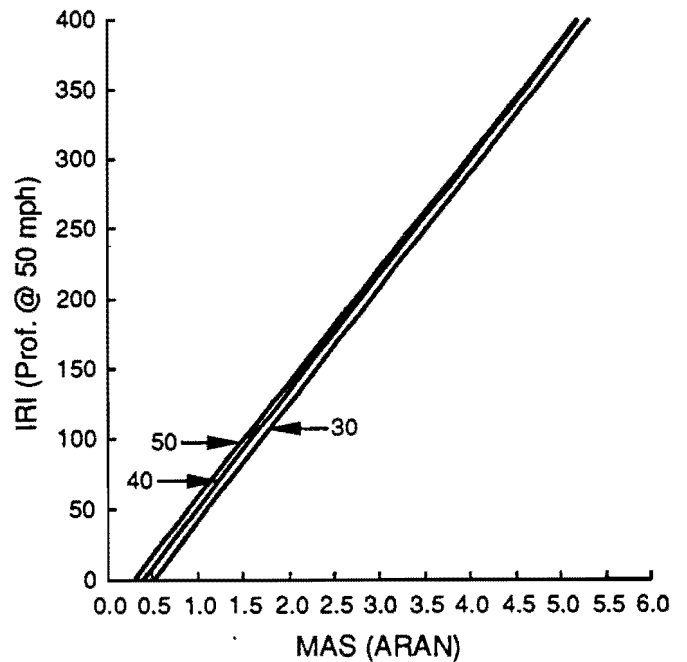


Fig B.12 Correlations between MAS (ARAN) and IRI profilometer at 50 mph.

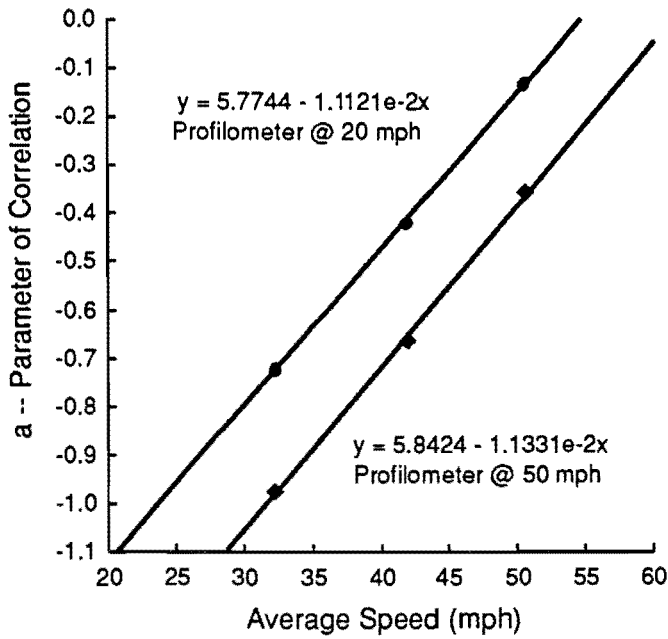


Fig B.13 Parameter of correlation (A) between SI (ARAN) and SI (Profilometer), as a function of average speed.

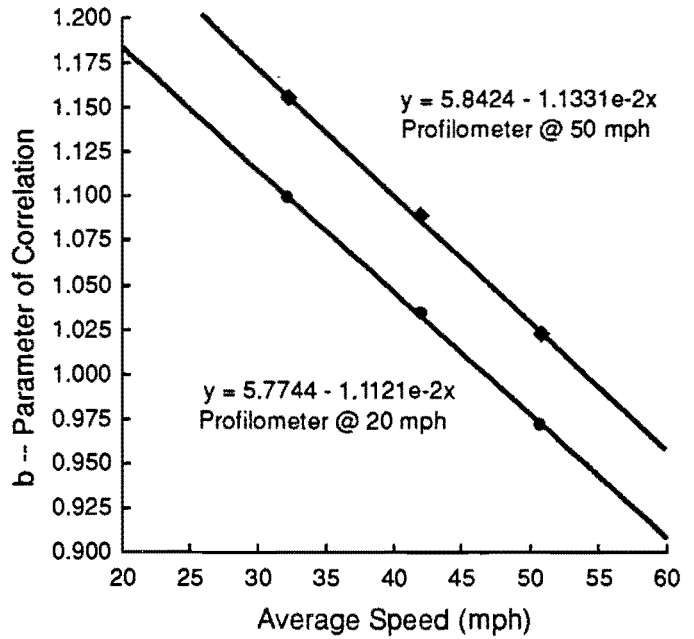


Fig B.14 Parameter of correlation (B) between SI (ARAN) and SI (Profilometer), as a function of average speed.

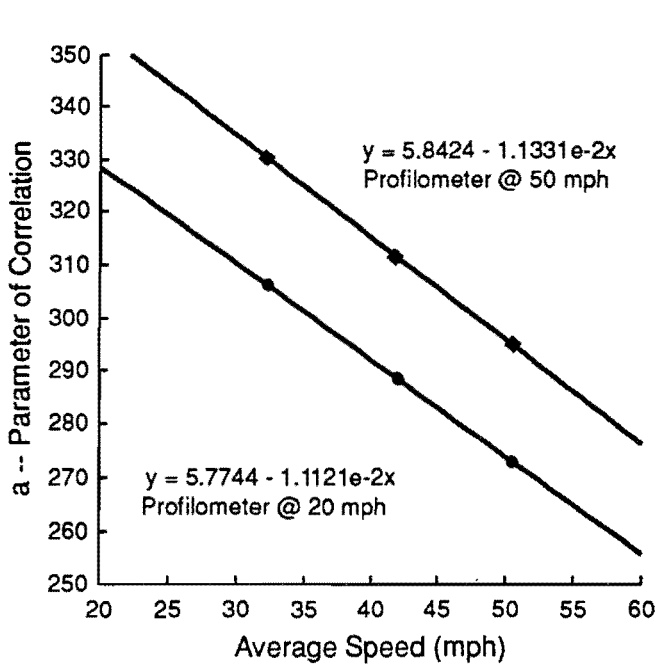


Fig B.15 Parameter of correlation (A) between SI (ARAN) and MO (Profilometer), as a function of average speed.

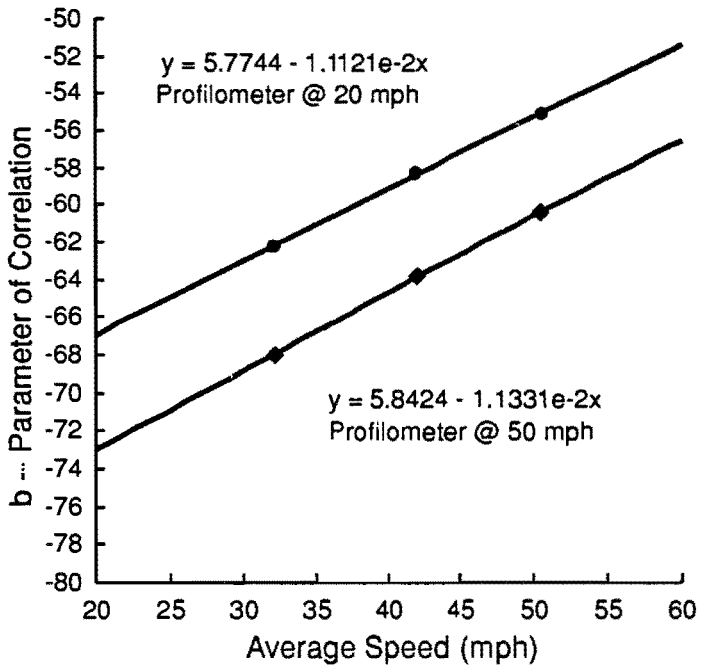


Fig B.16 Parameter of correlation (B) between SI (ARAN) and MO (Profilometer), as a function of average speed.

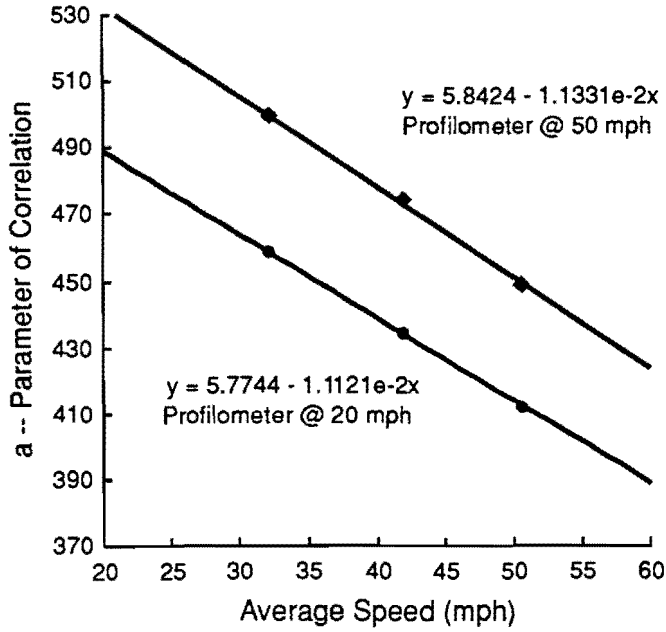


Fig B.17 Parameter of correlation (A) between SI (ARAN) and IRI (Profilometer), as a function of average speed.

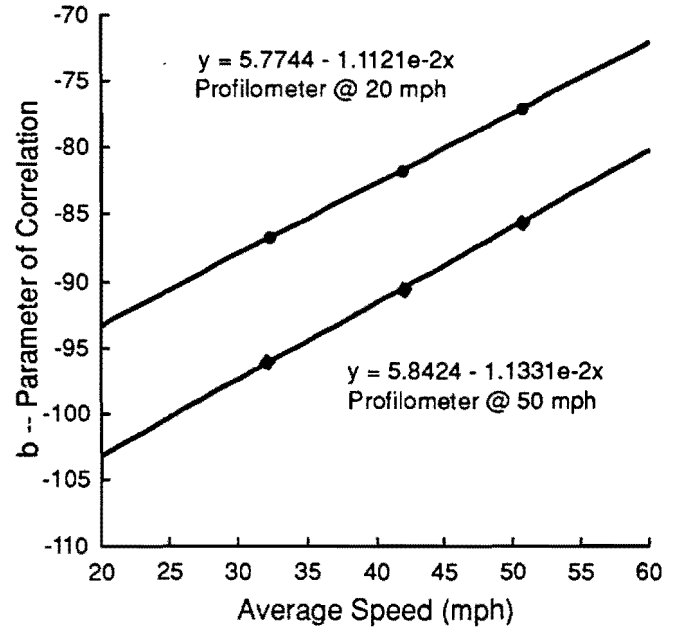


Fig B.18 Parameter of correlation (B) between SI (ARAN) and IRI (Profilometer), as a function of average speed.

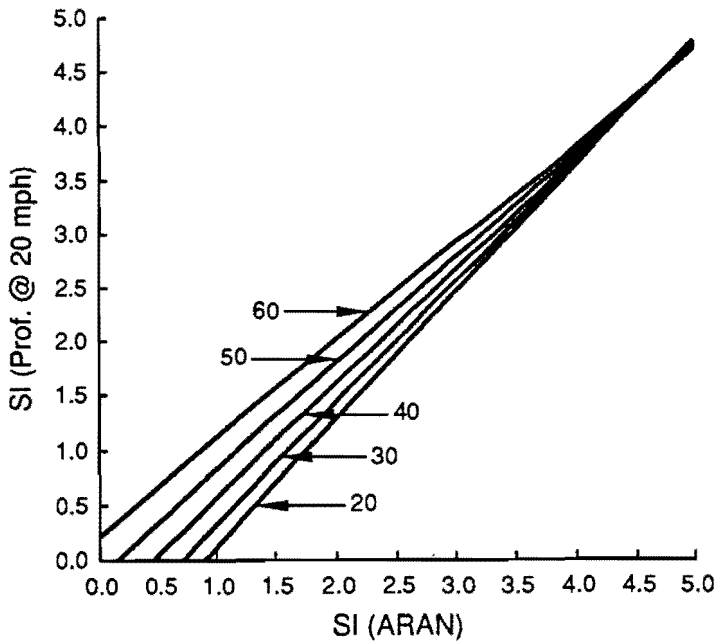


Fig B.19 Correlations between SI (ARAN) and SI profilometer at 20 mph.

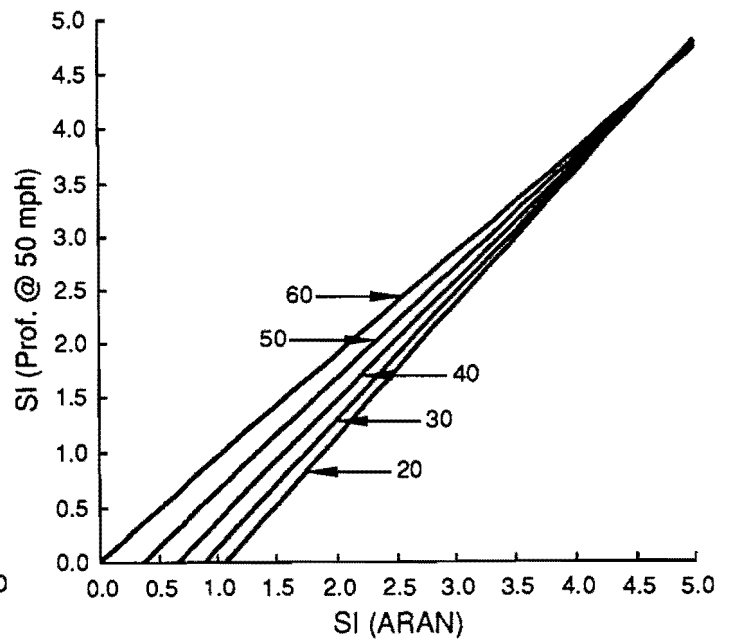


Fig B.20 Correlations between SI (ARAN) and SI profilometer at 50 mph.

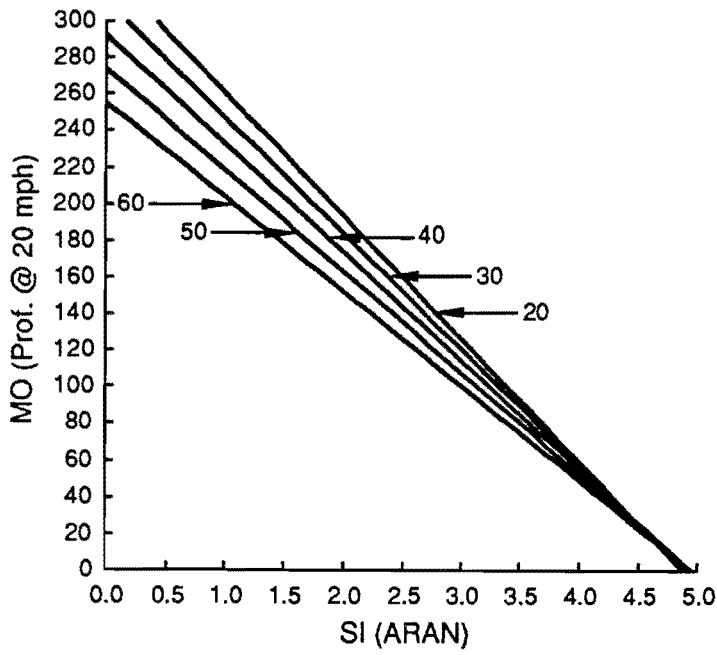


Fig B.21 Correlations between SI (ARAN) and MO profilometer at 20 mph.

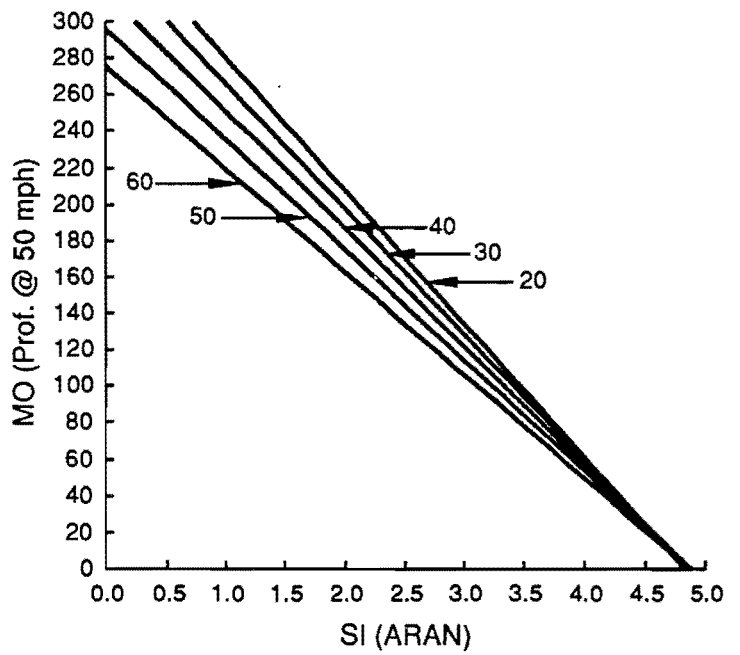


Fig B.22 Correlations between SI (ARAN) and MO profilometer at 50 mph.

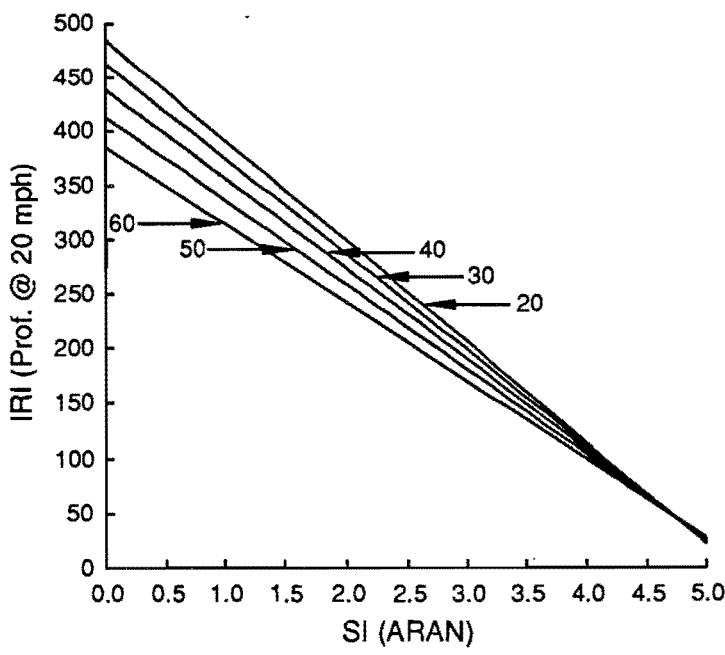


Fig B.23 Correlations between SI (ARAN) and IRI profilometer at 20 mph.

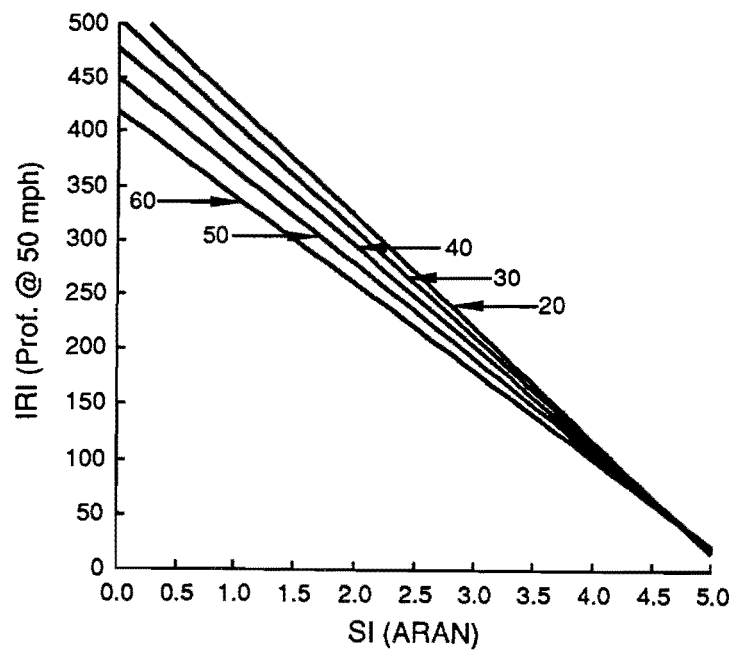


Fig B.24 Correlations between SI (ARAN) and IRI profilometer at 50 mph.

APPENDIX C. FIGURES FOR THE SPEED-EFFECT-CANCELING MODEL 2

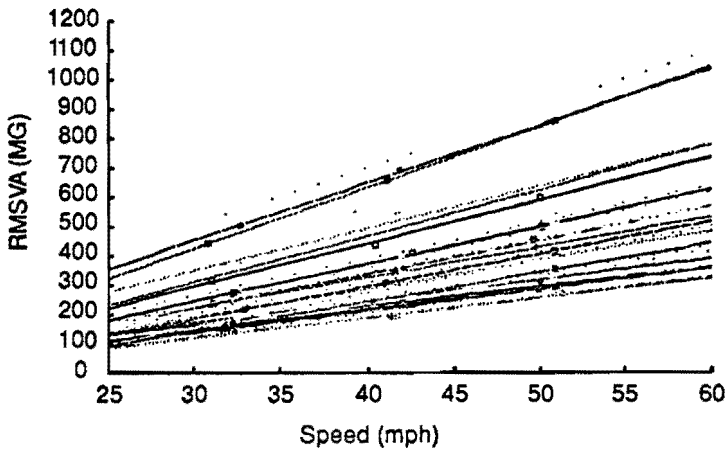


Fig C.1 Raw RMSVA (mg) versus testing speed.

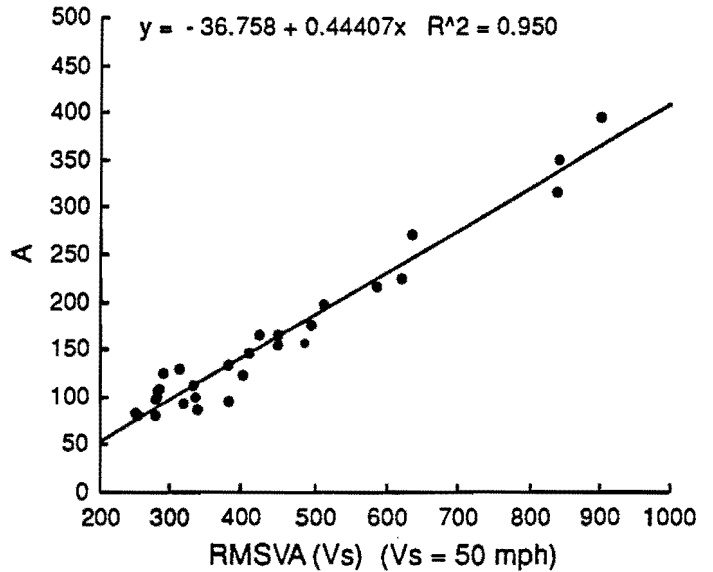


Fig C.2 Coefficient A versus RMSVA (Vs = 50 mph).

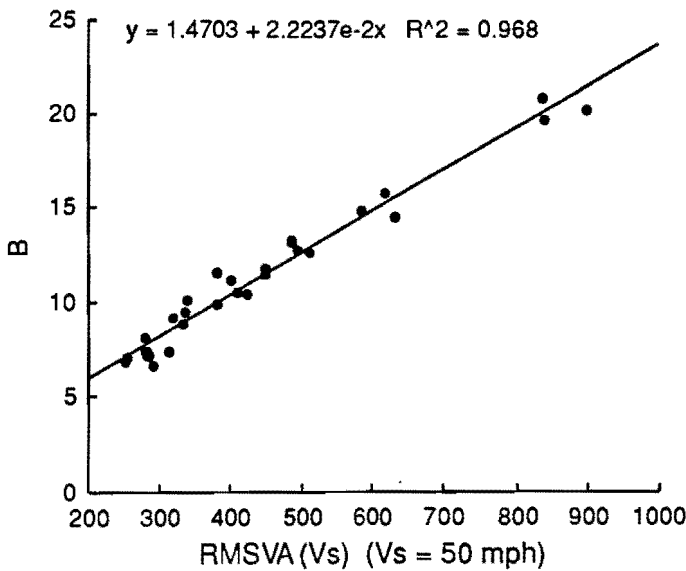


Fig C.3 Coefficient B versus RMSVA (Vs = 50 mph).

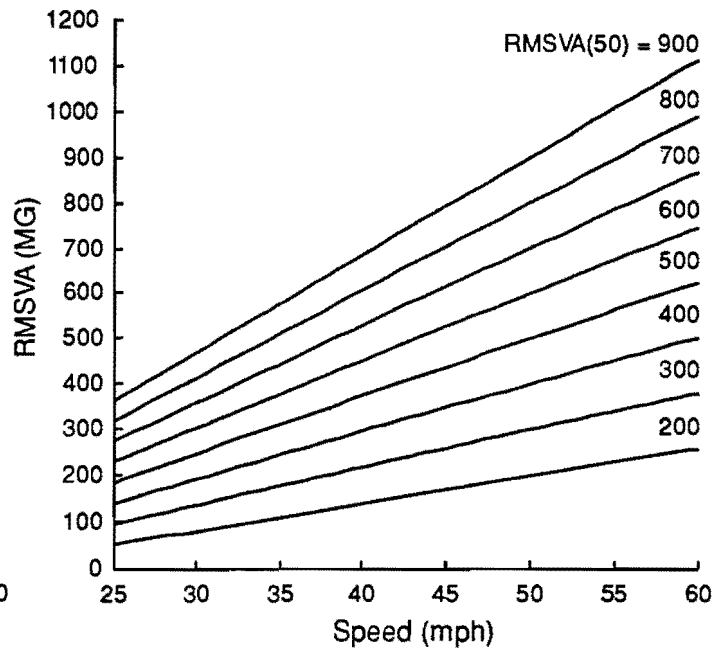


Fig C.4 Transformation of RMSVA at V_t to the standard RMSVA ($V_x = 50$ mph) by the speed-effect-canceling Model 2.

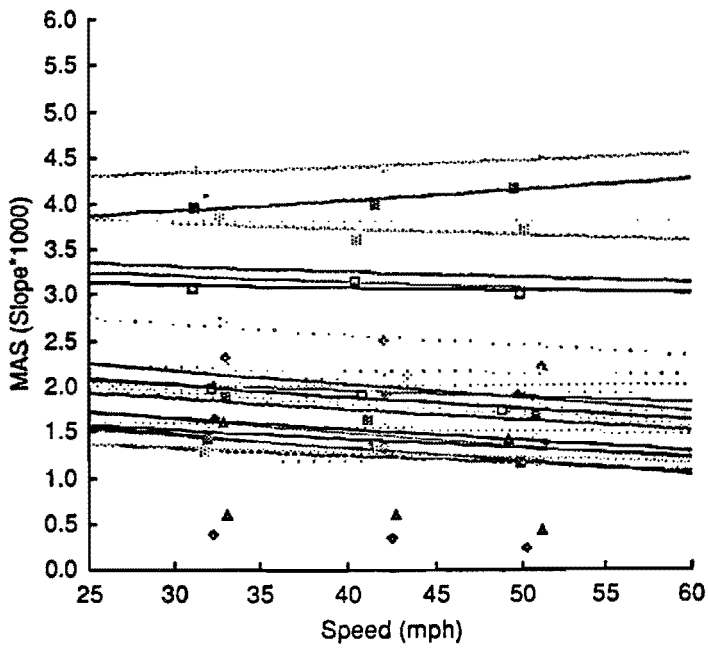


Fig C.5 Raw MAS (slope * 1000) versus testing speed.

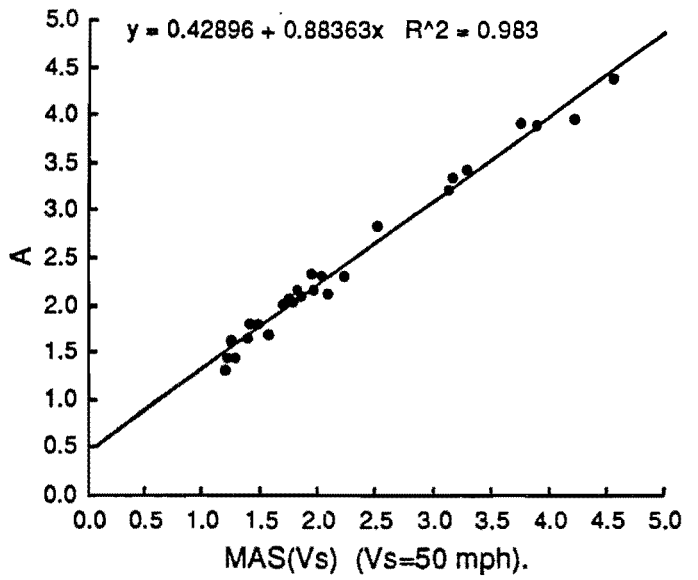


Fig C.6 Coefficient A versus MAS (Vs = 50 mph).

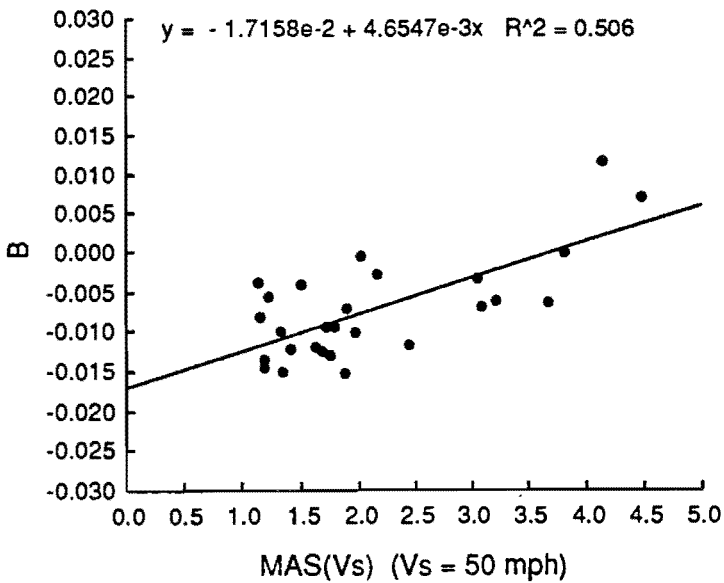


Fig C.7 Coefficient B versus MAS (Vs = 50 mph).

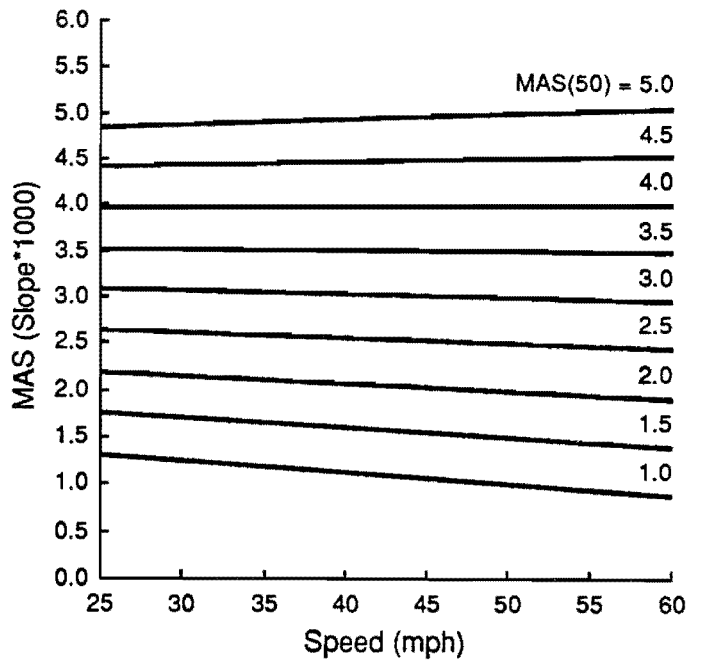


Fig C.8 Transformation of MAS at Vt to the standard MSA (Vs = 50 mph) by the speed-effect-canceling Model 2.

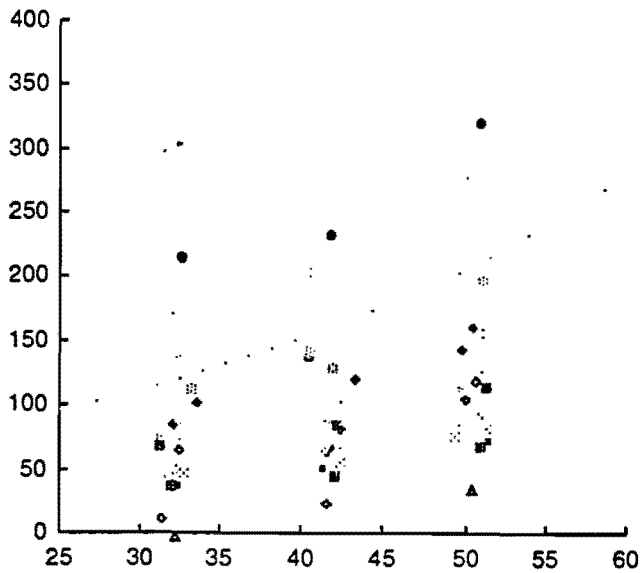


Fig C.9 Raw TEXTURE (mg) for flexible pavement versus testing speed.

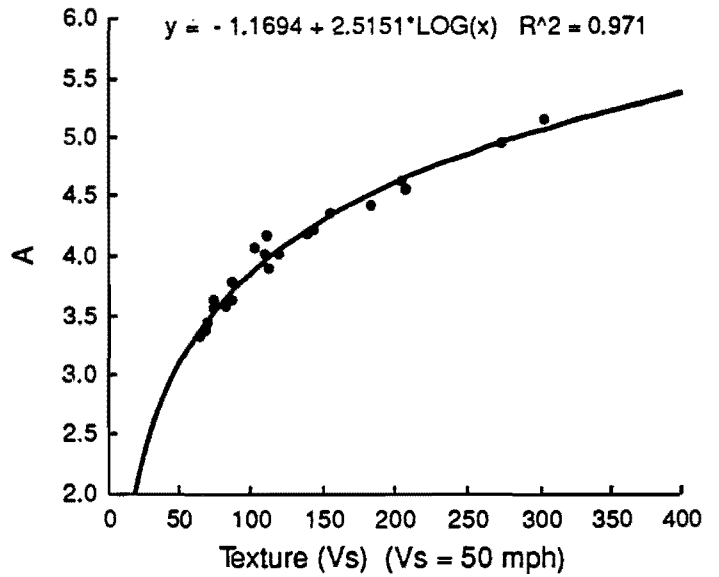


Fig C.10 Coefficient A versus TEXTURE for flexible pavement (Vs = 50 mph).

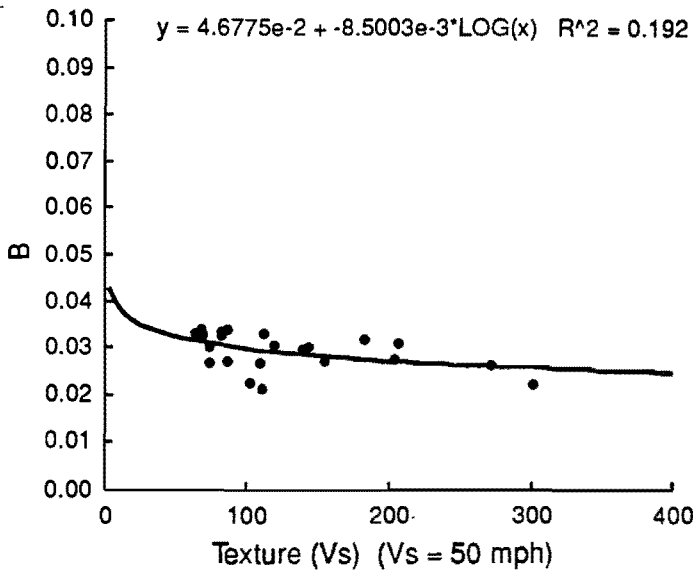


Fig C.11 Correlations between SI (ARAN) and SI profilometer at 20 mph.

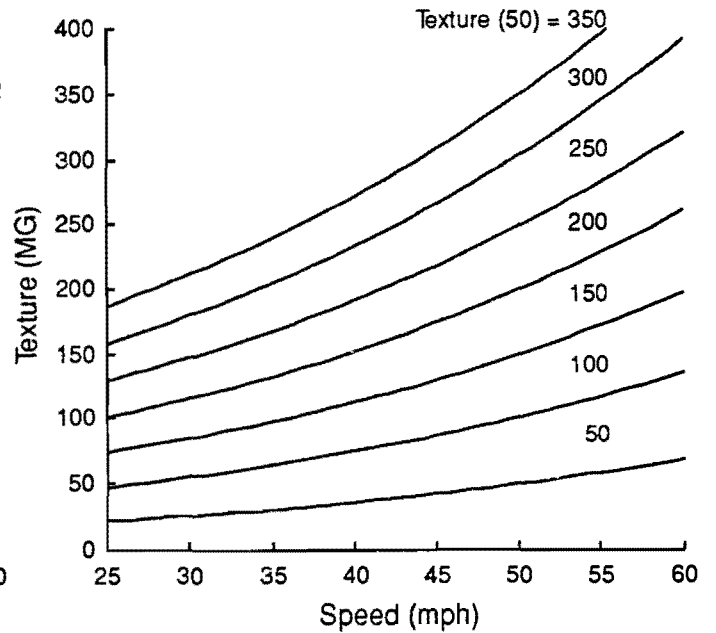


Fig C.12 Transformation of TEXTURE for flexible pavement at Vt to the standard RMSVA (Vs = 50 mph) by the speed-effect-canceling Model 2.

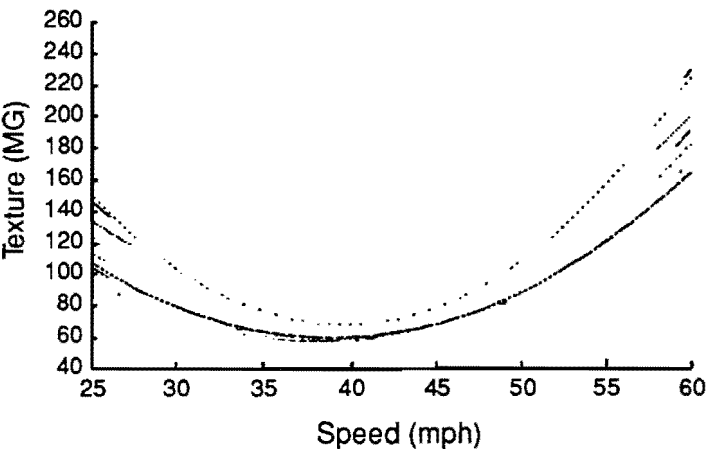


Fig C.13 Raw TEXTURE (mg) for rigid pavement versus testing speed.

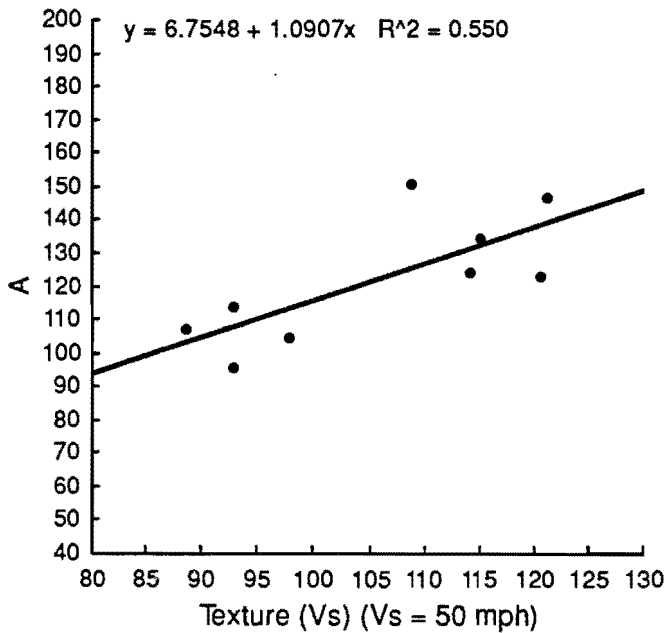


Fig C.14 Coefficient A versus TEXTURE for rigid pavement (Vs = 50 mph).

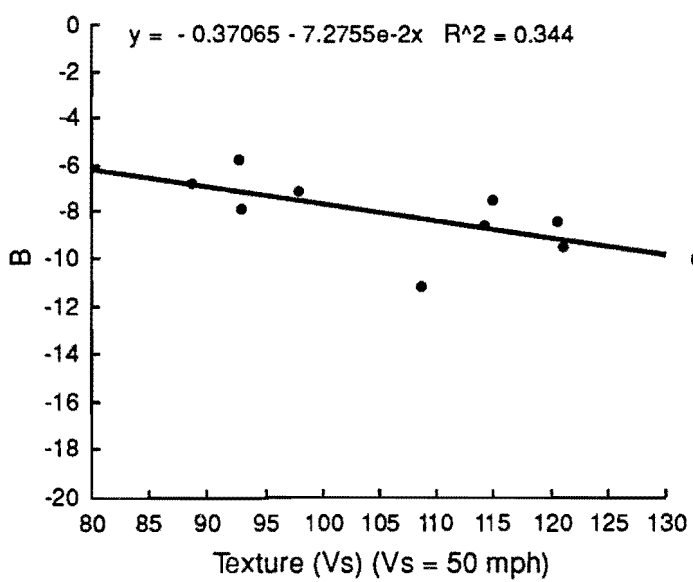


Fig C.15 Coefficient B versus TEXTURE for rigid pavement (Vs = 50 mph).

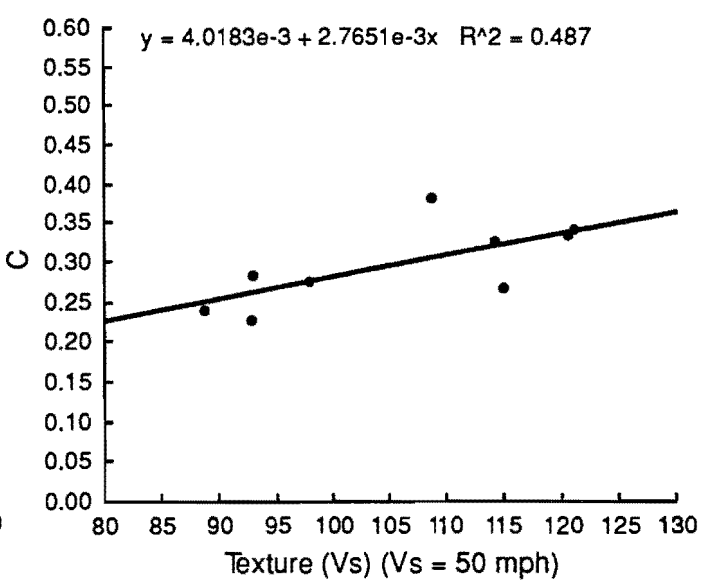


Fig C.16 Coefficient C versus TEXTURE for rigid pavement (Vs = 50 mph).

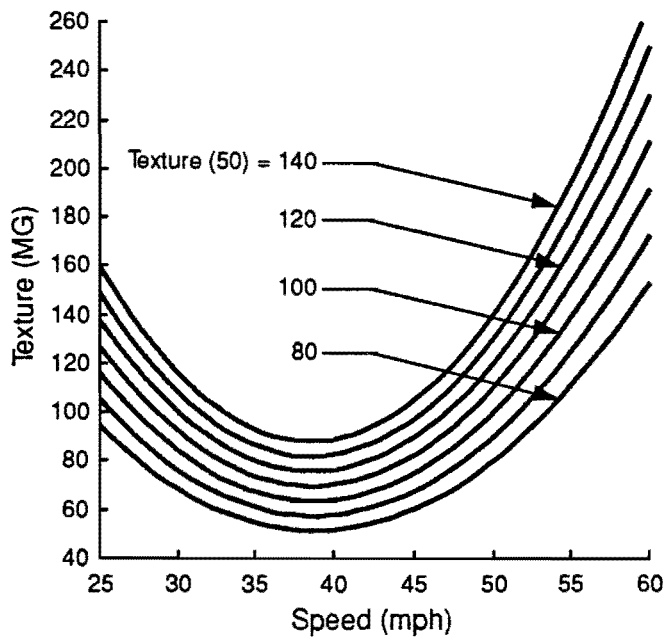


Fig C.17 Transformation of TEXTURE for rigid pavement at V_t to the standard RMSVA ($V_s = 50$ mph) by the speed-effect-canceling Model 2.

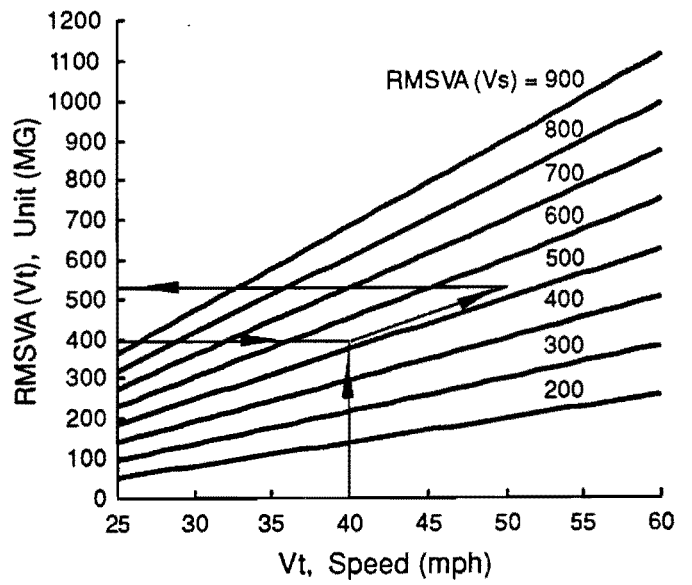


Fig C.18 Example: RMSVA ($V_t = 400$ mg) at $V_t = 40$ mph, then: RMSVA (50) = 533 mg, ($V_s = 50$ mph)

APPENDIX D. COMPUTER PROGRAM FOR NEW PSI MODELS

BACKGROUND

With the introduction last summer of a new PSI model of the ARAN Unit (Refs 1, 2, 3), the Texas SDHPT requested software that could be used to update the new model.

OBJECTIVE

That software has now been created, and this tech memo presents its particular structure and program lists (an example is also presented). The manual of operation will be provided in a later tech memo. (It should be mentioned that, although the new PSI model was developed for the K. J. Law Profilometer, the software can be used with other reference instruments as well.)

STRUCTURE OF THE SOFTWARE

Figure D.1 shows the software structure. The name of the data file is ABCDEFGH.XYZ, where

- AB = Test speed of reference instrument, such as 20
- CD = Test speed of ARAN, such as 50
- EF = Date of data collection (day), such as 01
- GH = Date of data collection (year), such as 89
- XYZ = Date of data collection (month), such as Aug.

The software is divided into two main blocks: (1) data inputs, and (2) data processing. The resulting outputs are:

- (1) New PSI model parameters
- (2) Root mean square error (RMSE)

$$RMSE = \sqrt{\frac{1}{N} \sum_{i=1}^N (x_i - \hat{x}_i)^2}$$

where

- N = the number of point
- x_i = SI value of the reference instrument
- \hat{x}_i = PSI of ARAN by new PSI model

(3) R² value (Ref 4)

$$R^2 = \frac{\left[\sum_{i=1}^N (x_i - \bar{x}) (\hat{x}_i - \bar{\hat{x}}) \right]^2}{\sum_{i=1}^N (x_i - \bar{x})^2 \sum_{j=1}^N (\hat{x}_j - \bar{\hat{x}})^2}$$

(4) Graphics of SI vs. PSI (option)

(5) The correlation parameter of SI (Reference Instruments) against PSI (ARAN)

$$SI = a + b PSI$$

where a and b are the correlation parameters. Theoretically, a and b should be

$$a \approx 0$$

$$b \approx 1$$

EXAMPLE D.1

Example D.1 shows the resulting outputs with data matrix given.

PROGRAM LISTS

Example D.2 shows the program lists of data input file, data processing file, and graphics file.

ACKNOWLEDGEMENTS

During the writing of this software, Terry Dossey provided invaluable assistance, particularly in the writing of the graphics file. I would like to express my thanks to him.

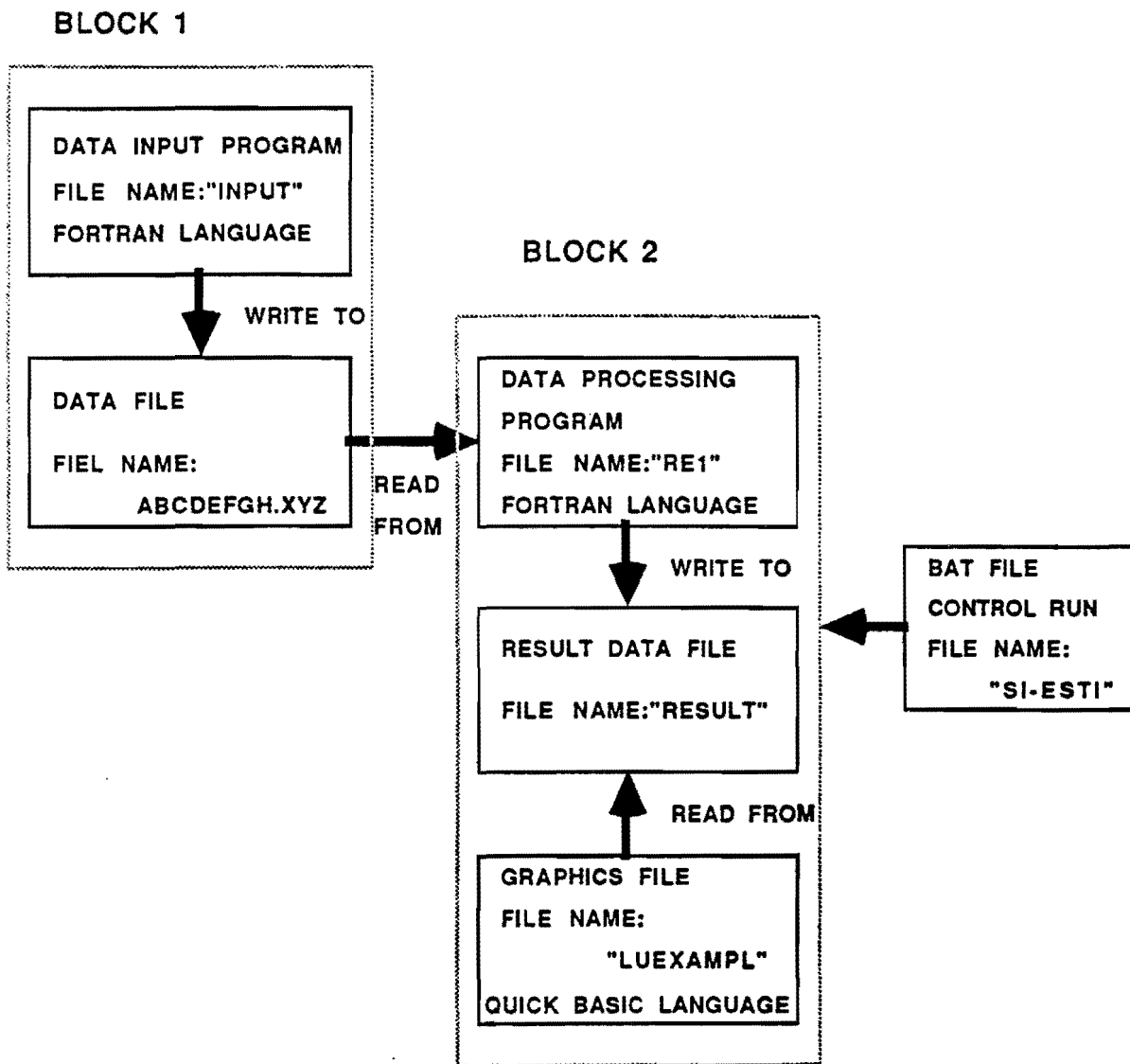


Fig D.1 New PSI software structure for estimating SI of reference instrument.

EXAMPLE D.1

EXAMPLE OF THE NEW PSI MODEL SOFTWARE

Data Matrix			
SI of Ref.	RMSVA	MAS	PSI of ARAN
1.96	311.80	3.08	2.51
3.66	240.00	2.03	3.49
1.42	346.00	3.84	1.81
4.46	176.00	1.30	4.19
3.40	157.00	1.90	3.68
3.80	222.30	1.97	3.56
4.36	178.30	1.20	4.27
4.02	174.00	1.51	4.01
.93	436.70	5.68	.12
1.19	235.70	4.37	1.45
2.01	233.30	3.96	1.81
4.19	133.70	1.57	3.99
3.53	176.00	2.21	3.39
1.62	530.00	3.85	1.63
4.33	148.00	1.46	4.08
1.91	324.00	3.14	2.44
2.15	267.00	2.91	2.70
3.73	135.70	1.66	3.91
4.16	131.00	1.29	4.24
2.35	496.30	3.23	2.21
2.75	259.50	2.00	3.50
3.86	308.00	1.89	3.55
4.14	161.00	1.71	3.84
4.02	160.70	1.62	3.92
4.39	148.30	1.42	4.11
3.03	372.30	2.49	2.97
2.94	298.70	2.38	3.13
2.84	294.00	2.78	2.79
2.76	404.30	2.90	2.58

Results — Coefficients:

A(1) = 5.487830

A(2) = -.000923

A(3) = -.873877

Root mean square error: RMSE = .3291E + 00

R square value: R² = .904

Model coefs between SI of ref and PSI of ARAN:

A = .0000

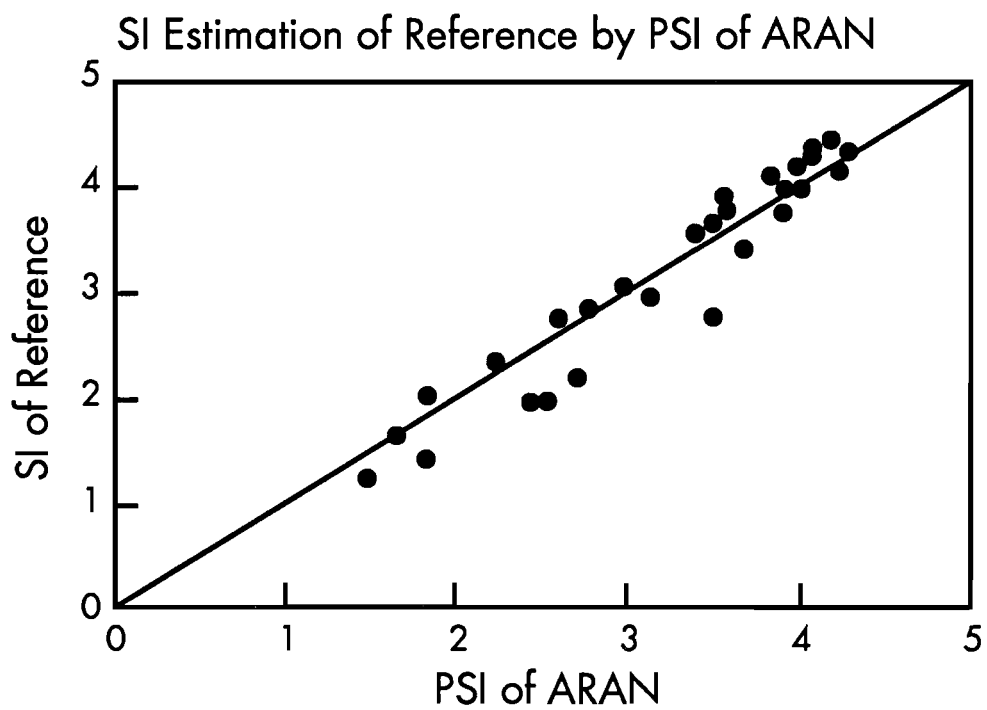
B = 1.0000

Date of data processing: Jan 01, 89

Speed of ref. instrument: SPEED = 20 (mph)

Speed of ARAN: SPEED = 30 (mph)

Data file name: 20300189 Jan



20300189.JAN

EXAMPLE D.2

PROGRAM LISTS:

1. Data Input File
2. Data Processing File
3. Graphics File

```

C*****
CTHIS IS A DATA INPUT PROGRAM OF PSI ESTIMATION SOFTWARE OF ARAN
CDEVELOPED BY JIAN LU OF THE CENTER FOR TRANSPORTATION RESEARCH
COF THE UNIVERSITY OF TEXAS AT AUSTIN IN Oct., 1989.
C*****
CCLEANING SCREEN SUBROUTINE
SUBROUTINE CLEANSCREEN
DO 310 I=1,23
WRITE(*,300)
  300FORMAT(' ')
  310CONTINUE
RETURN
END
C DATA INPUT MAIN PROGRAM
PROGRAM DATAINPUT
DIMENSION SUM4(3,1000)
CHARACTER*12 SS
CHARACTER*11 SD
CHARACTER DATEDA(2)
CHARACTER DATEMO(3)
CHARACTER DATEYE(2)
CHARACTER SPEDAR(2)
CHARACTER SPEDPR(2)
CHARACTER FI(12)
CHARACTER FD(11)
CHARACTER*1 Q
EQUIVALENCE (SD, FD(1))
EQUIVALENCE (SS, FI(1))
  100CALL CLEANSCREEN
C SHOW SOME INSTRUCTIONS
WRITE(*,1)
  1FORMAT(//,9X,'< PSI ESTIMATION MODEL OF ARAN--DATA INPUT FILE >'\)
WRITE(*,2)
  2FORMAT(/,9X,' *****'\)
WRITE(*,3)
  3FORMAT(//,10X,' MODEL: PSI=A(1) + A(2)*RMSVA + A(3)*MAS'\)
WRITE(*,4)
  4FORMAT(//,10X,' INSTRUCTION OF DATA FILE NAME CREATION:\)
WRITE(*,5)
  5FORMAT(//,15X,'DATA FILE: ABCDEFGH.XYZ, e.g. 20500189.AUG'\)
WRITE(*,6)
  6FORMAT(//,18X,'AB-TEST SPEED (MPH) OF REF. INSTRUMENT, e.g. 20')
WRITE(*,7)
  7FORMAT(/,18X,'CD-TEST SPEED (MPH) OF ARAN, e.g. 50')
WRITE(*,8)
  8FORMAT(/,18X,'EF-DATE OF DATA PROCESSING (DAY), e.g. 01')
WRITE(*,9)
  9FORMAT(/,18X,'GH-DATE OF DATA PROCESSING (YEAR), e.g. 89')
WRITE(*,10)
  10FORMAT(/,18X,'XYZ-DATE OF DATA PROCESSING (MONTH), e.g. AUG'\)
WRITE(*,11)
  11FORMAT(//,10X,' NOTE: DATA FILE CAN BE REVISED BY EDIT'\)
WRITE(*,12)
  12FORMAT(//,' CONTINUE ? (Y/N)\)
READ (*,13) Q
  13FORMAT(A1)
IF (Q.NE.'Y') GOTO 210
C INPUT DATE OF DATA PROCESSING
WRITE(*,14)
  14FORMAT(//,' DATE=? (MONTH)\)
READ (*,15) DATEMO
  15FORMAT(3A1)
WRITE(*,20)
  20FORMAT(//,' DATE=? (DAY)\)
READ (*,25) DATEDA
  25FORMAT(2A1)
WRITE(*,30)
  30FORMAT(//,' DATE=? (YEAR)\)
READ (*,35) DATEYE
  35FORMAT(2A1)
C INPUT TESTING SPEED
WRITE(*,40)

```

```

40FORMAT(//,' SPEED=? (MPH) (REFERENCE INSTRUMENT)'\)\)
READ (*,45) SPEDPR
45FORMAT(2A1)
WRITE(*,50)
50FORMAT(//,' SPEED=? (MPH) (ARAN)'\)\)
READ (*,55) SPEDAR
55FORMAT(2A1)
ORGANIZE DATA FILE NAME
DO 60 I=1,2
60FI(I)=SPEDPR(I)
DO 70 I=1,2
70FI(I+2)=SPEDAR(I)
DO 80 I=1,2
80FI(I+4)=DATEDA(I)
DO 90 I=1,2
90FI(I+6)=DATEYE(I)
FI(9)='.'
DO 100 I=1,3
100FI(I+9)=DATEMO(I)
CINPUT NUMBER OF TEST SECTION
WRITE(*,101)
101FORMAT(//,' SECTION NUMBER L=?'\)\)
READ (*,*) L
ORGANIZE THE FORM OF DATE OF DATA PROCESSING
DO 102 I=1,3
102FD(I)=DATEMO(I)
DO 103 I=1,2
103FD(I+5)=DATEDA(I)
DO 104 I=1,2
104FD(I+9)=DATEYE(I)
FD(4)='.'
FD(8)='.'
CALL CLEANSCREEN
CSHOW INPUT PARAMETERS
WRITE(*,105) SD
105FORMAT(//,10X,'DATE OF DATA PROCESSING : ',A11,\)\)
WRITE(*,111) SPEDPR
111FORMAT(//,10X,'SPEED OF REF. INSTRUMENT = ',2A1,' (MPH)',\)\)
WRITE(*,112) SPEDAR
112FORMAT(//,10X,'SPEED OF ARAN = ',2A1,' (MPH)',\)\)
WRITE(*,113) L
113FORMAT(//,10X,'SECTION NUMBER : L=',I3,\)\)
WRITE(*,114) SS
114FORMAT(//,10X,'DATA FILE NAME : ',A12,\)\)
WRITE(*,116)
116FORMAT(//,' IS THIS INFORMATION CORRECT ? (Y/N)',\)\)
READ (*,118) Q
118FORMAT(A1)
IF (Q.NE.'Y') GOTO 1000
2000CALL CLEANSCREEN
CINPUT DATA OF FIELD TESTS
119WRITE(*,120)
120FORMAT(//,' ENTER -SI OF REF. INSTRUMENT-(REENTRE: PRESS Q)'\)\)
DO 130 I=1,L
WRITE(*,122) I
122FORMAT(//,' SI(',I3,')= '\)\)
130READ(*,*,ERR=119) SUM4(1,I)
CALL CLEANSCREEN
133WRITE(*,131)
131FORMAT(//,' ENTER -RMSVA OF ARAN-(REENTRE: PRESS Q)'\)\)
DO 140 I=1,L
WRITE(*,132) I
132FORMAT(//,' RMSVA(',I3,')= '\)\)
140READ(*,*,ERR=133) SUM4(2,I)
CALL CLEANSCREEN

```

```

143WRITE(*,141)
141FORMAT(//,' ENTER -MAS OF ARAN-(REENTRE: PRESS Q)'\)
DO 150 I=1,L
WRITE(*,142) I
142FORMAT(//,' MAS(',I3,')= '\)
150READ(*,*,ERR=143) SUM4(3,I)
CALL CLEANSCREEN
WRITE(*,*) ' WANT TO SEE DATA MATRIX ? (Y/N)'
READ(*,151) Q
151FORMAT(A1)
IF (Q.NE.'Y') GOTO 184
CALL CLEANSCREEN
CSHOW DATA INPUTED BY THE SCREEN
WRITE(*,160)
160FORMAT(//,10X,'INPUT DATA MATRIX, (USE PAUSE KEY)',\)
WRITE(*,165)
165FORMAT(//,15X,' SI OF REF. RMSVA      MAS',\)
WRITE(*,170)
170FORMAT('')
DO 185 JJ=1,L
WRITE(*,175) (SUM4(I1,JJ),I1=1,3)
175FORMAT(15X,3F10.2)
DO 180 KK=1,3000
DO 179 MM=1,100
KKK=0
179CONTINUE
180CONTINUE
185CONTINUE
WRITE(*,182)
182FORMAT(//,' IS THIS DATA CORRECT ? (Y/N)',\)
READ(*,183) Q
183FORMAT(A1)
IF (Q.NE.'Y') GOTO 2000
CSAVE DATA TO DISC
184OPEN(5,FILE=SS, STATUS='NEW')
WRITE(5,*) L
DO 200 I=1,L
WRITE(5,190) (SUM4(K,I),K=1,3)
190FORMAT(2X,3F8.2)
200CONTINUE
CLOSE (5)
210STOP

```

```

C*****
CTHIS IS A DATA PROCESSING PROGRAM OF PSI ESTIMATION SOFTWARE OF
CARAN DEVELOPED BY Mr. JIAN LU OF THE CENTER FOR TRANSPORTATION
CRESEARCH OF THE UNIVERSITY OF TEXAS AT AUSTIN IN Oct., 1989.
C*****
CINSTRUCTION SUBROUTINE
SUBROUTINE INSTRUCTION
CHARACTER*1 Q
WRITE(*,1)
  1FORMAT(//,9X,'< PSI ESTIMATION MODEL OF ARAN-PROCESSING FILE >'\\)
WRITE(*,2)
  2FORMAT(/,9X,' *****'\\)
WRITE(*,3)
  3FORMAT(//,10X,' MODELt - PSI=A(1) + A(2)*RMSVA + A(3)*MAS'\\)
WRITE(*,4)
  4FORMAT(//,10X,' INSTRUCTION OF DATA FILE NAME CREATION:'\\)
WRITE(*,5)
  5FORMAT(//,15X,'DATA FILE: ABCDEFGH.XYZ, e.g. 20500189.AUG'\\)
WRITE(*,6)
  6FORMAT(//,18X,'AB-TEST SPEED (MPH) OF REF. INSTRUMENT, e.g. 20')
WRITE(*,7)
  7FORMAT(/,18X,'CD-TEST SPEED (MPH) OF ARAN, e.g. 50')
WRITE(*,8)
  8FORMAT(/,18X,'EF-DATE OF DATA PROCESSING (DAY), e.g. 01')
WRITE(*,9)
  9FORMAT(/,18X,'GH-DATE OF DATA PROCESSING (YEAR), e.g. 89')
WRITE(*,10)
  10FORMAT(/,18X,'XYZ-DATE OF DATA PROCESSING (MONTH), e.g. AUG'\\)
WRITE(*,11)
  11FORMAT(//,' CONTINUE ? (Y/N)'\\)
READ(*,12) Q
  12FORMAT(A1)
  IF (Q.NE.'Y') GOTO 13
  RETURN
  13STOP
END
CREGRESSION SUBROUTINE
SUBROUTINE TRIREG(N,M,NN,IO,SUM,U,V,R,P,MAX,IC)
DIMENSION SUM(N,M),U(N),V(N),R(NN),IC(N)
K1=0
      DO 19 I1=1,N
        19U(I1)=0.0
      DO 20 I1=1,NN
        20R(I1)=0.0
      DO 30 I1=1,M
        DO 40 J1=1,N
          40V(J1)=SUM(J1,I1)
        J1=0
      DO 30 I2=1,N-
        D=V(I2)
        U(I2)=U(I2)+D
      DO 30 I3=I2,N
        J1=J1+1
        30R(J1)=R(J1)+V(I3)*D
      J1=1
      A=1.0/FLOAT(M)
      DO 50 I1=1,N
        P=R(J1)-(U(I1)**2)*A
        IF(P-1.0E-0)51,51,52
        51V(I1)=0.0
      GO TO 53
        52V(I1)=1.0/SQRT(P)
        53R(J1)=1.0
        50J1=J1+N+1-I1
      J1=1
      DO 60 I1=1,N
        D=A*U(I1)
        P=V(I1)
        J1=J1+1
        U(I1)=D
        I11=I1+1
      DO 60 I2=I11,N

```

```

R(J1)=(R(J1)-D*U(I2))*V(I2)*P
60J1=J1+1
I1=-N
I2=N+1
DO 70 I3=1,N
I1=I1+I2-I3
70IC(I3)=I1
ID1=ID+1
DO 110 I1=ID1,N
J1=IC(I1)
IF(V(I1).EQ.0.0) GO TO 210
J11=J1+I1
P=1.0/R(J11)
IF(P.GT.PMAX) GO TO 210
R(J11)=P
I11=I1-1
DO 120 I2=1,I11
J2=IC(I2)
J12=J2+I1
A=P*R(J12)
DO 120 I3=I2,N
IF(I3-I1)130,120,150
130J3=IC(I3)
J13=J3+I1
D=R(J13)
GO TO 140
150J113=J1+I3
D=-R(J113)
140J123=J2+I3
R(J123)=R(J123)+D*A
120CONTINUE
I11=I1+1
DO 160 I2=I11,N
J112=J1+I2
A=P*R(J112)
J2=IC(I2)
DO 160 I3=I2,N
J123=J2+I3
J113=J1+I3
160R(J123)=R(J123)-A*R(J113)
220I11=I1-1
DO 170 I2=1,I11
J2=IC(I2)+I1
170R(J2)=-P*R(J2)
J111=J1+I1+1
NJ1=N+J1
DO 180 I2=J111,NJ1
180R(I2)=P*R(I2)
GO TO 110
210P=0.0
K1=K1+1
J111=J1+I1
R(J111)=0.0
GO TO 220
110CONTINUE
D=1.0/FLOAT(M-N+ID-1+K1)
DO 310 I1=1,ID
IF(V(I1).EQ.0.0)GO TO 330
A=0.0
P=1.0/V(I1)
J1=IC(I1)
ID1=ID+1
DO 320 I2=ID1,N
IF(ABS(R(I2)).LT.1.0E-8) GO TO 320
J112=J1+I2
R(J112)=-R(J112)*V(I2)*P
A=A+R(J112)*U(I2)
320CONTINUE
J111=J1+I1
V(I1)=(2-R(J111))*D/V(I1)**2
R(J111)=U(I1)-A

```

```

GO TO 310
  330J1=IC(11)
  J11=J1+11
  JN1=J1+N
DO 340 I2=J11,JN1
  340R(12)=0.0
  310CONTINUE
A=1.0/FLOAT(M)
ID1=ID+1
DO 410 I1=ID1,N
  IF(V(I1).NE.0.0) V(I1)=A/V(I1)**2
  410CONTINUE
RETURN
END
CCLEAN SCREEN SUBROUTINE
SUBROUTINE CLEANSCREEN
DO 701 I=1,23
WRITE(*,700)
  700FORMAT(' ')
  701CONTINUE
RETURN
END
CMAIN PROGRAM
PROGRAM TR
CMULTI. REGRESSION--SEE FORTRAN PROGRAM COLLECTION VOL.2 P444-CHINA
CN=3
CCD=3 -- # OF COEFFICIENT
CM=NUMBER OF SECTION
CNN=N*(N+1)/2
CID=1
CDIMENSION SUM4(N,M),U4(N),V4(N),R4(NN),IC4(N)
DIMENSION SUM4(3,1000),U4(3),V4(3),R4(6),IC4(3)
CHARACTER*12 SS
CHARACTER*11 SD
CHARACTER DATEDA(2)
CHARACTER DATEMO(3)
CHARACTER DATEYE(2)
CHARACTER SPEDAR(2)
CHARACTER SPEDPR(2)
CHARACTER FI(12)
CHARACTER FD(11)
EQUIVALENCE (SS,FI(1))
EQUIVALENCE (SD,FD(1))
  601CALL CLEANSCREEN
CALL INSTRUCTION
CALL CLEANSCREEN
CDATA FILE NAME INPUT
WRITE(*,600)
  600FORMAT('/', ' DATE=? (MONTH)'\')
READ(*,605) DATEMO
  605FORMAT(3A1)
WRITE(*,610)
  610FORMAT('/', ' DATE=? (DAY)'\')
READ(*,615) DATEDA
  615FORMAT(2A1)
WRITE(*,620)
  620FORMAT('/', ' DATE=? (YEAR)'\')
READ(*,625) DATEYE
  625FORMAT(2A1)
WRITE(*,630)
  630FORMAT('/', ' SPEED=? (MPH) (REFERENCE INSTRUMENT)'\')
READ(*,635) SPEDPR
  635FORMAT(2A1)
WRITE(*,640)
  640FORMAT('/', ' SPEED=? (MPH) (ARAN)'\')
READ(*,645) SPEDAR
  645FORMAT(2A1)
DO 650 I=1,2
  650FI(I)=SPEDPR(I)
DO 660 I=1,2
  660FI(I+2)=SPEDAR(I)

```

```

DO 670 I=1,2
  670FI(I+4)=DATEDA(I)
DO 680 I=1,2
  680FI(I+6)=DATEYE(I)
  FI(9)='.'
DO 690 I=1,3
  690FI(I+9)=DATEMO(I)
DO 691 I=1,3
  691FD(I)=DATEMO(I)
DO 692 I=1,2
  692FD(I+5)=DATEDA(I)
DO 693 I=1,2
  693FD(9+I)=DATEYE(I)
  FD(4)='.'
  FD(8)='.'
  CSHOW TESTING CONDITIONS AND DATE OF DATA PROCESSING ON SCREEN
  CALL CLEANSSCREEN
  WRITE(*,700) SD
  700FORMAT(/,10X,'DATE OF DATA PROCESSING: 'A11,\)
  WRITE(*,701) SPEDPR
  701FORMAT(/,10X,'SPEED OF REF. INSTRUMENT: SPEED=',2A1,' (MPH)',\))
  WRITE(*,702) SPEDAR
  702FORMAT(/,10X,'SPEED OF ARAN: SPEED=',2A1,' (MPH)',\))
  WRITE(*,703) SS
  703FORMAT(/,10X,'DATA FILE NAME: ',A12,\)
  WRITE(*,706)
  706FORMAT(/,' IS THIS INFORMATION CORRECT ? (Y/N)',\))
  READ(*,704) Q
  704FORMAT(A1)
  IF (Q.NE.'Y') GOTO 601
  COPEN PRINTER
  OPEN(1,FILE='LPT1:')
  CPRINT TESTING CONDITIONS AND DATE OF DATA PROCESSING
  WRITE(*,694) SD
  WRITE(1,694) SD
  694FORMAT(/,' DATE OF DATA PROCESSING: ',A11,\)
  WRITE(*,695) SPEDPR
  WRITE(1,695) SPEDPR
  695FORMAT(/,' SPEED OF REF. INSTRUMENT: SPEED=',2A1,' (MPH)',\))
  WRITE(*,696) SPEDAR
  WRITE(1,696) SPEDAR
  696FORMAT(/,' SPEED OF ARAN: SPEED=',2A1,' (MPH)',\))
  WRITE(*,697) SS
  WRITE(1,697) SS
  697FORMAT(/,' DATA FILE NAME: ',A12,\)
  COPEN DATA FILE AND READ IT

  N=3
  ND=3
  NN=N*(N+1)/2
  ID=1
  OPEN(3,FILE=SS)
  READ(3,*) M
  DO 496 JJ=1,M
    496READ(3,*) (SUM4(II,JJ),II=1,N)
  CLOSE (3)
  PEP=10.0E8
  CTRANSFER TO REGRESSION SUBROUTINE
  CALL TRIREG(N,M,NN,ID,SUM4,U4,U4,R4,PEP,IC4)
  CPRINT DATA MATRIX
  WRITE(*,501)
  WRITE(1,501)
  501FORMAT(/,2X,'DATA MATRIX'\)
  WRITE(*,1000)
  WRITE(1,1000)
  1000FORMAT(/,2X,' SI OF REF. RMSUA      MAS      PSI OF ARAN',\))
  WRITE(*,502)
  WRITE(1,502)
  502FORMAT('')
  DO 504 JJ=1,M
    PSI=R4(1)+R4(2)*SUM4(2,JJ)+R4(3)*SUM4(3,JJ)
  WRITE(*,503) (SUM4(II,JJ),II=1,N),PSI
  WRITE(1,503) (SUM4(II,JJ),II=1,N),PSI
  503FORMAT(2X,4F10.2)
  504CONTINUE

```

```

CPRINT REGRESSION COEFFICIENTS
WRITE(*,510)
WRITE(1,510)
  510FORMAT(/,' RESULTS--COEFFICIENTS:\')
WRITE(*,511)
WRITE(1,511)
  511FORMAT('')
DO 520 I=1,3
WRITE(*,512) I, R4(I)
WRITE(1,512) I, R4(I)
  512FORMAT(2X,'A(',I1,')=' ,F12.6)
  520CONTINUE
CCALCULATE ROOT MEAN SQUARE ERROR AND R-SQUARE VALUE
SV=0
RX=0
RY=0
DO 550 I=1,M
XI=R4(1)+R4(2)*SUM4(2,I)+R4(3)*SUM4(3,I)
RX=RX+XI
RY=RY+SUM4(1,I)
SV=(SUM4(1,I)-XI)*(SUM4(1,I)-XI)+SV
  550CONTINUE
RMSE=SQRT(SV/M)

RX=RX/M
RY=RY/M
XY=0
XX=0
YY=0
DO 560 I=1,M
XI=R4(1)+R4(2)*SUM4(2,I)+R4(3)*SUM4(3,I)
XY=XY+(XI-RX)*(SUM4(1,I)-RY)
XX=XX+(XI-RX)*(XI-RX)
YY=YY+(SUM4(1,I)-RY)*(SUM4(1,I)-RY)
  560CONTINUE
CCALCULATE COEFS. OF REGRESSION MODEL OF SI OF REF. Vs. PSI OF ARAN
B=XY/XX
A=RY-B*RX
R=XY/SQRT(XX*YY)
RSQUARE=R*R
CPRINT ROOT MEAN SQUARE ERROR
WRITE(*,570) RMSE
WRITE(1,570) RMSE
  570FORMAT(/,' ROOT MEAN SQUARE ERROR: RMSE=' ,E10.4)
CPRINT R-SQUARE VALUE
WRITE(*,580) RSQUARE
WRITE(1,580) RSQUARE
  580FORMAT(/,' R SQUARE VALUE: R^2=' ,F5.3)
CPRINT COEFS. OF REGRESSION MODEL OF SI OF REF. Vs. PSI OF ARAN
WRITE(*,572)
WRITE(1,572)
  572FORMAT(/,' MODEL COEF.s BETWEEN SI OF REF. AND PSI OF ARAN:',\)\)
WRITE(*,574) A,B
WRITE(1,574) A,B
  574FORMAT(/,' A=' ,F6.4, ' B=' ,F6.4)
WRITE(*,582)
WRITE(1,582)
  582FORMAT(/,' ***** END *****',\)\)
WRITE(*,584)
WRITE(1,584)
  584FORMAT('')
CSAVE RESULTS
CLOSE (1)
OPEN(5,FILE='RESULT',STATUS='NEW')
WRITE(5,585) SS
  585FORMAT(2X,A12)
WRITE(5,586) A,B,R4(1),R4(2),R4(3)
  586FORMAT(2X,5F12.6)
CLOSE(5)
587STOP
END

```

```

5 DIM SI(500), RMSVA(500), MAS(500)
10 XL = 0: XH = 5: YL = 0: YH = 5
20 XL$ = "PSI OF ARAN": YL$ = "SI OF REFERENCE": XG = 1: YG = 1
30 GT$ = "SI ESTIMATION OF REFERENCE BY PSI OF ARAN": XS = 1: SM = 9:
40 OPEN "RESULT" FOR INPUT AS #1
50 INPUT #1, SS$
60 INPUT #1, A
70 INPUT #1, B
80 FOR I = 1 TO 3
90 INPUT #1, R4(I)
100 NEXT
110 CLOSE #1
120 OPEN SS$ FOR INPUT AS #1
130 INPUT #1, N
140 FOR I = 1 TO N
150 INPUT #1, SI(I)
160 INPUT #1, RMSVA(I)
170 INPUT #1, MAS(I)
180 NEXT
190 CLOSE #1
500 GOSUB 16000:
1000 GOSUB 17000: END
15100 REM***** Yes or NO *****
15110 t = 0: d$ = INKEY$: z = LEN(d$): IF z = 0 THEN 15110
15120 IF d$ = "Y" OR d$ = "y" THEN t = 1
15130 RETURN
16000 REM***** FULL SCREEN PLOT ROUTINE *****
16002 REM** x and y are points to be plotted
16003 REM** n is number of points
16004 REM** xl and yl are x and y lower WINDOW limits
16005 REM** xh and yh are x and y upper WINDOW limits
16006 REM** xl$ is x axis label, yl$ is y axis label
16007 REM** vertical grids at xg, horiz grids at yg, 0 for none
16008 REM** gt$ is the graph title, at the top
16009 REM** xs$ is 1 for label every x tic, 2 for every other, etc
16010 REM** SM is screen mode, 9 for hi-res, 2 for printer plot
16013 SCREEN 0: CLS : SCREEN SM:
16015 IF SM = 9 THEN COLOR 15, 1: VIEW (93, 62)-(570, 272), , 15
16016 IF SM = 2 THEN VIEW (93, 35)-(565, 155), , 15:
16017 WINDOW (XL, YL)-(XH, YH): CLS
16020 REM***** draw plot line *****
16030 SARAN = 0: SB = A + B * SARAN: SARAN = 5: SE = A + B * SARAN
16031 LINE (0, SB)-(5, SE)
16032 FOR I = 1 TO N: PSI = R4(1) + R4(2) * RMSVA(I) + R4(3) * MAS(I)
16034 IF PSI < 0 THEN 16036
16035 CIRCLE (PSI, SI(I)), .02: CIRCLE (PSI, SI(I)), .01
16036 NEXT
16040 REM***** draw vertical grid lines *****
16050 IF XG = 0 THEN GOTO 16080: REM** no vert. grid lines **
16060 n1 = INT((XH - XL) / XG) - 1
16070 FOR I = 1 TO n1: LINE (XG * I, YL)-(XG * I, YH), , , &H8888: NEXT
16080 REM***** draw horizontal grid lines *****
16085 IF YG = 0 THEN GOTO 16110: REM** no horiz grid lines **
16090 n1 = INT((YH - YL) / YG) - 1
16100 FOR I = 1 TO n1: LINE (XL, YL + YG * I)-(XH, YL + YG * I), , , &H8888: NE
16110 REM***** draw graph title *****
16115 L = LEN(gt$): LOCATE 2, 42 - INT(L / 2): PRINT gt$
16120 L = LEN(SS$): LOCATE 22, 10 - INT(L / 2): PRINT SS$
16130 REM***** draw x axis label *****
16140 L = LEN(XL$): LOCATE 22, 42 - INT(L / 2): PRINT XL$
16150 REM***** label y axis grid lines *****
16160 yinc = 16 / (YH - YL): n1 = INT((YH - YL) / YG)
16170 FOR I = 0 TO n1: yy = 15 * YG * I / (YH - YL): y$ = STR$(YL + YG * I)
16175 l1 = LEN(y$): LOCATE 20 - INT(.5 + yy), 11 - l1: PRINT y$: NEXT
16180 REM***** draw y axis label *****
16190 L = LEN(YL$): LOCATE 11 - INT(L / 2), 6 - l1: PRINT YL$
16200 REM***** label x axis grid lines *****
16210 xinc = 60 * XG / (XH - XL): n1 = INT((XH - XL) / XG) + 1
16220 FOR I = 1 TO n1 STEP XS: x$ = STR$(XL + XG * (I - 1)): L = LEN(x$)
16230 LOCATE 21, xinc * I - L + 1: PRINT x$: NEXT: BEEP: RETURN
17000 REM***** Hardcopy of Plot on Printer *****
17005 LOCATE 24, 22: PRINT "<Press Y for Hardcopy, N to continue>":
17020 GOSUB 15100: IF t = 1 THEN SM = 2: GOSUB 16000: CALL interrupt(5, 2, 2)
17025 SM = sm0: RETURN

```